

DELAYED ADMINISTRATION OF ANGIOTENSIN II TYPE 2 RECEPTOR (AT2R) AGONIST COMPOUND 21 IMPROVES STROKE OUTCOMES IN DIABETES

By

LADONYA JACKSON

(Under the Direction of Susan C. Fagan and Advije Ergul)

ABSTRACT

A disabling consequence of stroke is cognitive impairment, occurring in up to 48% of patients, for which there is NO therapy. A critical barrier is the lack of understanding of how post-stroke cognitive impairment (PSCI) develops. While 70% of stroke victims present with comorbid diseases such as diabetes & hypertension, the limited use of comorbid disease models in preclinical research further contributes to this lack of progress. Since otherwise healthy rats recover motor and cognitive function almost fully post-stroke, deficits that develop overtime in the comorbid environment, as in stroke patients, go unrecognized and remain understudied. To this end, we used a translational model of diabetes to study the development of PSCI. We then investigated whether the chronic inflammatory state of diabetes contributed the development of PSCI. Stimulation of angiotensin II type 2 receptor (AT2R) has emerged as a novel therapeutic strategy in vascular and nervous system diseases by virtue of its anti-inflammatory, anti-proliferative and tissue regenerating properties. To this end, we evaluated the application of compound 21 (C21), for the treatment of PSCI *in vivo* in a double blinded manner, with a strict inclusion criteria and a delayed administration time-point. Lastly, we employed a global knockdown with intracerebroventricular (ICV) instillation of lentiviral shRNA for colony-stimulating factor 1 receptor (CSF1R), to silence microglia and investigate its therapeutic

potential while deciphering underlying mechanisms of cognitive decline. We discovered that diabetes drastically exacerbated cognitive decline after a stroke and this was mediated by the elevated inflammatory state within these animals. When microglia activation was polarized toward an anti-inflammatory state with C21 or reduced by global knockdown the decline in cognition post-stroke was reduced. This highly translational study demonstrated that 1) the progressive nature of PSCI offers an opportunity to prevent cognitive decline; 2) AT2R agonism is a promising therapeutic tactic in the prevention of PSCI; and 3) microglia activation is a contributing mechanism. Evaluating the therapeutic potential in our comorbid model may pave the road for a move toward more translational preclinical studies that may lead to a higher number of successful clinical trials and FDA approved stroke therapies.

INDEX WORDS: diabetes, cognition, inflammation, microglia

**DELAYED ADMINISTRATION OF ANGIOTENSIN II TYPE 2 RECEPTOR
(AT2R) AGONIST COMPOUND 21 IMPROVES STROKE OUTCOMES IN
DIABETES**

By

LADONYA JACKSON

MS, Ohio University, 2015

BS, Utah State University, 2013

A Dissertation Submitted to the Graduate Faculty of the University of Georgia in Partial
Fulfillment of the Requirements for the Degree

DOCTOR OF PHILOSOPHY

ATHENS, GEORGIA

2019

© 2019

Ladonya Jackson

All Rights Reserved

**DELAYED ADMINISTRATION OF ANGIOTENSIN II TYPE 2 RECEPTOR
(AT2R) AGONIST COMPOUND 21 IMPROVES STROKE OUTCOMES IN
DIABETES**

By

LADONYA JACKSON

MS, Ohio University at Athens, Ohio USA 2015

Major Professors: Susan C Fagan, PharmD

Adviye Ergul, MD, PhD

Advisory Committee Members: Phillip Holmes, PhD,

Franklin West, PhD,

Jessica Filosa, PhD

Electronic Version Approved:

Suzanne Barbour

Dean of the Graduate School

The University of Georgia

[August 2019]

DEDICATION

I dedicate this to my beautiful daughter Abigail. I pray that my journey inspires you to be the best version of yourself. I pray that my shoulders are your foot stands and that my ceiling is your floor.

ACKNOWLEDGEMENTS

I am grateful to my family who supports me unconditionally. To my fiancé who splits the load of parenthood with me and who inspires me to be the best at my craft. To Jamilah, whom made my timely thesis defense a possibility. Whom stepped in and mothered my family and me as I furthered my education. I would not have been able to defend my thesis in the time that I did without you.

I thank my mentors Drs. Ergul and Fagan, you both have been the largest blessing in my education. You both allow me to be an independent thinker, yet are there to guide when I need help, and even in the times that I needed help but did not know it. This is the mentorship style under which I flourish, I have learned and grown so much both scientifically and personally under your guidance. When I told you that my goal was to go to medical school, you two did everything in your power to support me. Dr. Ergul even reserved her space at Augusta University after to moving to the Medical College of South Carolina, to ensure that I finish in time. That was not an easy task and I do not take for granted the blessing that this was for me. I hope that one day I can help a young mentee in the way that you both have helped me, thank you.

Lastly, to the wonderful family that I have built both from the University of Georgia Clinical and Experimental Therapeutics program and from the Augusta University Physiology program. I am so grateful for all of the help that you all have provided me and for the great conversations that we have had.

Table of Contents

ACKNOWLEDGEMENTS	v
LIST OF TABLES	vi
LIST OF FIGURES	viii
1. CHAPTER 1 INTRODUCTION AND LITERATURE REVIEW	1
Problem Statement and Specific Aims	28
2. CHAPTER 2 DELAYED ADMINISTRATION OF ANGIOTENSIN II TYPE 2 RECEPTOR (AT2R) AGONIST COMPOUND 21 PREVENTS THE DEVELOPMENT OF POST-STROKE COGNITIVE IMPAIRMENT IN DIABETES THROUGH THE MODULATION OF MICROGLIA POLARIZATION	36
3. CHAPTER 3 MICROGLIA KNOCKDOWN REDUCES INFLAMMATION AND IMPROVES COGNITION IN DIABETIC ANIMALS	73
4. CHAPTER 4 INTEGRATED DISCUSSION	106

List of Tables

Table 1: Chart on rodent models used to study VCID 19

Table 2: Collective Tables for Chapter 2 70

Table 3: Table for Chapter 3 103

List of Figures

Figure 1.1: Acute Ischemic Cascade.....	2
Figure 1.2: Proposed Timeline of Pathological Mechanisms Contributing to Stroke Injury	4
Figure 1.3: Spreading Depression Induced Alterations in Hemodynamic Responses, Ionic Imbalance, and Cytotoxic Edema.....	8
Figure 1.4: Microglia Polarization States	11
Figure 1.5: Prevalence of Post-Stroke Cognitive Impairment across the World	14
Figure 1.6: Synergistic Interplay of Factors Mediating the Development of PSCI.....	17
Figure 1.7: Diabetes Increases the Incidence of PSCI	20
Figure 1.8: Diabetes Stroke Results in Vasoregression.....	22
Figure 1.9: Diabetes Results in a dysfunctional NVU which Contributes to Poor Stroke Recovery	23
Figure 1.10: Schematic representation of the biological actions of the angiotensin system in the brain	25
Figures 2.1-2.8: Collective Figures from Chapter 2.....	59
Figures 3.1-3.7: Collective Figures from Chapter 3.....	95
Figure 4.1: Cognitive “Trajectory” in Stroke	112

CHAPTER 1

INTRODUCTION AND LITERATURE REVIEW

1. Acute ischemic stroke

1.1 Epidemiology & etiology

In the United States (U.S), over 800,000 new strokes occur annually and there are currently more than 7 million stroke survivors [1], many of whom are burdened with residual long-term disabilities. The vast majority (87%) of all strokes are ischemic, resulting from the occlusion of the blood vessels within the brain. [2]. When a blood vessel is occluded, the area which it supplies is left void of nutrients and oxygen. This leads to cell death and the wide spread activation of a neuroinflammatory cascade. With recent advances in recanalization procedures and better acute stroke care, more patients are surviving stroke events. In the U.S, stroke-related deaths show consistent trend of steady decline each year, especially among people aged ≥ 65 (by 54.1%), compared to their than younger counterparts (by 45.9 - 53.6%)[3]. In fact, in 2018 new clinical trial evidence supported the extension of the time by which eligible patients can be selected for recanalization therapy to 24 hours after initial stroke symptoms. This has, and will continue to lead to more stroke victims receiving life-saving recanalization therapies. As a result, more surviving patients will develop long-term disabilities.

In the U.S, stroke is a major cause of long-term disability and the 3rd and 5th leading cause of death in women and men, respectively. At least 6.6 million adults (aged ≥18 years) have a stroke, translating to a prevalence rate of about 2.7-3.0 %. Each year, it is estimated that about 800,000 people in the US experience first-time (610,000) or recurrent (185,000) strokes.

1.2 Pathophysiology of acute Ischemic injury

Ischemia activates a cascade of biochemical events and pathophysiological responses leading to cell death, the degree of which often depends on the duration of ischemia. Since neurons rely on the continuous flow of blood into the brain, arterial occlusion leaves that particular area of the brain depleted of energy substrates

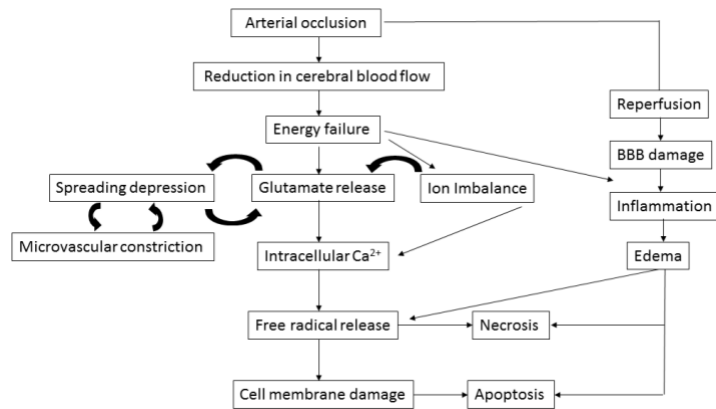


Figure 1.1: Acute Ischemic Cascade

Depicts the cascade of events that occur as the consequence of an ischemic stroke. This includes ionic imbalances, excitotoxicity and spreading depression, which all culminate in cell death.

Adapted from Bates 2015, Restor Neurol Neurosci.

essential to neuronal survival (i.e. glucose, ATP and oxygen). These ischemic conditions trigger excitotoxicity as a result of glutamate release, spreading depression (SD), ionic imbalance and inflammation, all of which perpetuate the injury leading to cell death (Figure 1) [4, 5]. The bulk of the cell death is concentrated within the ischemic core. This is an area of severe ischemia where the blood flow is below 10% to 25%. The area surrounding this core is defined as the penumbra. As the excitotoxicity and the waves of SDs progress, this penumbra has the potential to turn ischemic or be salvaged depending on the duration of time before intervention.

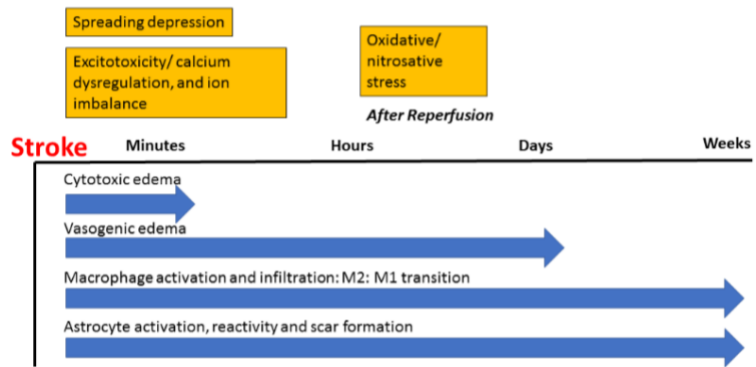
The ionic balance of Ca^{2+} , Na^+ , K^+ and Cl^- within the brain parenchyma is essential for cell survival. Events such as excitotoxicity and spreading depolarization further drive the perturbations of ionic balances leading to a large cellular influx of Na^+ , Ca^{2+} , and Cl^- ions, and a large efflux of K^+ into the extracellular space which in turn, activate a repertoire of calcium-dependent enzymes including phospholipases, endonucleases, and proteases. These proteolytic enzymes destroy key cellular components, especially the cytoskeleton, membrane, and DNA, resulting in excitotoxic cell death [4]. Additionally, the imbalanced influx of Na^+ drives the Cl^- influx via chloride channels, resulting in increased osmolarity. The active extrusion of Na^+ is essential to maintain homeostasis and requires ATP. Without continual blood supply, ATP is depleted, resulting in disrupted Na^+/K^+ pumps and causing a massive influx of Na^+ [6, 7]. This then drives the influx of water via aquaporin channels and cytotoxic edema, which inevitably leads to oncotic or necrotic cell death of mostly astrocytes and neurons [6].

1.2.1 Excitotoxicity

As the flow of blood and essential energy supply is interrupted, the neuronal and astrocytic membrane potentials are lost. This results in depolarization events, voltage-dependent Ca^{2+} channel activation and excessive glutamate release [8]. As cell death occurs, the glutamate release is exponentially amplified, since the intracellular contents of glutamate far surpass the homeostatic extracellular concentrations. Glutamate, as the main excitatory neurotransmitter within the brain, stimulates N-methyl-D-aspartate (NMDA) and α -amino-3-hydroxy-5-methyl-4-isoxazolepropionic acid (AMPA) receptors. The receptor activation leads to Ca^{2+} influx and overload into the mitochondria. This depolarizes the membrane, and induces mitochondrial dysfunction, while contributing to the evolution of spreading depression,

cytotoxic edema and cell death [4, 7, 8]. Since energy is limited in the absence of blood flow, the ion pumps involved in the presynaptic recycling of glutamate are also reduced in activity, further contributing to the large excess of glutamate in the extracellular space [8].

Additionally, NMDA activity can directly contribute to the



generation of reactive oxygen species (ROS) through the activation of NADPH oxidase activity [8].

Astrocytes are positioned between neurons and blood vessels and are able to transmit bidirectional information [9]. They have been implicated as key intermediaries in neurovascular coupling [9]. To maintain ionic balance as well as homeostatic concentrations of neurotransmitters under normal

Figure 1.2: Proposed Timeline of Pathological Mechanisms Contributing to Stroke Injury
 Depicts the timeline of pathogenic events that occur after an ischemic stroke. This includes ionic imbalances, excitotoxicity and spreading depression, as well as the resulting edema formation and immune activation.
 Adapted from McCrary 2017, J Anesth Perioper Med.

physiologic conditions, astrocytes rapidly remove excess K^+ and glutamate. As discussed previously, extracellular K^+ is increased after stroke due to the depletion of ATP and the loss of active transport regulation [10]. Astrocytes are involved in glutamate uptake through two transporters, GLAST (EAAT1) and GLT-1 (EAAT2) [10]. Na^+ , H^+ and K^+ electrochemical gradients work with the two transporters to bring glutamate into the astrocyte [10]. Increased uptake of K^+ within astrocytes actually leads to a reduction in the amount of glutamate reuptake, further contributing to the excitotoxicity (Figure 2).

1.2.2 Spreading depression

Spreading depressions and spreading depolarizations are both referred to as SD events and were first discovered by a Brazilian physiologist, Aristides Leao as the depression of cortical activity. Although spreading depressions were initially believed to be separate entities from the previously described spreading depolarizations observed after a stroke, these two were later found to be two ends of the same phenomenon [11]. Together this phenomenon is commonly referred to as SDs and it defines propagating waves that spread through the brain tissue and can expand ischemic injury. As this wave spreads, it induces persistent depolarization in the ischemic core, spreading depression in the periphery, and intermediate-duration depolarizations in the intervening penumbra [11, 12]. Due to the ionic imbalances that culminate after an ischemic stroke, the spreading depolarizations that propagate throughout the core are so large that repolarization of the membrane is not possible, ultimately resulting in depression of neuronal activity. The prolonged duration of SDs indicates the insufficiency of membrane ion pumps to repolarize neurons and is speculated to increase severity [13]. Delayed lesion expansion in focal ischemia occurs in a similar fashion, triggered by secondary spontaneous SDs that induce persistent/terminal depolarization and excitotoxic injury in the penumbra [7].

Ionic imbalances & cytotoxic cell death

After the onset of acute ischemic brain injury, spontaneous waves of intense neuronal and astrocytic mass-depolarizations occur minutes later and may be sustained for several days (Figure 2) [13]. SDs occur as the absence of blood flow leads to the depletion of energy needed

to maintain neuronal membrane potential and results in the loss of ion homeostasis, in particular high intracellular Na^+ , Ca^{2+} and Cl^- and high extracellular K^+ . The extracellular K^+ first rises slowly over 2–4 min until it reaches 9–11mM, a “ceiling level” in the cortex [11]. SDs then lead to a massive rise in K^+ to a new equilibrium up to 75mM [11]. This then signals the onset of persistent depolarization and a sharp increase in neuronal, followed by astrocytic intracellular Ca^{2+} [11, 12]. The insufficiency of membrane ion pumps (i.e. Na/K) further perpetuates the ionic imbalance because the concentration of negatively charged ions (Cl^-) rises higher within the cells than in the extracellular space [6, 7]. This in turn creates a driving force for water to enter the cells [12]. The influx of water induced during SD is the principle mechanism of cytotoxic edema (Figure 3) [12]. Cytotoxic edema leads to swelling of the neuronal soma and dendritic beading [12]. The reduction in the mobility of intracellular water along the main axis of each dendrite can be detected as increased DWI intensity, and a decrease of the ADC and MR diffusion [12].

Astrocytes contribute to the development of cytotoxic edema through multiple avenues. They function to siphon the excess glutamate and K^+ from the extracellular space. The increased K^+ influx within astrocytes leads to NKCC1 activation, which causes the K^+ influx to be followed by Na^+ and Cl^- [12]. The extracellular acidosis and increased lactate through the Na^+/H^+ or $\text{HCO}_3^-/\text{Cl}^-$ exchangers also lead to intracellular osmolytes and the influx of water [12]. Additionally, as astrocytes remove excess glutamate from the excitotoxic cloud occurring post-stroke, water is translocated through glutamate transporters such as EAAT1 [12].

Aquaporin-4, (AQP4) is normally responsible for removing excess water to prevent cytotoxic edema and cell lysis. Although cytotoxic edema occurs shortly within minutes, the

uncoupling of AQP4 from astrocytic end-feet contributes to both the immediate cytotoxic edema response, as well as later vasogenic edema after stroke [12]. Vasogenic edema is due to the opening of the BBB and involves the net increase in cerebral water content by the movement of water into the extracellular space, causing swelling within the brain parenchyma [14].

Altered Hemodynamic Responses

In addition to preserving constant blood flow, the brain has the ability to increase cerebral blood flow (CBF) in proportion to the activity and energy consumption of a specific brain region [15]. This phenomenon known as functional hyperemia forms the basis of functional MRI (fMRI). Functional hyperemia can occur as a result of neurovascular coupling which is defined by the coupling between neural activity and CBF and comprises the idea that brain activity, and more specifically, the metabolites produced by neuronal activity can elicit changes in cerebral perfusion [15]. Just as the metabolites produced by neuronal activity elicit increased perfusion, the vascular changes induced by neural activity are necessary to feedback and fulfill the increased metabolic needs of active brain regions [15]. The flow increase may also be needed to clear the brain of potentially toxic by-products of brain activity (i.e. lactate, CO₂, adenosine, H⁺, the amyloid- β peptide (A β), tau), and for brain temperature regulation [15]. Astrocytes are essential for proper hemodynamic responses and modulate the activity of large neuronal populations and vascular networks to ensure functional hyperemia [16]. The gap junction protein, connexin 43, functionally couples astrocytic end-feet surrounding parenchymal arterioles to the glia limitans, the thick layer of astrocytic processes surrounding pial vessels that supply the brain circulation, to ensure an efficient increase in CBF during functional hyperemia [16].

SD leads to vasodilation in healthy tissue, and vasoconstriction in ischemic tissue. In healthy tissue, a proper ionic balance between K^+ , Na^+ and Ca^{2+} and intact neurovascular coupling response

exists. During this

process, neuronal

depolarization

stimulates increases in

endfoot astrocytic Ca^{2+} ,

which activates BK

channels and the resulting

release of K^+ [16].

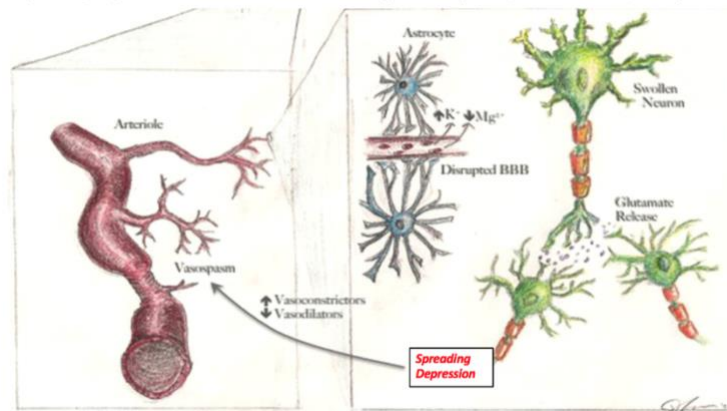


Figure 1.3: Spreading Depression Induced Alterations in Hemodynamic Responses, Ionic Imbalance, and Cytotoxic Edema

Depicts the sub-events that occur as a result of the propagating waves of spreading depression. These specifically include ionic imbalances, cytotoxic cell death and altered hemodynamic responses.

Adapted from Kramer 2016, J Clin Neurosci.

Depending on the concentration of K^+ (below 20 mM), this then activates vascular smooth muscle cell (VSMC) Kir channels causing hyperpolarization, which closes the voltage gated Ca^{2+} channels. This decreases intracellular Ca^{2+} within the VSMC and ultimately leads to vasodilation and hyperemia [17].

Within the ischemic tissue, SDs produce adverse hemodynamic responses characterized by a brief initial drop of CBF, transient hyperemia, followed by sustained hypoperfusion also known as spreading oligemia [13]. While the vasodilation associated with hyperemic CBF responses contributes to the tissue salvage, this beneficial response is often overridden by vasoconstriction, which culminate in tissue damage (Figure 3) [13]. Upon ischemic neuronal hyperpolarization (increased extracellular K^+ and increased intracellular Na^+), adenosine-mediated suppression of vesicular transmitter release reduces energy consumption as a

survival response to ischemia [11]. The neuronal hyperpolarization is termed as 'nonspreading depression' of activity and is thought to be the pathophysiological correlate of the sudden, simultaneous neurological deficit in different modalities which is typical of transient ischemic attacks and stroke [12, 18]. This electrical inactivity, termed 'nonspreading depression' occurs seconds before it triggers the first SD [12]. Thus, brain activity is already partially depressed before SD erupts in ischemic tissue, leading to opposing effects to those observed in healthy tissue [12]. In the ischemic tissue, the elevated K^+ (above 20 mM) and decreased Na^+ within the extracellular space, along with the dysregulated Na^+/K^+ pump leads to increased Ca^{2+} in the astrocytic end-feet which, contrary to that observed in healthy tissue, then activates VSMC Kir channels to depolarize and open the voltage gated Ca^{2+} channels, increasing intracellular Ca^{2+} within VSMCs and ultimately leading to vasoconstriction [17]. The nitric oxide (NO)-mediated vasodilator response to increased Ca^{2+} mobilization in endothelial cells would normally outweigh the increased vasoconstrictor response caused by augmented Ca^{2+} mobilization in astrocytes and VSMC [12]. Since oxygen is necessary for NO synthesis, NO bioavailability is decreased under ischemic conditions, leading to the elimination of this compensatory mechanism and ultimately spreading ischemia [12]. The spreading ischemia propagates in the tissue due to the microvascular constriction and it also feeds back to prolong the SD and increase the chance of transitioning into cell death [12]. The influx of K^+ within astrocytes not only activates signaling pathways to induce microvascular constriction, but also leads to swelling of the astrocytic end-feet, which has been hypothesized as a potential mechanism to restrict perfusion even further, contributing to the hypoperfusion during SD [19]. This

restriction has also been postulated to occur as an acutely neuroprotective method to limit the spread of neuroinflammation and neuronal death [8].

Although SDs are largely recognized as detrimental, recent publications have suggested the contrary. One study observed that when microglia were knocked out prior to ischemic insult, SDs were attenuated, resulting in continuous neuronal depolarizations and exacerbated cumulative Ca^{2+} overload within the cell [20]. This actually led to an increased infarct size in a mouse model [20]. Additional studies within rats found that the advancement of age reduced the frequency of K^+ induced SDs as well as spontaneous SDs and increased the latency between subsequent SD events [13]. A clinical study also reported a lower incidence of SDs in older versus younger patients after brain injury [21]. Since aging is associated with exacerbated outcomes after stroke, the exact role of SDs in these outcomes remain to be elucidated.

1.2.3 Cell death pathways

Ischemia can induce cell death via multiple pathways: apoptosis, necrosis, programmed necrosis, ferroptosis and autophagy [8]. Apoptosis is classified as controlled cell death which converges on caspase pathways where DNA and organelles are fragmented into smaller parts and ingested by phagocytes with minimal release of inflammatory cytokines [8]. Apoptotic cells generally induce an anti-inflammatory response, such as the release of transforming growth factor (TGF)- β and interleukin (IL)-10 by engulfing macrophage, resulting in an immunologically silent event [22]. Necrosis on the other hand, is caused by overwhelming stress, such as ischemic conditions, and it is not regulated like apoptosis. It actually involves disintegration of the cell walls, ROS production and excessive inflammation [8]. After a stroke, approximately 70% of the ischemic

core consists of necrotic tissue [8]. As an intermediate, programmed necrosis has also been identified as a defense against intracellular pathogens that block apoptosis activation [3].

Programmed necrosis involves the activation of

programmed cell death via TNF α and FasL

pathways [8]. Ferroptosis is a form of cell death

which was first reported in 2012 [23]. This

distinct form of cell death is characterized by the

iron-dependent accumulation of toxic lipid ROS

[24]. Unlike the other forms of cell death,

ferroptosis does not require the transcriptional

upregulation or posttranslational modification

of any specific cell death effector or pore-

forming protein, but is characterized morphologically by the

vanishing of mitochondria membranes [24, 25]. Rodent

models of stroke have shown increased iron levels within the

ipsilateral hemisphere after an ischemic event, which

perpetuates ferroptosis, ROS accumulation, and thusly

activation of the other various cell death cascades. Lastly, autophagy involves lysosomal

processes of cell components, it is the self-eating pathway through which long-lived proteins,

damaged organelles and misfolded proteins are degraded and recycled for the maintenance of

cellular homeostasis and normal cellular functions [8, 26]. It is a cellular protection pathway but

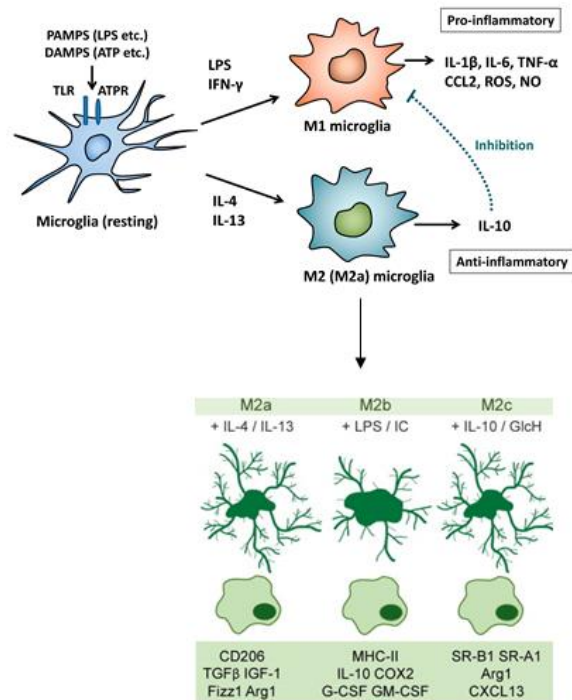


Figure 1.4: Microglia Polarization States

Microglia are dynamic cells that can exist in a plethora of states. Overall, M1 is regarded as an inflammatory state while the M2 is regarded as an anti-inflammatory state.

Adapted from Franco R 2015, *Prog Neurobiol.* and Nakagawa 2014, *Pharmaceuticals*

can be beneficial or detrimental depending on the rate of induction and/or duration [26]. Regardless of the pathway, the massive cell death is concentrated within the ischemic core.

1.2.4 Neuroinflammation

The aforementioned cell death pathways lead to the release of damage associated molecular pathogens (DAMPs), pro-inflammatory cytokines, chemokines and ROS which activate microglia (resident immune cells of the brain) to initiate neuroinflammatory responses. Neuroinflammation further perpetuates the release of pro-inflammatory cytokines, chemokines, ROS and second messengers [27]. The inflammatory response then additionally contributes to secondary neuronal damage and the recruitment of peripheral immune cells, blood brain barrier (BBB) breakdown, edema and tissue damage [27, 28], [29].

Microglia are primarily responsible for the initiation of an immune response. Microglia constitute around 10% of the cells within the CNS [27]. Microglia are derived from myeloid cells and migrate into the CNS very early on in development [27]. In a healthy brain, neurons secrete immunosuppressive signals such as CD200, CX3CL1, and other neurotransmitters and neurotrophins, that keep microglia in an inactive state and their primary role consists of scanning for disturbances [30]. Upon activation, they exist as two broadly classified phenotypes referred to as 'M1' or 'M2' (Figure 4) [30]. Although M2 consists of many sub-types, overall they promote immune suppression, injury resolution and participate in phagocytosis and matrix maintenance [30]. M1 on the other hand, promotes the release of pro-inflammatory cytokines and recruitment of peripheral inflammatory cells [30]. Microglia have a relatively low turnover rate in the absence of pharmacological intervention, making them susceptible to pro-inflammatory effects of age, injury or stress [27]. Although microglia are infamous for their detrimental role in

neurodegeneration, it was demonstrated in a mouse model that after an ischemic stroke event, microglia were actually initially polarized toward a M2 phenotype, which peaked within 5 days after the initial injury [31]. In a different mouse model of stroke, infarction was exacerbated in the absence of microglia, most likely due to the beneficial effects mediated by M2 microglia acutely post-stroke [20]. After 3-5 days the microglia begin to shift toward a M1 phenotype [31]. This resolves within weeks to months in the absence of comorbidities [32].

2. Post-Stroke Cognitive Impairment (PSCI)

Stroke is the leading cause of long-term disability worldwide, with the onset of cognitive impairment being a large contributor [33]. Vascular cognitive impairment and dementia (VCID) is the second most common cause of cognitive decline [34]. PSCI is a type of vascular dementia which is characterized by the progressive decline in cognition, and 25-30% of stroke survivors develop it within the first 3 months after stroke [1]. The term VCID is used since not all cognitively impaired stroke survivors meet the criteria of the dementia [35]. The term VCID is used for all forms of cognitive disorders associated with cerebrovascular disease, regardless of the pathogenesis (i.e., cardioembolic, atherosclerotic, ischemic, hemorrhagic, or genetic) [36]. It encompasses a spectrum of clinical disease states [1–4] that range from post-stroke mild cognitive impairment or dementia following a large artery stroke, through ‘sporadic’ small vessel disease (SVD), to pure genetic small vessel arteriopathy (CADASIL, CARASIL, COL4A1/4A2 mutations) [37]. Most of VCID involves a combination of microinfarction, microvascular changes related to blood–brain barrier damage, neuronal cell death and co-existing neurodegenerative

pathology [13]. For the purpose of this dissertation we will focus primarily on PSCI, a specific type of VCID.

2.1 Epidemiology & etiology

PSCI has been recorded to have a prevalence rate ranging from 20-50% [1, 35, 38, 39] (Figure 5). Aside from regional differences, the wide prevalence estimates could be attributed to the difference in sociodemographic characteristics between countries, races, and the diagnostic criteria, especially the Diagnostic and Statistical Manuals of Mental Disorders IV (DSMMD-IV) and Mini-Mental State Examination (MMSE) score versus the Montreal Cognitive Assessment (MoCA). These evaluation tools have huge variability in gauging PSCI [38]. When the two tests were compared side by side in patients with Parkinson’s Disease (PD) the MMSE was found to be more sensitive but less specific than the MoCA. The Rotterdam study was a large population-based cohort study that utilized the MMSE to evaluate age-related disorders in over 10, 000 older individuals who were stroke free and cognitively normal at baseline.

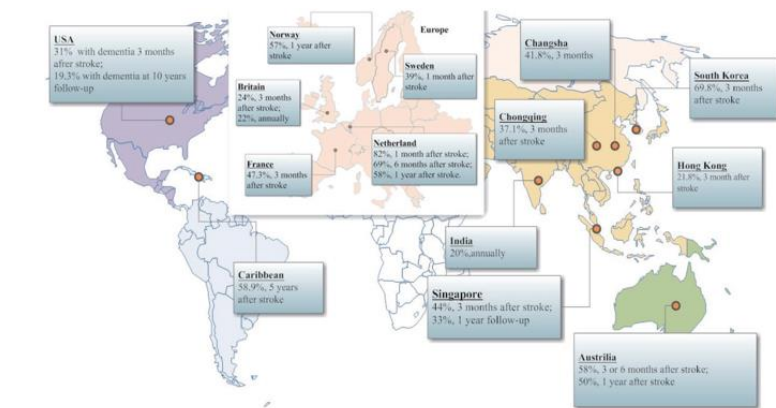


Figure 1.5: Prevalence of Post-Stroke Cognitive Impairment across the World
 Depicts the range of prevalence of PSCI across the world 3 months to 1 year after stroke.
 Adapted from Sun 2014, Ann Transl Med.

Findings from the Rotterdam study and statements from the

American Heart Association (AHA) conclude that in general, having a stroke increases the risk of dementia 2-fold. [36, 40, 41]. The risk of dementia increases with increased age, fewer years of education, history of diabetes mellitus and atrial fibrillation, and recurrent stroke. The

REGARDS trial (Reasons for Geographic and Racial Differences in Stroke) was the first study to demonstrate a progressive decline in cognition after one stroke event. Results from the REGARDS trial indicate that 25-30% of stroke survivors develop it within the first 3 months after stroke [1]. This study enrolled over 30,000 patients and actually utilized the SIS (six item screener), AFT (animal fluency test) and WLD (word list delayed recall) instead of MMSE or MoCa, due to the ability to conduct these assessments over the phone. The ASPIRE trial looked at cognitive impairment 6 months after stroke utilizing the MoCa in 256 stroke patients and found that 57% of patients developed cognitive impairment [3]. With the varying tools used to measure cognition, we can expect 25-57% of patents to develop PSCI within the acute phase (first 3-6 months) after stroke. Although variations between populations are to be expected, the use of one standardized tool to measure PSCI across clinical trials would allow for more consistent and replicable findings to derive conclusion from.

2.2 Acute versus progressive cognitive changes after stroke

Although the REGARDS study showed that patients that exhibited cognitive impairment at 3 months exhibited an accelerated and persistent decline in global cognition and executive function over 6 years, there is conflicting evidence on whether the development of PSCI is sustained over time. A population-based study in Rochester, Minnesota [42] evaluated 971 cognitively normal patients with first-ever ischemic stroke and found a 9-fold increase in dementia compared to the general population 3 months after stroke. This later declined to a 2-fold increase over a 5-year period. It is possible that the decreased risk may be due to the unaccounted mortality. Stroke survivors with cognitive impairment at 3 months have been shown to experience a 53% increased risk of death compared with those with no known

cognitive impairment at the same time point [38]. A study based in England study found that in patients aged older than 75 (non-demented at baseline), the patients that did not die within 6 years after stroke developed delayed dementia at a 24% rate, similar to the rate found in the REGARDS trial [43]. Interestingly, of the patients that died within 6 years, more than 75% met the criteria for vascular dementia [43]. They additionally found that the risk of progression to delayed dementia after stroke is related to the presence of vascular risk factors, such as diabetes [43].

2.3 Pathophysiology of PSCI

The impact of vascular pathology on the development of PSCI is influenced by morphology (focal or multifocal; large or small vessel), volume of brain destruction, and location and number of lesions [44, 45]. PSCI is associated with marked alterations in cerebral microvascular structure, including thickened basement membranes, increased tortuosity, and vasoregression [36]. These features are also abundant in the pathophysiology of diabetes [46]. Additionally, arterioles undergo hyaline degeneration (lipohyalinosis), a cause of microhemorrhages, also similar to that observed in diabetes [36]. Neurovascular dysfunction further increases the brain's susceptibility to injury by altering regulation of the cerebral blood supply, disrupting BBB function, and reducing trophic factors. Just as the previous features, these two are also present in the pathophysiology of diabetes [36].

Brain Atrophy

A multitude of studies have associated hippocampal atrophy with cognitive decline [35, 47]. In fact, cerebral atrophy is speculated to explain why inflammatory microglia and astrocytes exhibit a dampened cytokine response in the production of IL-6 and IL-8 in those stroke subjects that develop dementia compared to those who do not [48, 49]. After a stroke, IL-6 and IL-8 have been shown to be significantly lower in dementia patients than in non-demented patients in every region although high plasma levels have been associated with cognitive impairment [49]. However, atrophy alone does not directly predict the severity of cognitive impairment. The infarct volume was only found to explain a small proportion of the variability of cognition in the stroke patients, but rather the strategic site of the lesion plays a larger role in the manifestation of cognitive impairment after stroke and is associated with the severity of the dementia [35, 50].

Lesions in areas such as the frontal cortex, cortical limbic areas, the hippocampus and the white matter, explain half of the variability in MMSE of patients after a stroke [48].

Additionally the combination of vascular risk factors, strategic lesions sites and neurogenerative processes

may work together to lower the threshold required by each to induce the clinically manifestation of cognitive impairment [50] (Figure 6).

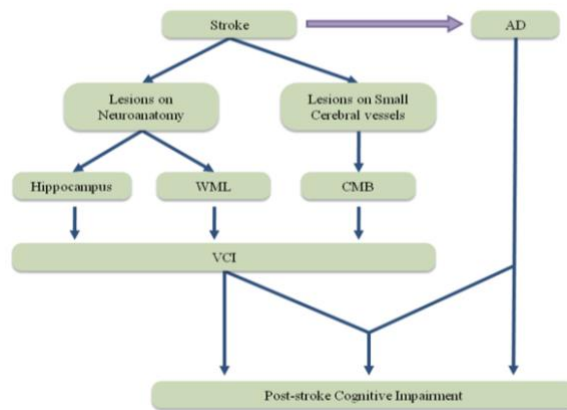


Figure 1.6: Synergistic Interplay of Factors Mediating the Development of PSCI

Depicts the factors that contribute to the development of PSCI.

Adapted from Sun 2014, *Ann Transl Med*.

White matter damage

Lesions within the white matter (WM) may lead to cortical thinning, contributing to the atrophy impairing the executive function and verbal fluency [51]. WM changes observed in cognitively impaired patients are most prominent in the frontal lobe and appear linked with frontal -subcortical disconnection [48]. A study performed in 448 patients with symptomatic atherosclerotic disease from the cohort of SMART-MR in a 4 years follow-up, also suggested that the interaction between brain atrophy and WM lesions or infarcts work together aggravate the cognitive decline [52].

Dysfunction of the neurovascular unit (NVU) and mechanisms regulating CBF particularly in the deep WM are important components of the pathophysiological processes underlying PSCI [48]. The infiltration of reactive astrocytosis and activated microglia within the white matter are associated with expression of hypoxia-inducible genes, suggesting local hypoxia [36]. Clasmatoendrocytes are astrocytes that exhibit swollen and vacuolated cell bodies, indicative of irreversibly injury. Clasmatoendrocytes are well described in hypoxic-ischemic injury but have also been recently indicated in post-stroke dementia [53]. High ratios of clasmatoendrocytes to total astrocytes in the frontal WM were shown to be consistent with lower MMSE scores in demented subjects [48]. The percentage of clasmatoendrocytes were shown to be increased by 2- fold in demented compared to non-demented subjects and by 11- fold in older normal controls versus young controls in the frontal WM [53]. These were associated with aberrant co-localization of AQP4 in reactive GFAP+ astrocytes with disrupted end-feet juxtaposed to microvessels [48, 53]. This is consistent with the fact that WM BBB alterations are early findings in VCID [36]. It was similarly shown here that WM lesions and

brain atrophy, such as medial temporal lobe atrophy, subcortical atrophy, and cortical atrophy are independently related to VCID, and can accelerate the detrimental impact of WM lesions on VCID [54].

2.3.1 Animal studies on the development of VCID

A number of animal models have been used to study the development of PSCI following ischemic stroke [37]. They include rat/mice models of thromboembolic stroke (TES), middle cerebral artery occlusion (MCAO), chronic hypoperfusion (CHP), and bilateral carotid artery stenosis (BCAS) as summarized in Table 1.

Table 1.1: Chart on rodent models used to study VCID

Citations	Animal model	Brain gross pathology	Brain neuropathology	Cognitive changes
[28, 37, 55-57]	MCAo rat/mice (Post-stroke cognitive impairment)	Focal ischemic infarcts; brain atrophy in cortex and hippocampus	White matter lesions, impaired BBB, immune infiltration and microglia activation	Cognitive deficits in spatial, working and reference memory. Typically resolves within 1-2 weeks in non-comorbid animals. Persistent cognitive impairment is observed when hypertension or diabetes is present
[58, 59]	BCAS mice, CHP rat/mice	n/a	White matter lesions, impaired BBB, microglia activation	cognitive deficits in working and reference memory

3. Diabetic Stroke and the Development of PSCI

More than 40% of stroke patients present at the time of stroke with pre-existing diabetes. In fact, the risk of stroke is up to 2-6 fold greater in diabetics [60, 61]. Diabetes not only increases the risk of stroke, but also the severity of symptoms, including cognitive impairment [28]. In a

large clinical trial, the Rotterdam study, diabetes was associated with a 2-fold increased prevalence of dementia [60, 62].

3.1. The impact of diabetes on ischemic injury resolution

Clinical and experimental studies have shown altered hemodynamic states, chronic inflammation and increased brain atrophy in diabetic subjects [46, 47, 61, 63-65]. Both diabetic patients and diabetic rodent models demonstrate lower CBF at baseline [46, 63]. This is accompanied by dysfunctional angiogenesis and elevated oxidative stress which is associated with an upregulation of hypoxia inducible factor 1 (HIF-1) (Figure 7). The hypoxic state within the diabetic brain contributes to the impaired cognition observed in diabetics [63]. Hypoxia encourages the infiltration of inflammatory cells, resulting in reactive astrocytosis and activated microglial within areas sensitive to damage, such as white matter [36]. Our lab has shown that pro-inflammatory T helper cells (Th17) are upregulated within the brain parenchyma of diabetics prior to any ischemic injury [66]. The chronically elevated neuroinflammatory state also aids in increasing cell death and perpetuating brain atrophy, as diabetes has consistently been

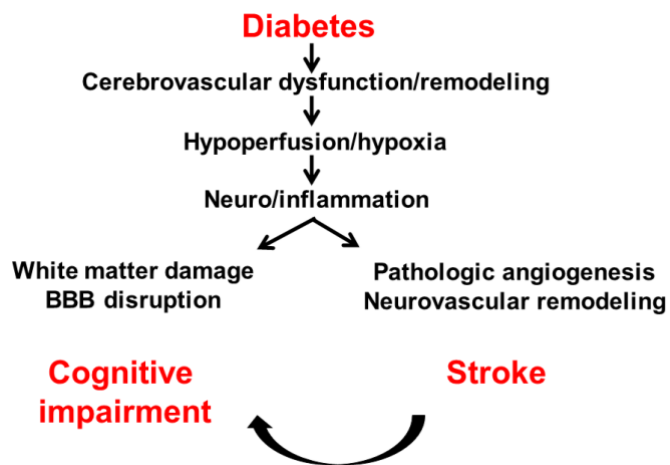


Figure 1.7: Diabetes Increases the Incidence of PSCI
An illustration of the cycle of pathogenic remodeling which contributes to the increased prevalence of PSCI after diabetic stroke.
Adapted from Ergul 2014, J Cerebr Blood F Met.

associated with hippocampal atrophy both in human patients and in experimental rodent models [47, 64, 65]. In conclusion, at baseline prior to a large ischemic event, diabetes have

lower CBF levels, elevated inflammation and hippocampal atrophy, all of which impact the acute and chronic recovery phases after an ischemic event (Figure 7).

3.1.1 Acute ischemic injury

Since both stroke and diabetes are vascular diseases, diabetes-induced dysfunction and pathological remodeling of the cerebrovasculature ultimately affects stroke injury and recovery [46]. Our lab has demonstrated, in numerous rodent models, that diabetic animals exhibit greater vascular injury after a stroke characterized by increased bleeding within the brain (hemorrhagic transformation) and greater edema [46]. Diabetic animals exhibit a reduced astrocytic response acutely, associated with greater BBB damage and stunted brain repair processes [67]. As previously discussed, astrocytes contribute to the development of cytotoxic edema in multiple ways, one of which is through AQP4 channels, which are responsible for removing excess water to prevent cytotoxic edema and cell lysis. Our lab has shown increased uncoupling of astrocytic AQP4 channels in diabetic animals compared to control animals after a stroke [67]. The increased uncoupling of AQP4 from astrocytic end-feet observed in these diabetic animals contributes to both the immediate cytotoxic edema response, as well as later vasogenic edema from the BBB after stroke [12]. Previous studies have correlated the reduction in astrocytic reactivity acutely after stroke to increased BBB breakdown [68]. The elevation of activated microglia also contributes to the BBB breakdown and the recruitment of peripheral immune cells. Unfortunately, due to their chronic inflammatory state, diabetic subjects have elevated M1 microglia at baseline. In addition, they do not experience the acute rise in M2 microglia after a stroke, which aid in injury resolution. Instead, diabetic animals experience an immediate increase in M1 microglia, which further signal for immune cell infiltration [69]. Our

lab has shown that diabetic animals have more pro-inflammatory T helper cells (Th1) within the brain parenchyma 3 days after a stroke when compared to control animals [66]. The severity of WM injury is known to correlate with poor functional prognosis in patients with stroke [70]. Greater disruptions in WM integrity have been observed in diabetic patients compared with

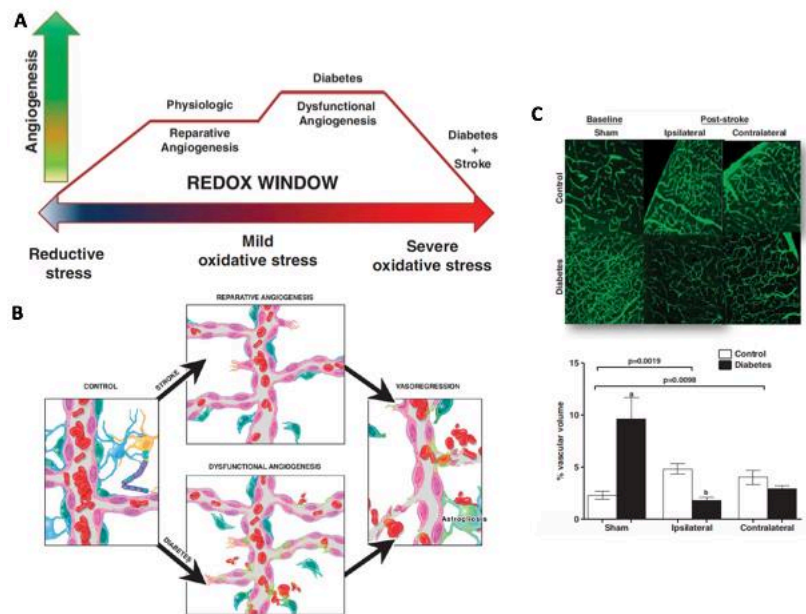


Figure 1.8: Diabetes Stroke Results in Vasoregression

Diabetes induces dysfunctional angiogenesis which results in an overall increased amount of blood vessels, but the vessels are immature and prone to injury. After an ischemic event diabetic animals have been shown to undergo vasoregression, which contributes to the chronic hypoperfusion.

Adapted from Ergul 2014, *J Cerebr Blood F Met.*

age-matched nondiabetic controls [69]. The acute rise in in astrocytic reactivity and increased M1 activation also contributes to the demyelination that occurs acutely and persists chronically after stroke in diabetic animals [68, 69]. The combination of these processes alter the NVU and culminate in increased cell death, particularly in the hippocampus and the cortex, and exacerbate already present atrophy of the brain (Figure 7) [28, 67].

3.1.2 Chronic Recovery

Diabetic patients not only experience increased mortality due to the aforementioned cascade of events, but the ones who survive also exhibit increased morbidity after a stroke event. Data from the Rotterdam study suggest that diabetes doubles the risk of VCI [71]. This

may be in part perpetuated by the altered hemodynamic states and the increased neuroinflammation. Diabetes results in increased angiogenesis, but the vessels formed are immature and dysfunctional. After a stroke, they experience greater vasoregression, of which is only partly reversed with glycemic control (Figure 8) [46]. This perpetuates chronic hypoperfusion and

perpetuates neuroinflammation (Figure 7). Potential contributing mechanisms include alterations to cells of the NVU and oxidative stress

(Figure 8 and 9) [70]. Pericytes contribute to the induction and maintenance of the BBB, microvascular stability, endothelial cell survival and angiogenesis, neurovascular coupling and blood flow regulation, and clearance of extracellular molecules by phagocytosis [70]. When pericyte number is decreased, there is a proliferative response leading to pathological angiogenesis [70]. When a second hit such as a stroke then leads to greater pericyte loss, which exceeds 50%, endothelial cells start undergoing apoptosis and vasoregression [70]. Although diabetic animals were shown to display an acute reduction in the astrocytic response, associated with a breakdown of the BBB, chronically 14 days after stroke diabetic animals display amplified astrocyte reactivity associated with loss of vasculature and poorer outcomes [72]. Potential molecular mechanisms contributing to the vasoregression includes nitrate

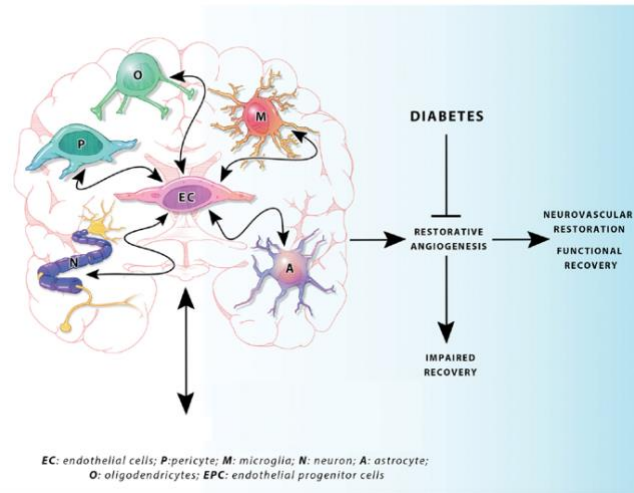


Figure 1.9: Diabetes Results in a dysfunctional NVU which Contributes to Poor Stroke Recovery
 An illustration of the NVU dysfunction and resulting vasoregression that occurs as a result of diabetes and contributes to the worsened stroke recovery.
 Adapted from Ergul 2016, Brain Res.

switch, since diabetic animals have greater peroxynitrite formation in association with greater endothelial apoptosis.

Although control animals experience a resolution of neuroinflammation and M1 activation, our lab has shown that diabetic rodents remain chronically elevated 2 weeks after stroke, which contributes to deficits in cognition [28, 67]. Indeed, other animal models have also demonstrated elevated M1 activation in diabetic animals compared to control animals 2 week after a stroke, which contributed to ongoing WM damage and impaired cognition [69]. Since both diabetes and cognitive impairment are independently associated with neuroinflammation, we postulate that this may be a causative link in diabetic PSCI that warrants further investigation [60]. Taken together, these findings suggest that modulation of the M1:M2 ratio in diabetics may favor better outcomes in the chronic recovery stage.

4. Central Angiotensin System

Within the brain, there are peripheral and central angiotensinergic pathways [30]. The main peripheral pathway is the forebrain pathway, which integrates the circumventricular organs (CVOs) that surround the third and fourth ventricles and consists of fenestrated capillaries to allow for the peripheral access of angiotensin [30]. Due to the restricted access by the BBB, the majority of brain regions have to synthesize angiotensin locally [30]. The main central pathway connects the hypothalamus and medulla and is the primary contributor of locally synthesized angiotensin [30]. To supplement this, angiotensin is also synthesized in various other brain regions [30]. Both peripheral and central angiotensin production contributes significantly to cardiovascular homeostasis [30]. AT1R is infamous for its role in

vasoconstriction, and AT2R for its role in vasodilation, but they additionally have pleiotropic roles within microglia, neurons and astrocytes. We will focus on their roles within the microglia. Further details on the cell specific actions of various components of the angiotensin system within the brain can be reviewed here [30].

4.1 Angiotensin II type 1 receptor (AT1R)

AT1Rs on microglia are undetectable under non-pathologic conditions but they are upregulated as part of a pro-inflammatory response in parallel with M1-like microglia [2]. AT1Rs are expressed on the cell surface of microglia but additionally have an intracellular angiotensin system [2]. Intracellular activation of AT1R leads to the further upregulation of AT1Rs and a shift toward a predominately M1-like phenotype [2]. Activation of cell surface and/or intracellular AT1R signaling leads to the

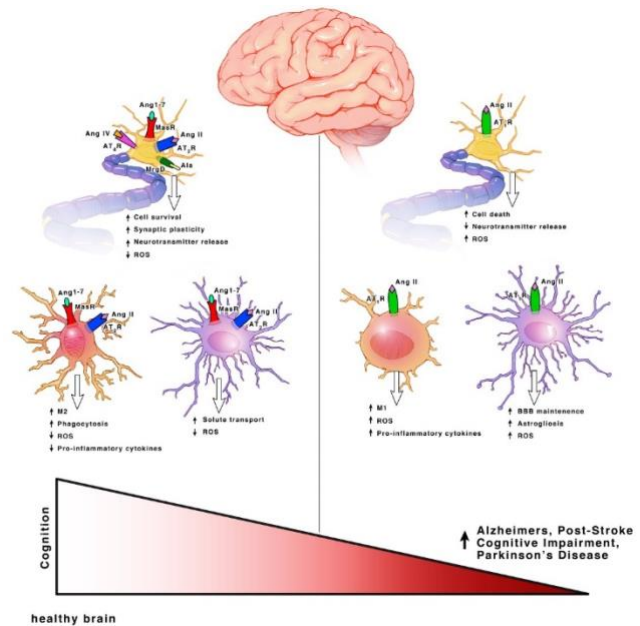


Figure 1.10: Schematic representation of the biological actions of the angiotensin system in the brain

In disease states such as PSCI Ang II effects driven by the AT1R predominate and exacerbate the development of cognitive impairment.

Adapted from Jackson 2018, *Int J Mol Sci*.

production of pro-inflammatory cytokines that can exacerbate ROS production and cell death in regions key to cognitive function such as the prefrontal cortex and hippocampus (Figure 10) [2]. AT1R upregulation in cortical and hippocampal M1-like microglia is linked to both neuroinflammation and cognitive impairment in rodents [2].

4.2 Angiotensin II type 2 receptor (AT2R)

AT2Rs are also undetectable in healthy microglia, but rapidly upregulated as part of a pro-inflammatory response [30]. AT2Rs are usually upregulated with AT1Rs as a compensatory mechanism, but this paired upregulation has been shown to be blunted in aging [30]. We suspect that this may also be the case in conditions such as diabetes and PSCI. AT2R signaling facilitates enhanced cognition, cell survival, synaptic maintenance and have both antioxidant and anti-inflammatory properties (Figure 10) [30]. Cell surface and intracellular signalling suppress ROS [30]. Additionally, intracellular activation of AT2Rs leads to the further upregulation of AT2Rs and shifts the microglia toward a M2-like phenotype. This also leads to the production of anti-inflammatory cytokines and the upregulation of phagocytic receptors [30]. Additionally, upon M2 microglia polarization, mBDNF production is enhanced to promote cell survival and synaptic plasticity [30].

4.2.1 Brain-derived neurotrophic factor (BDNF)

BDNF is a major neurotrophin found in all cell types. BDNF has two major forms; proBDNF and a cleaved form, mBDNF. Abnormally low mBDNF to proBDNF ratios are associated with cognitive disorders [30, 73]. The neuroprotective effects of ARBs and AT2R agonism are associated with increased mBDNF release [30]. Within microglia, BDNF promotes synaptic plasticity through pruning as well as learning-related synapse formation [30]. Upon M2 polarization, microglial-derived BDNF production increases, accounting for 80% of microglia-derived BDNF production [30]. This leads us to believe that AT2R stimulation may enhance BDNF

production to improve cognition by promoting cell survival and exerting antioxidant and anti-inflammatory effects [30].

4.2.2 Compound 21 (C21)

Our lab and others have shown that the effects of ARBs are mediated through the blockage of the AT1R which leads to the activation of the AT2R, due to the increased amount of unbound Ang II able to bind to the AT2R [30, 56]. C21 is a selective AT2R agonist and has been shown by multiple laboratories to ameliorate ischemic damage in different models of MCAO [30, 56, 74-78]. Our lab has shown that a single dose of C21, given at reperfusion or up to 24 hours after is neurovascular protective and improves stroke outcome with no effect on blood pressure in rats [30, 56, 74, 77]. It has recently been shown to mediate some of its neuroprotective effects through increases in BDNF after stroke [30, 79]. It has also been shown to downregulate activated microglia [56, 77]. C21 administration has additionally been shown to prevent cognitive decline when administered for 4 weeks in a mouse model of diabetes and rat models of hypertension [30, 56, 77, 80]. Taken together this leads us to believe that therapeutic intervention with delayed administration of C21 post-stroke in diabetic rats may modulate microglia polarization to alleviate cognitive deficits.

5. Problem Statement and Specific Aims

5.1 Specific Aims

Stroke is an important cause of adult disability in the United States, leaving more than 60% of its victims struggling to perform daily activities. One of the most disabling consequences of stroke is cognitive impairment, occurring in 12%-48% of patients, for which there is NO therapy. At a time when stroke mortality is decreasing due to advancements in therapy, the rate of post-stroke cognitive impairment (PSCI) has almost doubled since 1990. This increases the urgency for treatment development in this area. A critical barrier to progress in the development of new therapeutic strategies is the lack of understanding of how PSCI develops. While 70% of stroke victims present with comorbid diseases such as diabetes and hypertension, the limited use of comorbid disease models in preclinical research further contributes to the lack of progress. The goal of this translational proposal is to address this gap by 1) elucidating mechanisms contributing to the evolution of PSCI using a clinically relevant model of diabetes, a major risk factor for stroke and cognitive impairment, and 2) developing angiotensin II type 2 receptor (AT2R) agonism as a therapeutic target.

Microglia are the resident immune cells of the brain and their polarization toward a pro-inflammatory M1 and away from anti-inflammatory M2 phenotype initiates the inflammatory cascade. Comorbid diseases such as diabetes and hypertension may pre-dispose stroke victims to M1 hyper-activation and block injury resolution leading to chronic neuroinflammation that progressively perpetuates cognitive impairment. We hypothesize that diabetes will exacerbate the development of PSCI through chronic activation of microglia into a pro-inflammatory M1

phenotype, and that AT2R stimulation will attenuate PSCI by decreasing the pro(M1)/anti(M2) inflammatory balance. This hypothesis is built upon the following scientific premise and past findings in the Ergul and Fagan laboratories. AT2R agonism has additionally been shown to enhance cognition and downregulate M1 activation independent of changes in blood pressure [74]. Our studies suggest that 1) while control rats recover from stroke-induced cognitive deficits, diabetic rats do not improve; 2) stroke promotes profound microglial activation, 3) modulation of AT2R is restorative post-stroke in control rats.

Hypothesis

The central hypothesis of this study is that diabetes will exacerbate the development of PSCI through chronic activation of microglia into a pro-inflammatory M1 phenotype, and that AT2R stimulation will attenuate PSCI by decreasing the pro(M1)/anti(M2) inflammatory balance. This hypothesis will be addressed in two Aims:

Specific Aim 1: Determine whether the accumulation of cognitive deficits post-stroke is augmented in diabetes and if it can be therapeutically targeted.

We will test the hypothesis that:

1. Diabetes exacerbates the progressive development of PSCI.
2. AT2R agonist C21 can ameliorate the evolution of PSCI in diabetic rats.

Specific Aim 2: Determine whether sustained pro-inflammatory microglia activation is the underlying mechanism of PSCI in diabetes. We will test the hypothesis that:

1. Chronic pro-inflammatory microglia activation is correlated with the enhanced development of PSCI in diabetic rats.
2. AT2R agonist C21 can downregulate the M1:M2 ratio in (A) diabetic rats as well as (B) rodent microglia cells.
3. Microglia knockdown will prevent the progressive development of PSCI.

References

1. Levine, D.A., et al., *Trajectory of Cognitive Decline After Incident Stroke*. JAMA, 2015. **314**(1): p. 41-51.
2. Shukla, V., et al., *Cerebral ischemic damage in diabetes: an inflammatory perspective*. J Neuroinflammation, 2017. **14**(1): p. 21.
3. Writing Group, M., et al., *Executive Summary: Heart Disease and Stroke Statistics--2016 Update: A Report From the American Heart Association*. Circulation, 2016. **133**(4): p. 447-54.
4. Sekerdag, E., I. Solaroglu, and Y. GURSOY-OZDEMIR, *Cell Death Mechanisms in Stroke and Novel Molecular and Cellular Treatment Options*. Curr Neuropharmacol, 2018. **16**(9): p. 1396-1415.
5. Mohr, J.P., et al., *American Heart Association Prevention Conference. IV. Prevention and Rehabilitation of Stroke. Etiology of stroke*. Stroke, 1997. **28**(7): p. 1501-6.
6. Liang, D., et al., *Cytotoxic edema: mechanisms of pathological cell swelling*. Neurosurg Focus, 2007. **22**(5): p. E2.
7. Ernst, A.S., et al., *EphB2-dependent signaling promotes neuronal excitotoxicity and inflammation in the acute phase of ischemic stroke*. Acta Neuropathol Commun, 2019. **7**(1): p. 15.
8. Myles R. McCrary, S.W., and Ling Wei, *Ischemic Stroke Mechanisms, Prevention, and Treatment: The Anesthesiologist's Perspective*. J Anesth Perioper Med, 2017. **4**: p. 76-86.
9. Filosa, J.A., et al., *Beyond neurovascular coupling, role of astrocytes in the regulation of vascular tone*. Neuroscience, 2016. **323**: p. 96-109.
10. Milton, M. and P.D. Smith, *It's All about Timing: The Involvement of Kir4.1 Channel Regulation in Acute Ischemic Stroke Pathology*. Front Cell Neurosci, 2018. **12**: p. 36.
11. Hartings, J.A., et al., *The continuum of spreading depolarizations in acute cortical lesion development: Examining Leao's legacy*. J Cereb Blood Flow Metab, 2017. **37**(5): p. 1571-1594.
12. Dreier, J.P., et al., *Spreading depolarization is not an epiphenomenon but the principal mechanism of the cytotoxic edema in various gray matter structures of the brain during stroke*. Neuropharmacology, 2018. **134**(Pt B): p. 189-207.
13. Farkas, E. and F. Bari, *Spreading depolarization in the ischemic brain: does aging have an impact?* J Gerontol A Biol Sci Med Sci, 2014. **69**(11): p. 1363-70.
14. Kimelberg, H.K., *Water homeostasis in the brain: basic concepts*. Neuroscience, 2004. **129**(4): p. 851-60.
15. Iadecola, C., *The Neurovascular Unit Coming of Age: A Journey through Neurovascular Coupling in Health and Disease*. Neuron, 2017. **96**(1): p. 17-42.
16. Filosa, J.A. and J.A. Iddings, *Astrocyte regulation of cerebral vascular tone*. Am J Physiol Heart Circ Physiol, 2013. **305**(5): p. H609-19.
17. Filosa, J.A., et al., *Local potassium signaling couples neuronal activity to vasodilation in the brain*. Nat Neurosci, 2006. **9**(11): p. 1397-1403.
18. Dreier, J.P. and C. Reiffurth, *The stroke-migraine depolarization continuum*. Neuron, 2015. **86**(4): p. 902-922.

19. Ayata, C. and M. Lauritzen, *Spreading Depression, Spreading Depolarizations, and the Cerebral Vasculature*. *Physiol Rev*, 2015. **95**(3): p. 953-93.
20. Szalay, G., et al., *Microglia protect against brain injury and their selective elimination dysregulates neuronal network activity after stroke*. *Nat Commun*, 2016. **7**: p. 11499.
21. Fabricius, M., et al., *Cortical spreading depression and peri-infarct depolarization in acutely injured human cerebral cortex*. *Brain*, 2006. **129**(Pt 3): p. 778-90.
22. Szondy, Z., et al., *Anti-inflammatory Mechanisms Triggered by Apoptotic Cells during Their Clearance*. *Front Immunol*, 2017. **8**: p. 909.
23. Dixon, S.J., et al., *Ferroptosis: an iron-dependent form of nonapoptotic cell death*. *Cell*, 2012. **149**(5): p. 1060-72.
24. Magtanong, L. and S.J. Dixon, *Ferroptosis and Brain Injury*. *Dev Neurosci*, 2019: p. 1-14.
25. Wu, J.R., Q.Z. Tuo, and P. Lei, *Ferroptosis, a Recent Defined Form of Critical Cell Death in Neurological Disorders*. *J Mol Neurosci*, 2018. **66**(2): p. 197-206.
26. Wang, P., et al., *Autophagy in ischemic stroke*. *Prog Neurobiol*, 2018. **163-164**: p. 98-117.
27. DiSabato, D.J., N. Quan, and J.P. Godbout, *Neuroinflammation: the devil is in the details*. *J Neurochem*, 2016. **139 Suppl 2**: p. 136-153.
28. Ward, R., et al., *Post Stroke Cognitive Impairment and Hippocampal Neurovascular Remodeling: The Impact of Diabetes and Sex*. *Am J Physiol Heart Circ Physiol*, 2018.
29. Zhao, S.C., et al., *Regulation of microglial activation in stroke*. *Acta Pharmacol Sin*, 2017. **38**(4): p. 445-458.
30. Jackson, L., et al., *Within the Brain: The Renin Angiotensin System*. *Int J Mol Sci*, 2018. **19**(3).
31. Hu, X., et al., *Microglia/macrophage polarization dynamics reveal novel mechanism of injury expansion after focal cerebral ischemia*. *Stroke*, 2012. **43**(11): p. 3063-70.
32. Ceulemans, A.G., et al., *The dual role of the neuroinflammatory response after ischemic stroke: modulatory effects of hypothermia*. *J Neuroinflammation*, 2010. **7**: p. 74.
33. Mozaffarian, D., et al., *Heart disease and stroke statistics--2015 update: a report from the American Heart Association*. *Circulation*, 2015. **131**(4): p. e29-322.
34. Mijajlovic, M.D., et al., *Post-stroke dementia - a comprehensive review*. *BMC Med*, 2017. **15**(1): p. 11.
35. Sun, J.H., L. Tan, and J.T. Yu, *Post-stroke cognitive impairment: epidemiology, mechanisms and management*. *Ann Transl Med*, 2014. **2**(8): p. 80.
36. Gorelick, P.B., et al., *Vascular contributions to cognitive impairment and dementia: a statement for healthcare professionals from the american heart association/american stroke association*. *Stroke*, 2011. **42**(9): p. 2672-713.
37. Hainsworth, A.H., et al., *Translational models for vascular cognitive impairment: a review including larger species*. *BMC Med*, 2017. **15**(1): p. 16.
38. Douiri, A., A.G. Rudd, and C.D. Wolfe, *Prevalence of poststroke cognitive impairment: South London Stroke Register 1995-2010*. *Stroke*, 2013. **44**(1): p. 138-45.
39. Mellon, L., et al., *Cognitive impairment six months after ischaemic stroke: a profile from the ASPIRE-S study*. *BMC Neurology*, 2015. **15**(1): p. 31.
40. Hofman, A., et al., *The Rotterdam Study: 2010 objectives and design update*. *Eur J Epidemiol*, 2009. **24**(9): p. 553-72.

41. Ott, A., et al., *Prevalence of Alzheimer's disease and vascular dementia: association with education. The Rotterdam study.* BMJ, 1995. **310**(6985): p. 970-3.
42. Kokmen, E., et al., *Dementia after ischemic stroke: a population-based study in Rochester, Minnesota (1960-1984).* Neurology, 1996. **46**(1): p. 154-9.
43. Allan, L.M., et al., *Long term incidence of dementia, predictors of mortality and pathological diagnosis in older stroke survivors.* Brain, 2011. **134**(Pt 12): p. 3716-27.
44. Jellinger, K.A., *The pathology of "vascular dementia": a critical update.* J Alzheimers Dis, 2008. **14**(1): p. 107-23.
45. Stranahan, A.M., et al., *Diabetes impairs hippocampal function through glucocorticoid-mediated effects on new and mature neurons.* Nat Neurosci, 2008. **11**(3): p. 309-17.
46. Ergul, A., et al., *Cerebral neovascularization in diabetes: implications for stroke recovery and beyond.* J Cereb Blood Flow Metab, 2014. **34**(4): p. 553-63.
47. Qiu, C., et al., *Medial temporal lobe is vulnerable to vascular risk factors in men: a population-based study.* Eur J Neurol, 2012. **19**(6): p. 876-83.
48. Kalaria, R.N., R. Akinyemi, and M. Ihara, *Stroke injury, cognitive impairment and vascular dementia.* Biochimica et biophysica acta, 2016. **1862**(5): p. 915-925.
49. Chen, A., et al., *Multiplex analyte assays to characterize different dementias: brain inflammatory cytokines in poststroke and other dementias.* Neurobiol Aging, 2016. **38**: p. 56-67.
50. Zekry, D., et al., *The vascular lesions in vascular and mixed dementia: the weight of functional neuroanatomy.* Neurobiol Aging, 2003. **24**(2): p. 213-9.
51. Zi, W., D. Duan, and J. Zheng, *Cognitive impairments associated with periventricular white matter hyperintensities are mediated by cortical atrophy.* Acta Neurol Scand, 2014. **130**(3): p. 178-87.
52. Kooistra, M., et al., *Vascular brain lesions, brain atrophy, and cognitive decline. The Second Manifestations of ARterial disease--Magnetic Resonance (SMART-MR) study.* Neurobiol Aging, 2014. **35**(1): p. 35-41.
53. Chen, A., et al., *Frontal white matter hyperintensities, clasmotodendrosis and gliovascular abnormalities in ageing and post-stroke dementia.* Brain, 2016. **139**(Pt 1): p. 242-58.
54. Jokinen, H., et al., *Brain atrophy accelerates cognitive decline in cerebral small vessel disease: the LADIS study.* Neurology, 2012. **78**(22): p. 1785-92.
55. Ergul, A., et al., *Impact of Comorbidities on Acute Injury and Recovery in Preclinical Stroke Research: Focus on Hypertension and Diabetes.* Transl Stroke Res, 2016. **7**(4): p. 248-60.
56. Ahmed, H.A., et al., *RAS modulation prevents progressive cognitive impairment after experimental stroke: a randomized, blinded preclinical trial.* J Neuroinflammation, 2018. **15**(1): p. 229.
57. Li, W., et al., *Diabetes Worsens Functional Outcomes in Young Female Rats: Comparison of Stroke Models, Tissue Plasminogen Activator Effects, and Sexes.* Transl Stroke Res, 2017.
58. Wang, L.Y., et al., *Huoluo Yinao decoction mitigates cognitive impairments after chronic cerebral hypoperfusion in rats.* J Ethnopharmacol, 2019. **238**: p. 111846.

59. Ben-Ari, H., et al., *White matter lesions, cerebral inflammation and cognitive function in a mouse model of cerebral hypoperfusion*. Brain Res, 2019. **1711**: p. 193-201.
60. Hardigan, T., R. Ward, and A. Ergul, *Cerebrovascular complications of diabetes: focus on cognitive dysfunction*. Clin Sci (Lond), 2016. **130**(20): p. 1807-22.
61. Ergul, A., et al., *Cerebrovascular complications of diabetes: focus on stroke*. Endocr Metab Immune Disord Drug Targets, 2012. **12**(2): p. 148-58.
62. Wang, Q., et al., *Prediabetes is associated with post-stroke cognitive impairment in ischaemic stroke patients*. Brain Res, 2018. **1687**: p. 137-143.
63. Fukasawa, R., et al., *Identification of diabetes-related dementia: Longitudinal perfusion SPECT and amyloid PET studies*. J Neurol Sci, 2015. **349**(1-2): p. 45-51.
64. Peila, R., et al., *Type 2 diabetes, APOE gene, and the risk for dementia and related pathologies: The Honolulu-Asia Aging Study*. Diabetes, 2002. **51**(4): p. 1256-62.
65. Korf, E.S., et al., *Brain aging in very old men with type 2 diabetes: the Honolulu-Asia Aging Study*. Diabetes Care, 2006. **29**(10): p. 2268-74.
66. Ladonya Jackson, W.L., Yasir Abdul, Guangkuo Dong, Babak Baban, Adviye Ergul, *Diabetic Stroke Promotes a Sexually Dimorphic Expansion of T Cells*. NeuroMolecular Medicine 2019. **In Press**(71).
67. Ward, R., et al., *NLRP3 inflammasome inhibition with MCC950 improves diabetes-mediated cognitive impairment and vasoneuronal remodeling after ischemia*. Pharmacol Res, 2019. **142**: p. 237-250.
68. Jing, L., et al., *Temporal profile of astrocytes and changes of oligodendrocyte-based myelin following middle cerebral artery occlusion in diabetic and non-diabetic rats*. Int J Biol Sci, 2013. **9**(2): p. 190-9.
69. Ma, S., et al., *Diabetes Mellitus Impairs White Matter Repair and Long-Term Functional Deficits After Cerebral Ischemia*. Stroke, 2018. **49**(10): p. 2453-2463.
70. Ergul, A., et al., *Cellular connections, microenvironment and brain angiogenesis in diabetes: Lost communication signals in the post-stroke period*. Brain Res, 2015. **1623**: p. 81-96.
71. Ott, A., et al., *Diabetes mellitus and the risk of dementia: The Rotterdam Study*. Neurology, 1999. **53**(9): p. 1937-42.
72. Prakash, R., et al., *Vascularization pattern after ischemic stroke is different in control versus diabetic rats: relevance to stroke recovery*. Stroke, 2013. **44**(10): p. 2875-82.
73. Carlino, D., M. De Vanna, and E. Tongiorgi, *Is altered BDNF biosynthesis a general feature in patients with cognitive dysfunctions?* Neuroscientist, 2013. **19**(4): p. 345-53.
74. Alhusban, A., et al., *Compound 21 is pro-angiogenic in the brain and results in sustained recovery after ischemic stroke*. J Hypertens, 2015. **33**(1): p. 170-80.
75. Ahmed, H.A., et al., *Role of angiotensin system modulation on progression of cognitive impairment and brain MRI changes in aged hypertensive animals - A randomized double-blind pre-clinical study*. Behav Brain Res, 2017.
76. Fouda, A.Y., et al., *Role of interleukin-10 in the neuroprotective effect of the Angiotensin Type 2 Receptor agonist, compound 21, after ischemia/reperfusion injury*. Eur J Pharmacol, 2017. **799**: p. 128-134.

77. Ahmed, H.A., et al., *Angiotensin receptor (AT2R) agonist C21 prevents cognitive decline after permanent stroke in aged animals-A randomized double-blind pre-clinical study*. Behav Brain Res, 2018.
78. Ishrat, T., et al., *Dose-response, therapeutic time-window and tPA-combinatorial efficacy of compound 21: A randomized, blinded preclinical trial in a rat model of thromboembolic stroke*. J Cereb Blood Flow Metab, 2018: p. 271678X18764773.
79. Schwengel, K., et al., *Angiotensin AT2-receptor stimulation improves survival and neurological outcome after experimental stroke in mice*. J Mol Med (Berl), 2016. **94**(8): p. 957-66.
80. Iwanami, J., et al., *Possible synergistic effect of direct angiotensin II type 2 receptor stimulation by compound 21 with memantine on prevention of cognitive decline in type 2 diabetic mice*. Eur J Pharmacol, 2014. **724**: p. 9-15.

CHAPTER 2

DELAYED ADMINISTRATION OF ANGIOTENSIN II TYPE 2 RECEPTOR (AT2R) AGONIST COMPOUND 21 PREVENTS THE DEVELOPMENT OF POST-STROKE COGNITIVE IMPAIRMENT IN DIABETES THROUGH THE MODULATION OF MICROGLIA POLARIZATION¹

¹ Jackson L, Dong G, Althomali W, Sayed M, Eldahshan W, Baban B, Johnson M, Filosa J, Fagan S.C, Ergul A. Submitted to [*Translational Stroke Research*], [June 15 2019]

Abstract

A disabling consequence of stroke is cognitive impairment, occurring in 12%-48% of patients, for which there is no therapy. A critical barrier is the lack of understanding of how post-stroke cognitive impairment (PSCI) develops. While 70% of stroke victims present with comorbid diseases such as diabetes and hypertension, the limited use of comorbid disease models in preclinical research further contributes to this lack of progress. To this end, we used a translational model of diabetes to study the development of PSCI. In addition, we evaluated the application of compound 21 (C21), an angiotensin II Type 2 receptor agonist, for the treatment of PSCI by blinding the treatment assignment, setting strict inclusion criteria and implementing a delayed administration time point.

Methods: Diabetes was induced by a high fat diet (HFD) and low dose streptozotocin (STZ) combination. Control and diabetic rats were subjected to 1 hr middle cerebral artery occlusion (MCAO) or sham surgery. Adhesive removal task (ART) and 2-trial Y-maze were utilized to test sensorimotor and cognitive function. 3 days post-stroke, rats that met the inclusion criteria were administered C21 or vehicle in drinking water at a dose of 0.12 mg/kg/day for 8 weeks. Samples from freshly harvested brains were analyzed by flow cytometry and immunohistochemistry (IHC).

Results: Diabetes exacerbated the development of PSCI and increased inflammation and demyelination of the hippocampus. Delayed administration of C21 3 days post-stroke improved mortality, sensorimotor and cognitive deficits. It also improved inflammation and myelination through modulation of the M1:M2 ratio within the diabetic animals, while increasing macrophage infiltration within the control animals.

Introduction

Stroke is the leading cause of long-term disability worldwide, with the onset of cognitive impairment being a frequent contributor [1]. Vascular cognitive impairment and dementia (VCID) is the second most common cause of cognitive decline [2]. Post-stroke cognitive impairment (PSCI) is a type of VCID which is characterized by the progressive worsening of cognition, and 25-30% of stroke survivors develop it within the first 3 months after stroke [3]. With a large advancement in recanalization procedures, more patients are surviving stroke events. In the United States, stroke-related deaths show a steady decline each year, with a greater decline observed among people aged ≥ 65 (by 54.1%) than their younger counterparts (by 45.9 - 53.6%) [3]. In 2018, the time by which eligible patients can be selected for recanalization therapy was extended to 24 hours after initial stroke symptoms. This has and will continue to lead to more stroke victims receiving life-saving recanalization therapies. As a result, more surviving patients may also develop long-term disabilities, such as PSCI. This has resulted in an urgent need to discover possible therapeutic interventions. Unfortunately, poor understanding of how PSCI develops coupled with the incomplete modeling of PSCI in the laboratory setting poses a barrier for the development of new strategies and treatments. Our lab has shown that although there are acute cognitive deficits after stroke, young healthy male rats recover within 2 weeks [4, 5]. Diabetic rats, however, remain cognitively impaired at 2 weeks, making the first goal of this paper to discover the long-term effect of diabetes after stroke, in a clinically translational model of PSCI.

More than 40% of stroke victims present with pre-existing diabetes at the time of stroke. In fact, the risk of stroke is up to 2-6 fold greater in diabetic patients [6, 7]. Diabetes not only increases the risk of stroke, but also the severity of cognitive impairment [5]. In a large clinical

trial, the Rotterdam study, diabetes was associated with a 2-fold increased prevalence of vascular cognitive impairment (VCI) [6, 8]. Cognitive impairment after stroke is greatly understudied, partly due to the fact that the majority of laboratories utilize young and otherwise healthy male animals as previously described. The majority of patients present at the time of stroke with comorbid vascular risk factors, making studying PSCI in a comorbid disease model absolutely essential [9]. Utilizing a clinically relevant high fat diet (HFD)/ low dose streptozotocin (STZ) model, we evaluated the impact of diabetes on long-term cognition up to 8 weeks after a stroke.

Neuroinflammation has been linked to the development of cognitive impairment. Increased microglia activation, reactive astrocytes and white matter damage have all been associated with the development of cognitive impairment [10-12]. Diabetes, as a chronic inflammatory disease, also exhibits these same features [5, 13]. Our lab has shown that diabetes increases the amount of activated microglia as well as the amount of pro-inflammatory immune cells within both the blood and the brain of HFD/STZ animals [5, 14]. Although it is known that diabetes perpetuates neuroinflammation, it is not yet fully understood how diabetes impacts the microglia phenotype or chronic stroke recovery in an animal model. Microglia are the resident immune cells of the brain and have a major role in modulating neuroinflammation. Upon activation, they exist as two broadly classified phenotypes referred to as 'M1' or 'M2' [15]. Although M2 consists of many sub-types, overall they promote immune suppression, injury resolution and participate in phagocytosis and matrix maintenance [15]. M1 on the other hand, promotes the release of pro-inflammatory cytokines and recruitment of peripheral inflammatory cells [15]. Microglia have a relatively low turnover rate making them susceptible to pro-inflammatory effects of age, injury or stress, making the second goal of this study to discover how

diabetes impacts the M1:M2 ratio and inflammation within the diabetic brain, and how these alterations impact cognition.

After establishing a clinically translational model of PSCI and elucidating the key pathogenic mechanisms contributing to its development, we evaluated a potential therapeutic for disease intervention. In a blinded manner we evaluated the impact of a delayed administration of a therapeutic currently in clinical trials, compound 21 (C21). Our lab and others have shown that the effects of angiotensin receptor blockers (ARBs) are mediated through the blockage of the angiotensin II type I receptor (AT1R) which leads to the activation of the angiotensin type 2 receptor (AT2R), due to the increased amount of unbound Ang II able to bind to the AT2R [15, 16]. C21 is a selective AT2R agonist and has been shown by multiple laboratories to ameliorate ischemic damage in different models of MCAO [15, 17-21]. Our lab has shown that a single dose of C21, given at reperfusion, is neurovascular protective and improves stroke outcome with no effect on blood pressure in rats [15, 17]. It has recently been shown to mediate some of its neuroprotective effects through increases in brain-derived neurotrophic factor (BDNF) after stroke [15, 22]. It has also been shown to downregulate activated microglia, suggesting that therapeutic intervention with delayed administration of C21 post-stroke in diabetic rats may modulate microglia polarization to alleviate cognitive deficits. [16, 20]. Taken together, this led us to believe that therapeutic intervention with delayed administration of C21 post-stroke in diabetic rats may modulate microglia polarization to alleviate cognitive deficits. The third goal of this study was to evaluate whether C21 can attenuate PSCI and the mechanism by which it exerts its effect.

Methods

Animal model

Male Wistar rats (Envigo RMS, Inc., Indianapolis, IN) were housed in the animal care facility at Augusta University, which is approved by the American Association for Accreditation of Laboratory Animal Care. All experiments were conducted in accordance with the National Institute of Health (NIH) guidelines for the care and use of animals in research. Furthermore, all protocols were approved by the institutional animal care and use committee.

Middle Cerebral Artery Occlusion (MCAO) surgery

Male control and diabetic animals were subjected to transient focal cerebral ischemia (60 min MCAO) or sham surgery at 12-15 weeks of age using 4-0 silicon-coated nylon suture (Doccol 403756 or 403534), depending on the rat size. The animals that weighed 350g-425g received the 403756 suture, while animals weighing 300-350g received the 403534. This was optimized prior to the start of the study to result in similar infarct sizes across weight ranges. The animals were anesthetized using 2-5% isoflurane, a ventral mid-line neck incision was made, the right common carotid artery (CCA) was exposed and lightly tied, and the external carotid artery (ECA) was ligated and cut. The suture was marked at 1.8 and 2 mm then advanced from a nick at the ECA into the internal carotid artery (ICA) until positioned in-between the 1.8 and 2-mm marks, indicating the branching of the MCA. The suture was tied in place for the duration of the occlusion and the animals were allowed to recover from anesthesia. At the end of the 60-minute occlusion time, the animals were re-anesthetized, the suture was removed for reperfusion and the small nick at the ECA was permanently ligated. In

sham surgeries, the CCA was isolated and the ECA was cut and ligated without insertion of the suture. This led to a total of 6 groups: control sham (C sham, N=6), diabetic sham (D sham, N=5), control MCAO vehicle treatment (C veh N=6), diabetic MCAO vehicle treatment (D veh, N=7), control MCAO C21 treatment (C C21, N=7), diabetic MCAO vehicle treatment (D C21, N=6). In the post-operative period, blood glucose (BG) was monitored daily for 7 days and then weekly until 8 weeks.

Treatment and behavioral assessments

Dose and timing justification:

We chose Day 3 to start administering C21 because it is well out of the neuroprotective window of 6 hours and acute infarct evolution is likely to be complete. We chose an 8-week follow-up in an attempt to capture the progressive development of PSCI over time. The oral dose of 0.12 mg/kg was calculated based on an oral bioavailability of 0.25, so is equivalent to the intravenous (IV) dose of 0.03 mg/kg [17].

Blinding and randomization:

The treatment and vehicle groups were prepared by an individual not involved in the surgery or assessments and labeled as group A and group B. Each animal was numbered before baseline behavioral assessments were taken. After MCAO surgery, the animals that met the pre-set inclusion criteria were assigned to group A and B using a random number generator. All behavioral and histological assessments were coded and conducted by a blinded investigator. Drinking water groups were also blinded.

Inclusion criteria

In order to ensure inclusion of animals with a significant degree of ischemic injury, we implemented strict inclusion criteria. The inclusion criteria included assessment of sensorimotor function and weight loss. 3 days after MCAO, animals underwent the adhesive removal task (ART). Animals that had an ART above 30 seconds and had more than 11% weight loss were randomly assigned into C21 treatment and vehicle treatment groups.

Assessment of sensorimotor function:

Sensorimotor function was evaluated by composite neurological score and ART as previously described [23]. The composite score was comprised of the beam walk and Modified-Bederson score and was taken at baseline, day 3 and weeks 1, 2, 4, and 8 post-stroke. The Modified-Bederson score was comprised of circling bias, forelimb retraction, hind-limb retraction and resistance to push. Circling bias measures spontaneous ipsilateral circling 2 (best) to 0 (worst). For forelimb and hindlimb retraction, each limb was displaced laterally and the ability to recover the replaced limb was measured 1 (best) to 0 (worst). Resistance to push was scored as 1 (resistance) to 0 (no resistance). The animals were trained on the beam walk for 4 days prior to baseline assessments. Animals were given a score from 7 (best) to 1 (worst) based on their balance on a horizontal beam as described previously [24]. For the ART, the animals were trained for 4 days and then baseline measurements were recorded prior to stroke. 3 days post-stroke measurements were recorded to determine eligibility for inclusion in the study. If the rat was included in the study, then subsequent ART measurements were recorded at weeks 1, 2, 4, and 8 post-stroke. ART was carried out as previously described with modification [25]. Contact and removal latency of the adhesive paper dot was recorded and the average was taken from 3 trials with a maximum removal latency of 180 seconds per trial.

Assessment of cognitive function:

Cognition was assessed by the 2 trial Y-maze. The animals were trained 4 days prior to baseline testing. Testing was conducted at baseline prior to stroke, followed by weeks 1, 2, 4, and 8 post-stroke. The 2 trial Y-maze was used to examine spatial memory. In the first trial, animals were allowed to freely explore 2 open arms for 10 mins. The animal was returned to its home cage for a 15 min delay. In the second trial, animals were allowed to explore all 3 arms of the Y-maze apparatus freely for 3 mins. Total time spent in each arm was recorded. Results were expressed as % time spent in the novel arm (time in novel arm divided by total time in all arms x 100).

Euthanasia, specimen collection and molecular techniques

Animals were euthanized 8 weeks post-stroke or sham surgery using isoflurane overdose and cardiac puncture. Sections of the prefrontal cortex (PFC) and the hippocampus (Hipp) were taken for flow cytometric and immunocytochemistry.

Flow cytometry

The PFC and Hipp were isolated through separation of the B and D slice as indicated and figure 2.3A. The tissue was then minced into 1 mm³ pieces and was dissociated using Worthington's Papain Dissociation kit (catalog number LK003153) with the following modifications: 1) tissue was left in dissociation medium for 15–25 minutes and 2) oxygen was continuously perfused over (not bubbled within) the solution for the duration of the incubation period [26]. Microglia were isolated as described below.

Myelin debris removal and microglial isolation

A debris removal step was performed using modified protocols from Miltenyi Biotec's Myelin Removal Kit (catalog number (Miltenyi Biotec, Germany) and CD11b⁺ Microbeads (Miltenyi Biotec, Germany). Following dissociation, up to 10⁷ cells were suspended in 200 μL 0.5% BSA in PBS buffer and incubated with 20 μL anti-myelin microbeads for 15 mins at 4°C. The cells were then placed in the mini-MACS magnetic separator column and the clean supernatant was eluted out. The cells were then incubated with 20 uL of CD11b⁺ beads to isolate the microglia/macrophage population and isolated using the mini-MACS separator once again. CD11b⁺ cells were then further processed with surface and intracellular microglia makers.

Cellular staining

Cells were incubated with surface markers against pre-conjugated antibodies CD45-APC (ebioscience, San Diego, CA) and CD86-FITC (BD bioscience, San Jose, CA) for 20 minutes. Cells were then permeabilized for intracellular staining with a fixation/permeabilization solution kit (ebioscience, San Diego, CA). Cells were then separated into two groups and incubated with markers CD206 (Abcam, Cambridge, MA) or TNFα (BD bioscience, San Jose, CA) and TMEM119 (Novus, Centennial, CO). Secondary antibodies PE (ebioscience, San Diego, CA) and PerCP (BD bioscience, San Jose, CA) were used in both groups. Cells were then washed and analyzed using the Cytoflex (Beckman Coulter, Indianapolis, Indiana).

Imaging and analysis

To minimize false-positive events, the number of positive events detected with the negative staining control for each individual channel was subtracted from the number of positive cells stained with corresponding antibodies. Cells expressing a specific marker were reported as a percentage of the number of gated events. The gating strategy is shown in Table

1. Microglia were first identified as CD11b⁺ /CD45⁺ low. M1 microglia were further identified as CD86⁺, M2 cells were identified as CD206⁺. Residential microglia versus infiltrating macrophages were also identified as CD11b⁺/CD45⁺ without separation of low versus high. Residential microglia were then further identified as TMEM119⁺, while infiltrating macrophages were identified as TMEM119⁻. M1 macrophages were then identified as CD11b⁺/ CD45⁺/TMEM119⁻ /CD86⁺/TNFα⁺ cells.

Immunohistochemistry (IHC)

Brains were extracted and post-fixed in 4% PFA overnight. The B and D slices were derived as according to figure 2.3A. Free-floating 30 um sections were incubated overnight with anti-IBA-1 (Ionized calcium-binding adaptor molecule 1, 1:500, Wako, Japan) and anti-GFAP (Glial fibrillary acidic protein, 1:400, Sigma-Aldrich, Burlington, MA) for D slice sections containing the Hipp and with anti-MBP (Myelin Basic Protein, 1:100, Abcam, Cambridge, MA) and NF200 (Neurofilament, 1:1000, Abcam, Cambridge, MA) for the B slice containing the PFC. Cells were then incubated with Texas red and Alexa Flour 488-conjugated secondary antibodies (Cell Signaling Technology, Danvers, MA, USA) used at 1:200 for 2 h at room temperature. Nuclei were counterstained using Dapi (406-diamidino-2-phenylindole, Roche Basel, Switzerland) and sections were mounted. Imaging was performed using the Keyence Microscope (Itasca, IL) and Z stacked through the 30-um thickness at a 1-um pitch to obtain a complete count of the tissue area for IBA-1 and GFAP quantifications. Sections were derived from a single plane for MBP and NF200 quantifications.

Cell Culture

The direct effect of C21 on microglia polarization was determined in mouse cells (BV-2 line) by flow cytometry-based analysis of polarization markers. Cells were treated with LPS

(Lipopolysaccharide, 100 ng/ml) and IFN γ (interferon γ , 20 ng/ml) to induce activation and M1-like polarization. Cells were either pre-treated with C21 (100 nM), 6 hours prior, or post-treated, 6 hours post- LPS/IFN γ exposure to evaluate whether C21 impacts activation and polarization by preventing (pre-treatment) or reversing (post-treatment) M1-like polarization. The AT2R blocker, PD 123319 (0.1 μ M), was used to determine if the C21 effects were mediated through AT2R agonism.

Statistical Analyses

Statistical Analysis Software (SAS) software was used to analyze all behavioral data. Prism 7 was used to analyze all molecular data. Repeated ANOVAs were performed for measurements taken across time utilizing the last observation carried forward method for any missing data. Two-way ANOVAs were used to either compare (Control C vs Diabetes D) x (Sham vs Stroke) or (Control C vs Diabetes D) x (Veh vs C21), as indicated within the figure legends. Student's t test was used to compare 2 groups. The degree of significance was marked by the number of symbols: 1 symbol indicates $p < 0.05$, 2 indicate $p < 0.01$ and 3 indicate $p < 0.001$. * is used to symbolize an effect of time, + for an effect diabetes vs control (or LPS/IFN γ vs control) and \$ for an effect of C21 vs veh as indicated on the figures.

Results

Diabetes Increases Mortality, Worsens Stroke Recovery and Chronically Upregulates Inflammation

During the acute period of stroke recovery (up to 3 days) control animals exhibited a 25%

mortality rate, while the diabetic animals exhibited a 40% mortality rate (Table 2). In an effort to ensure inclusion of animals with a significant degree of ischemic injury, a strict inclusion criteria was employed (Fig 2.S1). 3 days after the animals underwent MCAO surgery, those that met the weight loss and sensorimotor deficit criteria were included in the study. After inclusion was determined none of the control animals experienced early mortality prior to week 8, while an additional 50% of the included diabetic animals experienced early mortality, with the bulk of the deaths occurring around week 4 (Fig 2.S2). The pre-set inclusion criteria resulted in maximum deficits in ART within both the control and diabetic groups at day 3 that improved with time (Fig 2.1A, $p < 0.001$). However, diabetic animals experienced a prolonged recovery period (Fig 2.1A $^{**}p < 0.01$). The neurological score of the animals displayed a similar trend of prolonged and exacerbated sensorimotor deficits within the diabetic animals. Even though both the control animals and diabetic animals experienced a significant degree of ischemic injury, 3 days after stroke the diabetic animals had a worse neurological score than the control animals which persisted resulting in a slower rate of improvement, thus distinctly dimorphic recovery processes (Fig 2.1B, $*p < 0.05$). Overall, the diabetic animals exhibited worsened stroke recovery as measured by both ART and the neurological score when compared to the control animals.

Similar to the worsened sensorimotor deficits, diabetic animals also exhibited exacerbated cognitive deficits. Both the control and diabetic animals exhibited a progressive decline after stroke, but the diabetic animals exhibited a consistently steeper decline than control animals (Fig 2.2A, $p < 0.001$ time, 0.01 diabetes). Eight weeks after stroke, the diabetic animals were significantly more impaired compared to control animals in both animals with a stroke and sham. This indicates that diabetes chronically impairs cognition after a stroke (Fig 2.2B, $p < 0.05$).

In fact, when the baseline of each animal was compared to their cognition at week 8, the control animals declined by an average of 10.6% after a stroke, while the diabetic animals declined by an average of 27.5%, indicating that the presence of diabetes more than doubled the decline of cognition chronically after a stroke (Fig 2.2B, $p < 0.05$). The threshold of cognitive impairment was set as scoring below the % chance (0.33) that the animal would explore the novel arm for an equal time of the 3 total arms. Through this method we found that although 0% of the control sham developed cognitive impairment which increased only to 20% after a stroke, 67% of the diabetic sham group developed cognitive impairment, which increased to 100% if they experienced a stroke (Fig 2.2C, $p < 0.05$).

Since diabetes is well-known to perpetuate a chronically elevated inflammatory state systemically, we evaluated the effects of diabetes on inflammation within the central nervous system (CNS) as an explanation for the exacerbated stroke deficits observed within these animals. We acquired images throughout the B slice (Fig 2.3A) from structures of the Prefrontal Cortex (PFC) as well as the limbic system, as these structures are essential to cognition. We acquired images from the organum vasculosum of the lamina terminalis (OVLT) since this structure is without a blood brain barrier (BBB) and allows access to components of systemic circulation, such as immune cells. We observed a drastic upregulation of IBA-1⁺ cells (microglia and macrophages) and GFAP⁺ (astrocytes) cells within each of these structures compared to the control animals (Fig 2.3B-E $p < 0.05$, 0.01). We observed a trend in the upregulation in IBA-1⁺ cells that failed to reach significance in diabetic sham animals compared to control sham animals in the absence of a stroke (Fig 2.S2). We then used flow cytometry to validate this upregulation in both the B and D slice and noted an increase in the number of CD11b⁺/CD45⁺ cells, indicative of

both microglia and macrophages (Fig 2.3A). We separated the two populations, utilizing a TMEM119 residential microglia marker. We discovered that the increase derived not from an increase in microglia but in macrophages (Fig 2.3H-J, $p < 0.01$ PFC, 0.05 Hipp). Utilizing IHC, we then evaluated the D slice, particularly the hippocampus, another area of the brain essential for learning and memory, for consequences of chronic inflammation such as demyelination (Fig 2.3F). Using MBP to stain myelin and NF200 to stain the axons, we evaluated the ratio of MBP:NF200 as a measure of myelination. Diabetic animals experienced significantly reduced myelination, or demyelination, compared to control animals (Fig 2.3G, $p < 0.01$). This suggests that the chronic inflammation observed in diabetes may contribute to the chronic impairment of cognition observed through resultant demyelination of areas responsible for learning and memory, such as the hippocampus.

Delayed Administration of C21 Decreases Mortality and Improves Stroke Recovery

Three days after stroke, the diabetic animals and the control animals that met the inclusion criteria were separated into vehicle treated and C21 treated groups. The study treatments were administered in the water bottles daily, and the doses were adjusted for weight and water consumption fluctuations weekly. Chronic administration of C21 resulted in a reduction of mortality without impacting blood glucose (BG), whereas the vehicle treated diabetic animals experienced an additional 50% mortality and the C21 treated diabetic animals did not experience any further mortality (Table 3, Fig 2.S3). Day 3 C21 administration was also associated with improvements in sensorimotor abilities, as measured by ART, as early as week 1 in both control and diabetic animals (Fig 2.4A and B, $p < 0.05$, 0.001).

The administration of C21 also preserved brain tissue volume within the control and diabetic animals after a stroke (Fig 2.5C, $p < 0.05$). C21 administration additionally improved myelination within the diabetic animals, but not the control animals ($p < 0.05$). This translated to the observed improvements in the cognitive deficits experienced by the diabetic animals and alleviated both the acute and chronic deficits in cognition observed in the diabetic animals, resulting in a dimorphic recovery from stroke (Fig 2.5F, Interaction $p < 0.05$). When the baseline of each animal was compared to their cognition at week 8, C21 administration not only prevented the 27.5% decline in diabetic animals, but actually resulted in a 5.6% increase from baseline after a stroke (Fig 2.5G, $p < 0.01$). When the threshold of cognitive impairment was set as scoring below the % chance (0.33) that the animal would explore the novel arm for an equal time of the 3 total arms, we discovered that C21 treatment reduced the development of cognitive impairment from 100% to 0%. By week 8, none of the diabetic animals that received C21 were cognitively impaired (Fig 2.5H).

C21 Modulates the Polarization of Microglia to Downregulate Inflammation in Diabetes

C21 administration did not reduce the number of GFAP⁺ cell nor IBA-1⁺ cells in the diabetic cohort (Fig 2.6A and B). Additionally, it did not impact the percentage of microglia which were activated (Fig 2.6C). Within the activated microglia population, it actually shifted the M1:M2 ratio toward a more anti-inflammatory profile. Flow cytometry was used to indicate the polarization status of the activated microglia. The CD86⁻/CD206⁺ cells were selected as illustrated in Fig 2.6D. The ratio of CD86⁺ to CD206⁺ cells was then compared as the M1:M2 ratio. E) Within the ipsilateral hemispheres containing both the PFC and hippocampus, the M1:M2 ratio was

upregulated within diabetic animals after a stroke compared to sham, but downregulated with C21 administration (Fig 2.6E, $p < 0.01, 0.05$). There was not a significant difference between any of the groups within the contralateral hemisphere (Fig 2.6E)

We then evaluated the direct impact of C21 on microglia *in vitro* using a BV2 mouse cell line. F4/80 was used to indicate activated microglia and from that population TNF α ⁺ cells were characterized as M1 and TNF- α ⁻ cells were further gated for CD206⁺ and IL-10⁺. The ratio of TNF α ⁺ to double positive CD206 and IL-10⁺ cells was then compared for the M1:M2 ratio as illustrated in Fig 2.7A. We discovered that LPS/IFN γ exposure did polarize the cells to a M1 phenotype and away from a M2 phenotype, as expected (Fig 2.7B-D). Both the pre- and post-treatment with C21 polarized the cells toward a M2 phenotype to ultimately decrease the M1:M2 ratio (Fig 2.7B-D). Post-treatment C21 was administered 6 hours after LPS/IFN γ exposure, yet it was still able to prevent the inflammatory effects of LPS/IFN γ exposure, highlighting the potency of this therapeutic application on microglia polarization. Interestingly, when the AT2R was blocked with PD, the effects were not reversed, suggesting that perhaps the microglia polarization effects of C21 are independent of the AT2R.

C21 Exerts Dimorphic Effects on Control and Diabetic animals

Although delayed administration of C21 improved sensorimotor deficits in control animals and preserved brain volume, it exerted dimorphic effects on the immune cell modulation when compared to its effects in diabetic animals. Within the control cohort, C21 administration increased the presence of IBA-1⁺ cells within the B slice in regions of the PFC, limbic system and the OVLT (Fig 2.8A $p < 0.01$), while it had no impact in diabetes (Fig 2.6A-C). We then used flow

cytometry to further assess the phenotype of the increased microglia in the control group. Using the TMEM119 marker to indicate residential microglia, we observed a similar trend of increase in the B slice, similar to that observed with IHC that did not reach significance. However, in the hippocampus, C21 administration increased the number of macrophages in control animals and tended to decrease them in diabetic animals (Fig 2.8C, interaction $p < 0.05$) exerting a dimorphic effect on each group. This suggested that the increase in IBA-1⁺ cells may be due to increased infiltration of macrophages. When further assessing the polarization of the macrophages, we found that although C21 increased their presence within the tissue, it actually decreased the percentage of M1 macrophages compared to vehicle treated control animals (Fig 2.8D, $p < 0.05$).

Discussion

The observation that the HFD/STZ model of diabetes increased stroke mortality, worsened sensorimotor deficits and exacerbated cognitive deficits, similar to that observed clinically, validated it as a translational animal model for the study of diabetic stroke and the development of PSCI. Clinically, more than 40% of stroke victims present at the time of stroke with pre-existing diabetes, which also increases the severity of cognitive impairment [8]. Similar to the increased occurrence of cognitive impairment in diabetes reported in the Rotterdam study, in our preclinical model, diabetic animals not only showed lower Y-maze scores indicative of worse cognitive function but also a 5-fold increased number of cognitively impaired rats after stroke in the diabetic cohort [6, 8].

Our lab has previously shown worsened cognition and increased inflammation within diabetic animals up to 2 weeks after a stroke, but to our knowledge this is the first study to

evaluate the long-term effect of diabetes on cognition and inflammation [5]. It was interesting to note that both diabetic and control animals experienced a similar degree of brain atrophy after a stroke, but only the diabetic animals developed impaired cognition at a significant rate. This may be due to the chronically elevated inflammatory presence in diabetic rats, as indicated by the increased number of astrocytes, microglia and by the advanced degree of demyelination. A similar effect of diabetes on microglia activation as well as impaired white matter and cognition has been reported in mice out to 35 days after stroke [13]. However, this is the first study to evaluate out to 60 days and confirm that the elevated inflammatory state produced by diabetes remains chronically elevated after a stroke without any apparent resolution. Although both control and diabetic animals experienced a similar degree of atrophy, the neuronal networks within the remaining tissue of the control animals appear to retain superior functionality and connectivity.

In this study we noted a large Mtrans phenotype, where the CD206 M2 marker and the CD86 marker often were co-expressed, even when intracellular markers were additionally implemented. Since this Mtrans population has been shown to be detrimental, similar to M1 microglia over-activation, this was gated out by only selecting M2 microglia from the CD86-population [27]. This leads us to speculate whether the M2 microglia maintain traditional M2 roles such as increased BDNF production, beneficial phagocytosis and synaptic plasticity in diabetes. Previous studies have reported increased phagocytosis and synaptic stripping by microglia in conjunction with impaired hippocampal function, which may suggest a reprogramming or a deleterious role within a sub-population of M2 microglia in diabetic animals [28].

After a stroke, many animals spontaneously recover. This may be due to the fact that they are not adequately stroked in comparison to the rest of the stroke group. It may also be due to compensatory mechanisms that vary between animals or to surgical variance. In either case, it can dilute or exaggerate the effectiveness of a therapeutic intervention. Our implementation of inclusion criteria served to address this problem and homogenize the stroke volumes in an effort to depict an accurate picture of the therapeutic potential of C21. In an added effort to increase the translatability of our studies, we blinded the experimenters and we implemented a delayed administration of C21, which served two purposes. First, many drugs are evaluated as a pre-treatment and show therapeutic efficacy but in clinical practice therapeutic interventions are rarely implemented in this manner. This ultimately contributes to the failure rate when translating an experimental therapeutic into clinical trials. Secondly, we wanted to elucidate the ability of C21 administration to impact the secondary neurodegenerative processes separate from acute neuroprotection. The observed preservation of brain tissue (lower brain atrophy) in the control and diabetic groups leads one to question, whether this is due to neuroprotection or prevention of secondary neurodegenerative processes. Since C21 was administered 3 days after stroke, when the infarct size has completed its evolution, this led us to believe that this may be due to secondary neurodegenerative processes, but further experiments are warranted.

Interestingly, the delayed administration of C21 did not reduce the number of IBA-1⁺ cells within the diabetic animals, nor their activation status. This is different than what our lab previously observed in spontaneously hypertensive rats (SHRs), where C21 drastically reduced microglia number and activation [16]. Difference may arise from differences within the comorbid background of diabetes versus hypertension. It may also arise from region of analysis. As

determined by flow cytometry, the microglia number was unchanged in the PFC of the diabetic animals but tended to decrease in the hippocampus of diabetic animals. Differences in activation induced by C21 may arise from the use of two completely different methods. In this study we used flow cytometry and the absence of M1/M2 markers to indicate activation status. Our lab previously utilized morphological analyses such as the transformation index (TI) and circularity index, which may be more indicative of M1 activated microglia (i.e. swollen cell body, shortened processes). This study did, in fact, show a reduction in M1 microglia [16]. Although C21 administration did not alter the number of microglia, it did shift the activated cells to a more anti-inflammatory phenotype. The treatment with C21 appears to work by polarizing the activated microglia toward a M2 phenotype. It is encouraging to observe that both the delayed administration of C21 *in vivo*, as well as the post-treatment of C21 in injured microglia resulted in significant improvements. Interestingly, in the absence of injury *in vivo* and *in vitro*, C21 did not alter the M1:M2 ratio. In the context of diabetes or when the cells were challenged with LPS and IFN γ , C21 markedly reduced the M1:M2 ratio. Studies have shown that M2 microglia and macrophages drive oligodendrocyte differentiation, which could underlie the improved MBP:NF200 ratio observed within the diabetic animals [28].

Interestingly, control animals treated with C21 experienced a dimorphic upregulation of macrophages, opposite to the downregulation observed in the diabetic animals. Upon further investigation into this phenomenon, it was discovered that even though C21 upregulated the macrophages in general, it drastically reduced the percentage of M1 macrophages within that population. This leads us to believe it is both recruiting macrophages into the control brain and impacting their polarization. Further investigation is warranted to evaluate whether this

potential massive recruitment of M2 macrophages observed only in the controls is accompanied by a breakdown of the BBB and whether this recruitment is actually beneficial or detrimental.

In summary, we found the HFD/STZ model of diabetic to be a highly translational model for the study of diabetic stroke and the development of PSCI, displaying both similar increased mortality, functional deficits, cognitive impairment and elevated inflammation to that observed clinically. We also found the implementation of the inclusion criteria to be a valuable tool to ensure ischemic injury and homogenization of the acute ischemic damage. C21 is currently in clinical trials for the treatment of pulmonary fibrosis. Since this therapeutic has already been shown to be safe for human consumption and granted orphan drug status, it has high repurposing potential. The level of AT2Rs within the brain is a highly debated concept, but our intriguing *in vitro* results suggest that this therapeutic may additionally act independent of these receptors [15]. Due to the complexity of our design, we included only the results obtained in male animals. Nevertheless, this translational study emphasizes the importance of incorporating disease models into dementia research to more closely mimic the clinical variables present within patient populations.

Acknowledgements: This study is from the doctoral thesis of Ladonya Jackson, presented to the University of Georgia. The authors would like to thank Dr. Darrell Brann for providing the BV2 cell line and Vicore Pharma for providing C21. We would also like to thank the Electron Microscope and Histology Core at Augusta University for the histological staining of our samples, with a special thanks to Ms. Penny Roon.

Funding: This study was supported by Veterans Affairs (VA) Merit Review (BX000347), VA Senior Research Career Scientist Award, National Institute of Health (NIH) R01 NS083559 to Adviy Ergul; R01 NS104573 to Adviy Ergul and Susan C. Fagan; and a TL1 award TL1 TR002382 and UL1TR002378 to Ladonya Jackson.

Conflict of Interest

The authors declare that they have no conflict of interest.

Compliance with Ethical Standards

Statement on the Welfare of Animals

All rats were housed in the animal care facility at Augusta University, which is approved by the American Association for Accreditation of Laboratory Animal Care. All experiments were conducted in accordance with the National Institute of Health (NIH) guidelines for the care and use of animals in research. Furthermore, all protocols were approved by the institutional animal care and use committee.

Figures

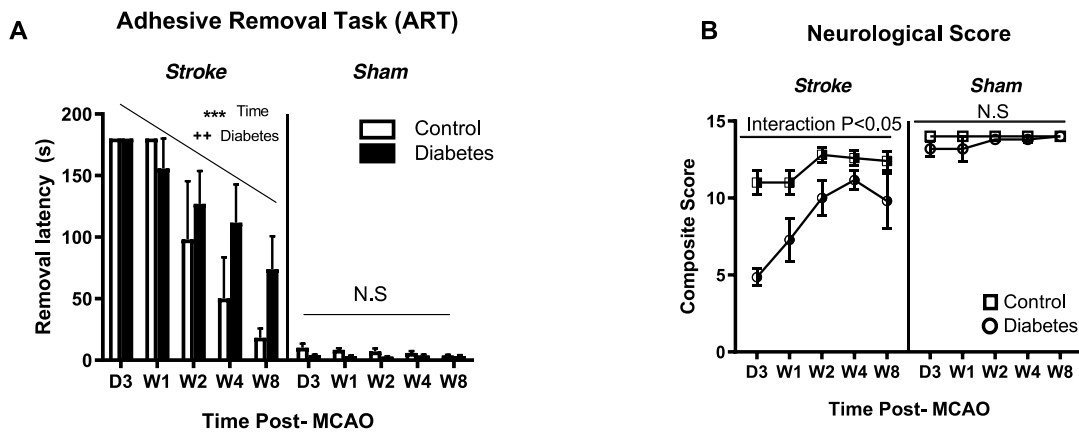


Figure 2.1: Diabetes worsened stroke-mediated functional deficits up to 8 weeks after recovery

A) Sensorimotor deficits were measured by adhesive removal task (ART) which indicated that diabetes prolonged the recovery after a stroke. *Repeated measures ANOVA, (Control C vs Diabetes D) *** main effect of time ($p < 0.001$), ** main effect of diabetes ($p < 0.01$).* B) Diabetic animals experienced greater deficits after a stroke compared to sham as measured by their neurological score. *Repeated measures ANOVA, (Control C vs Diabetes D) Interaction $p < 0.05$. ($n = 5-7/\text{group}$)*

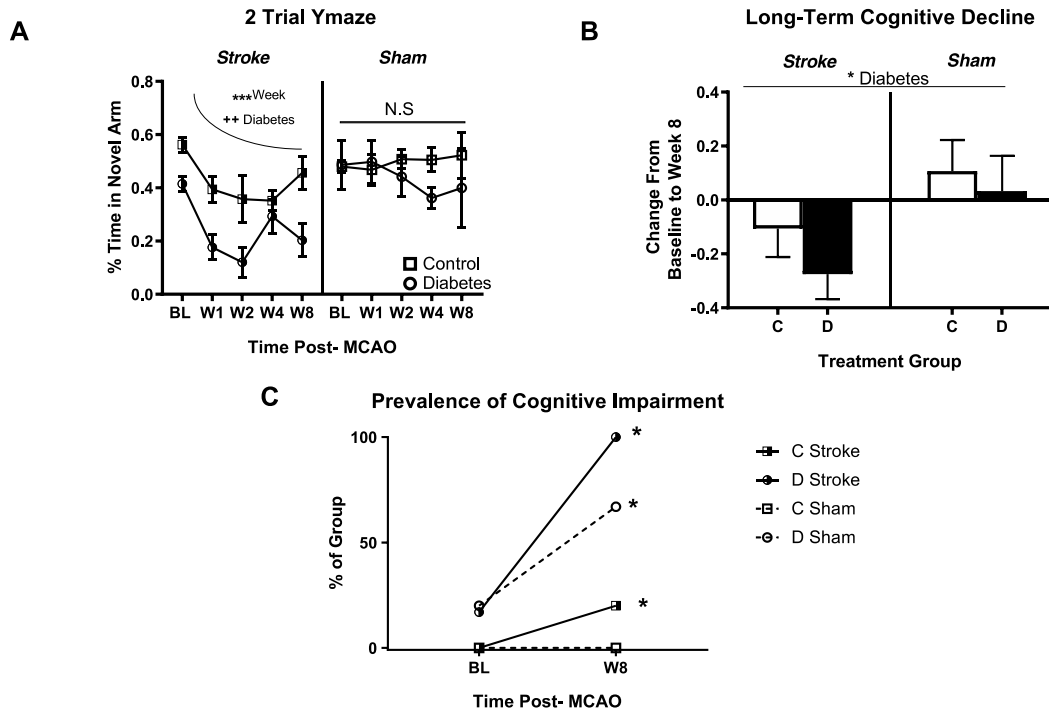


Figure 2.2: Diabetes exacerbated the development of cognitive Impairment

A) 2 trial Y-maze was used to examine cognition. Although both control and diabetic animals experienced an overall progressive decline in cognition after stroke, the diabetic animals experienced a steeper decline than the control animals. Repeated measures ANOVA, (Control C vs Diabetes D) *** main effect of time ($p < 0.001$), ++ main effect of diabetes ($p < 0.01$). B) Diabetes with or without the comorbid event of a stroke resulted in a net decline of cognition long-term. Two-way ANOVA, (Control C vs Diabetes D) (Sham x Stroke) * main effect of Diabetes ($p < 0.05$). C) A stroke event and/or diabetes increased the percentage of animals identified as “cognitively impaired”. Fisher’s Exact Chi Squared Test * association ($p < 0.05$). ($n = 5-7/\text{group}$)

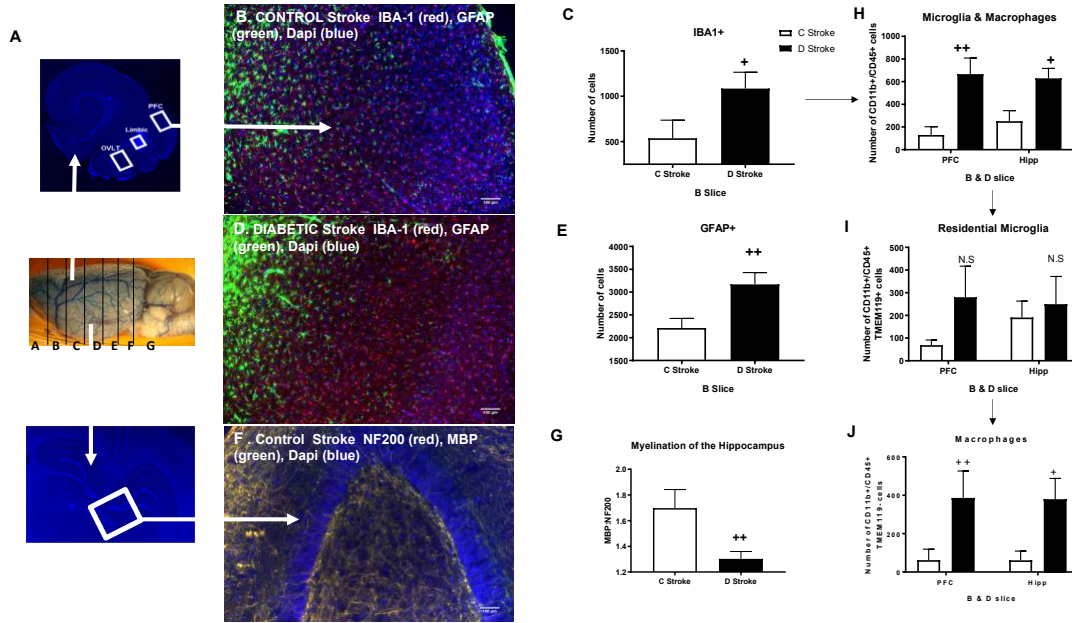


Figure 2.3: Diabetes chronically upregulated inflammation after a stroke

A) 30 μm sections from the B slice were co-stained with IBA-1 and GFAP as indicated in A. B) 10x images were taken from the structures within the PFC, limbic system and OVLT as indicated with squares in A. Images derived from control stroke (B) and a diabetic stroke groups (D) were Z stacked and quantified throughout the layer. 8 weeks after stroke, diabetic animals exhibited a chronic upregulation of C) IBA-1⁺ cell, and of E) GFAP⁺ cells compared to their control counter parts Student's t-test, (Control stroke C vs Diabetic stroke D) + compared to control stroke (p<0.05). E) Within the slice B histology GFAP⁺ cells were also upregulated. Student's t-test, (Control stroke C vs Diabetic stroke D) ++ compared to control stroke (p<0.01). F) 30 μm sections from the D slice were co-stained with MBP and NF200. Images were taken from the hippocampus as depicted in A and F and indicate that the diabetic animals also experienced a greater degree of demyelination (G) as measured by the ratio of MBP:NF200 axons, Student's t-test (Control stroke C vs Diabetic stroke D) ++ compared to control stroke (p<0.01). Flow cytometric analyses were performed on the B and D slice containing the PFC and Hipp, respectively, as indicated in Table 1. This also showed an upregulation of microglia and macrophages (H), with the upregulation deriving from an increase in the macrophage (I) but not microglia population (J). Student's t-test, (Control stroke C vs Diabetic stroke D) ++ and + compared to control stroke (p<0.01, 0.05). (n=5-7/group)

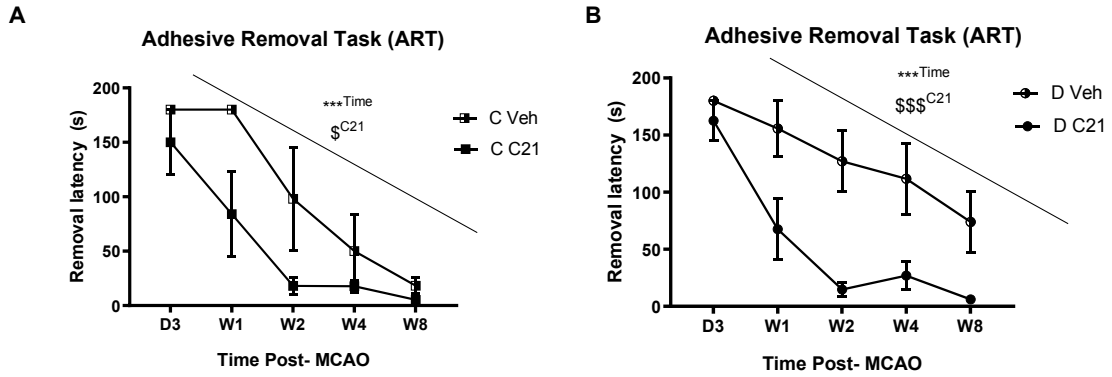


Figure 2.4: Delayed administration of C21 improved functional deficits

C21 administration improved functional deficits in A) control animals and B) diabetic animals as measured via ART. Repeated measures ANOVA, (Control C veh vs C C21) and (Diabetic D veh vs D C21) *** main effect of time ($p < 0.001$), + and +++ main effect of C21 ($p < 0.05$ C veh, 0.001 D veh). ($n = 5-7$ /group)

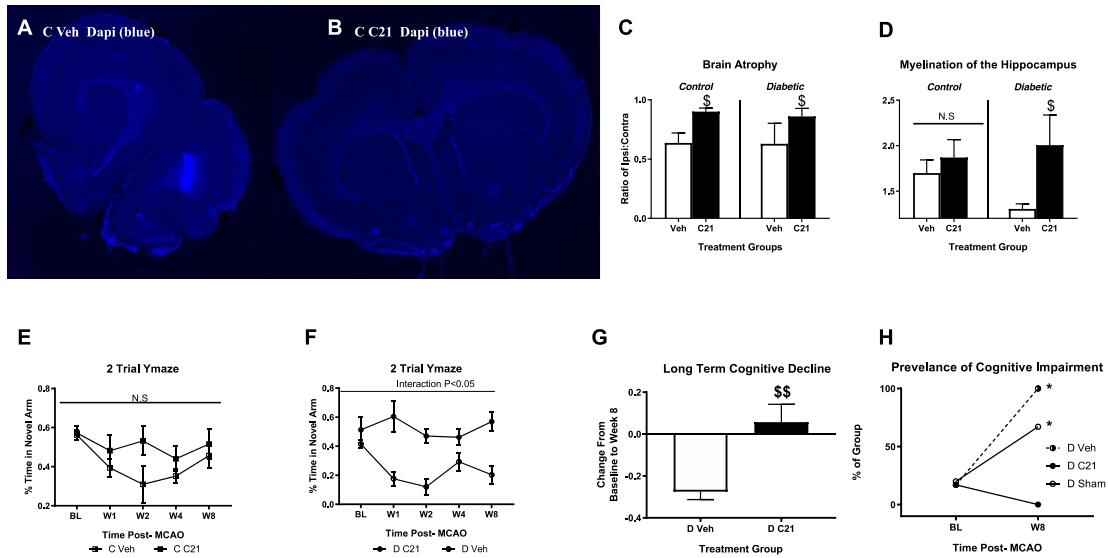


Figure 2.5: Delayed administration of C21 after a stroke reduced brain atrophy in both control and diabetic animals but only improves cognitive deficits in diabetic animals

A) Depicts an image of the B slice of a vehicle-treated control and B) C21-treated control 8 weeks after stroke. C) C21 treatment preserved brain volume in both control and diabetic animals. Student's t-test, (Diabetes D Veh vs Diabetes D C21) and (Control C Veh vs Control C C21) \$ compared to Veh ($p < 0.05$). D) It also drastically improved the myelination within the hippocampus from the D slice of the diabetic animals only. Student's t-test, (Diabetes D Veh vs Diabetes D C21) \$ compared to D Veh ($p < 0.05$). E) Although C21 treatment did not significantly improve cognition in control animals, it did significantly improve cognition in diabetic animals and prevented the progressive decline in cognition (F). Repeated measures ANOVA, (Control C vs Diabetes D) Interaction $p < 0.05$. G) C21 treatment actually resulted in a net improvement of cognition from baseline to 8 weeks after a stroke in diabetic animals. Student's t-test, (Diabetes D veh vs Diabetes D C21) \$\$ compared to D Veh ($p < 0.01$). H) C21 drastically reduced the percentage of "cognitively impaired" animals. Fisher's Exact Chi Squared Test * association ($p < 0.05$). (n=3-4/group for C and 5-7/group for D-H).

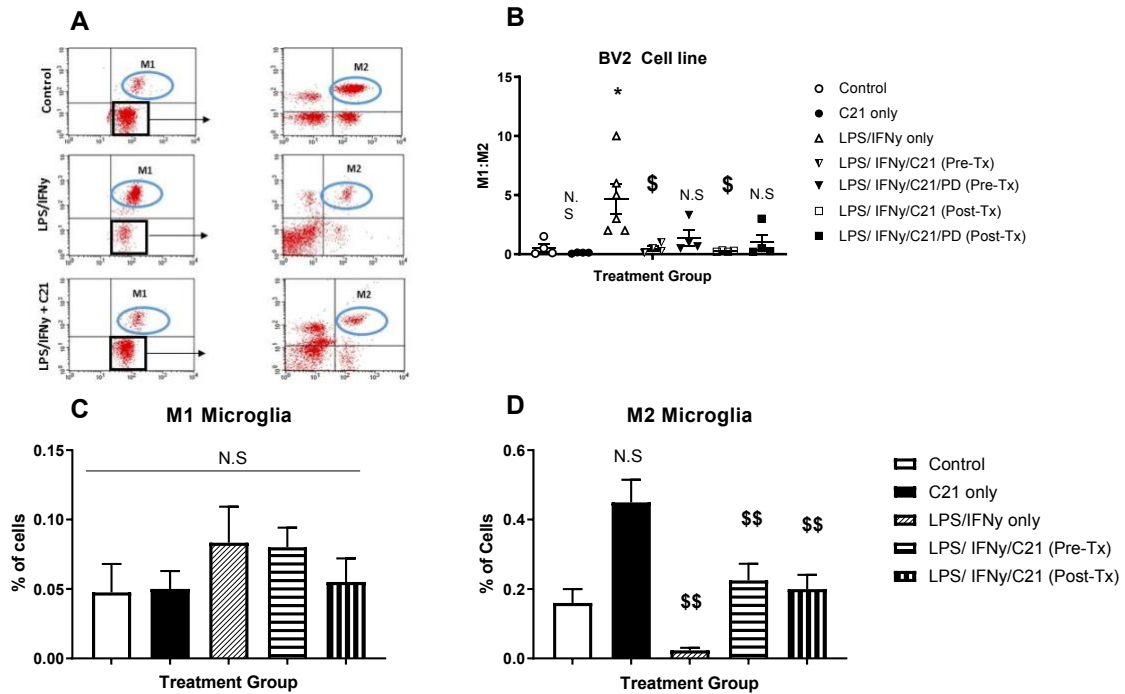


Figure 2.6: C21 may exert its beneficial effects on stroke recovery and cognition through modulation of the M1:M2 ratio in diabetic animals

Treatment with C21 did not impact the amount of A) GFAP⁺ cells or B) IBA-1⁺ cells that were stained histologically within the brain of the diabetic animals. C) It also did not impact the percentage of activated microglia, as measured by flow cytometry as indicated in Table 1. Flow cytometric analyses were conducted as illustrated in D), and indicated that C21 did however reduce the M1:M2 ratio within the ipsilateral hemisphere (E) without altering the contralateral hemisphere. Student's t-test, (Diabetes D veh vs Diabetes D sham) and (Diabetes D veh vs Diabetes D C21) ++ vs sham ($p < 0.01$) and \$ compared to D veh ($p < 0.05$). (n=5-7/group)

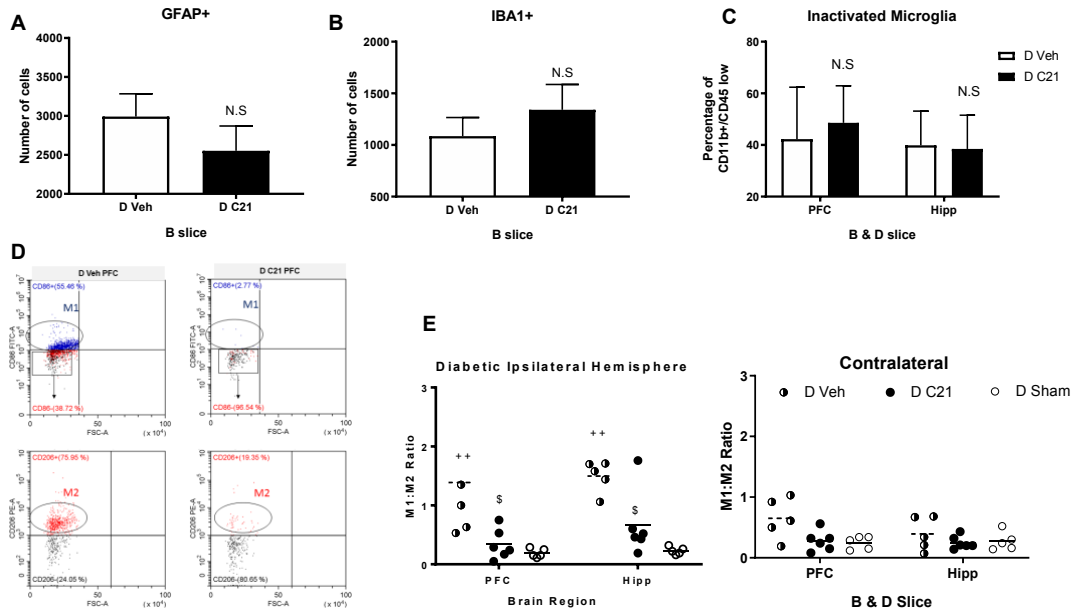


Figure 2.7: Delayed administration of C21 directly modulated microglia independent of AT2R activation

Flow cytometric analyses were conducted as illustrated in A. B) Within a BV2 cell line C21 also reduced the M1:M2 ratio in BV2 cells polarized toward a M1 phenotype with the incubation of both LPS and IFN γ . C21 improved the M1:M2 ratio independent of AT2R activation within microglia cells. Student's t-test (LPS/IFN γ vs control), (LPS/IFN γ vs LPS/IFN γ /C21 pre-tx) and (LPS/IFN γ vs LPS/IFN γ /C21 post-tx) * compared to control ($p < 0.05$), \$ compared to LPS/IFN γ ($p < 0.05$). C) Although C21 did not impact the M1 microglia polarization, it drastically upregulated E) M2 microglia polarization. Student's t-test (LPS/IFN γ vs control), (LPS/IFN γ vs LPS/IFN γ /C21 pre-tx) and (LPS/IFN γ vs LPS/IFN γ /C21 post-tx) * compared to control ($p < 0.01$), \$\$ compared to LPS/IFN γ ($p < 0.01$). (n=5-6/group)

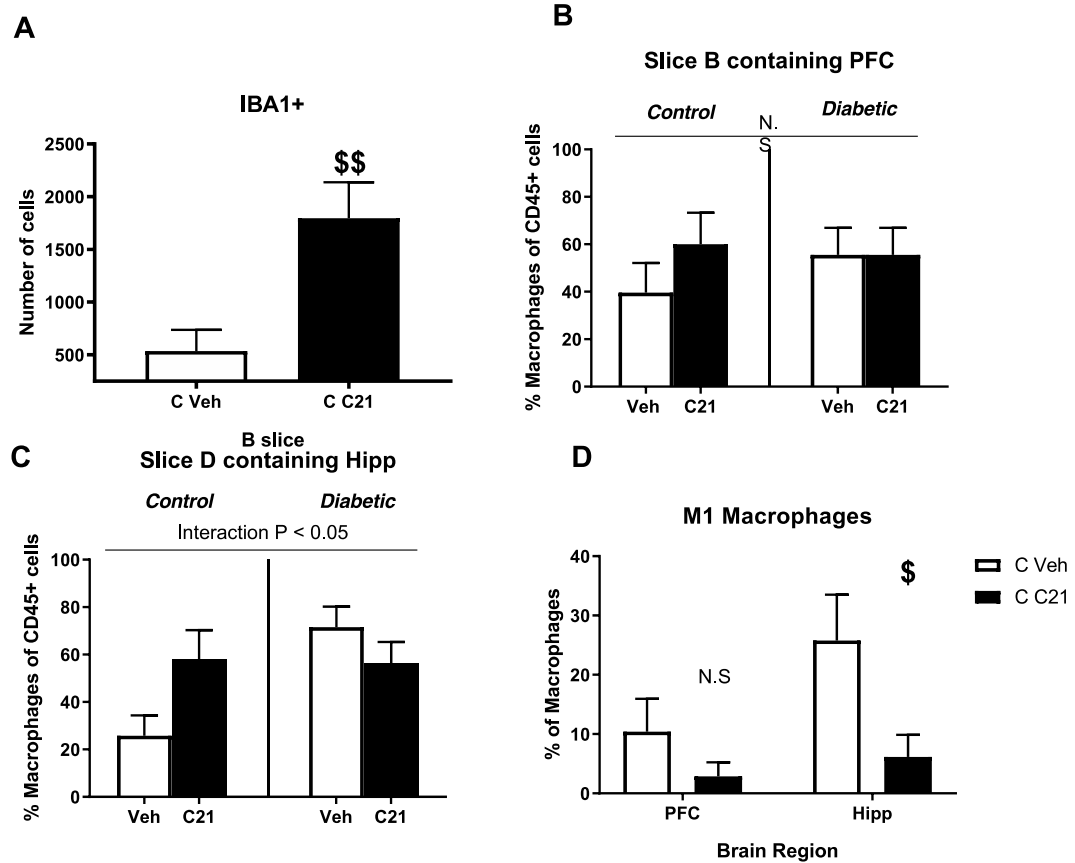


Figure 2.8: C21 administration exerted a dimorphic effect in diabetic and control animals

A) While C21 did not significantly impact the number of microglia nor the degree of macrophage infiltration in diabetic animals chronically after a stroke, it promoted a dimorphic increase in M2 macrophage infiltration of control animals. A) IHC staining with IBA-1 showed an increased amount of IBA-1⁺ cells within C21 treated control animals. Student's t-test (Control C veh vs C C21) \$\$ compared to C veh. B) Flow cytometric analyses indicated a dimorphic interaction of C21 to increase the TMEM119⁻ (macrophage) population within the CD45⁺ cells of the hipp of control animals, but not of diabetic animals. Two-way ANOVA (Control C veh vs C C21) x (Diabetic D veh vs D C21), interaction p<0.05. It also trended toward this within the PFC but did not reach significance B). Although C21 increased macrophage infiltration within the Hipp, within the macrophage population of the control animals C21 reduced the percentage of M1 macrophages within the Hipp. Student's t-test (Control C veh vs Control C C21) \$ compared to C veh (p<0.05). (n=5-6/group)

Lesion Size Analysis

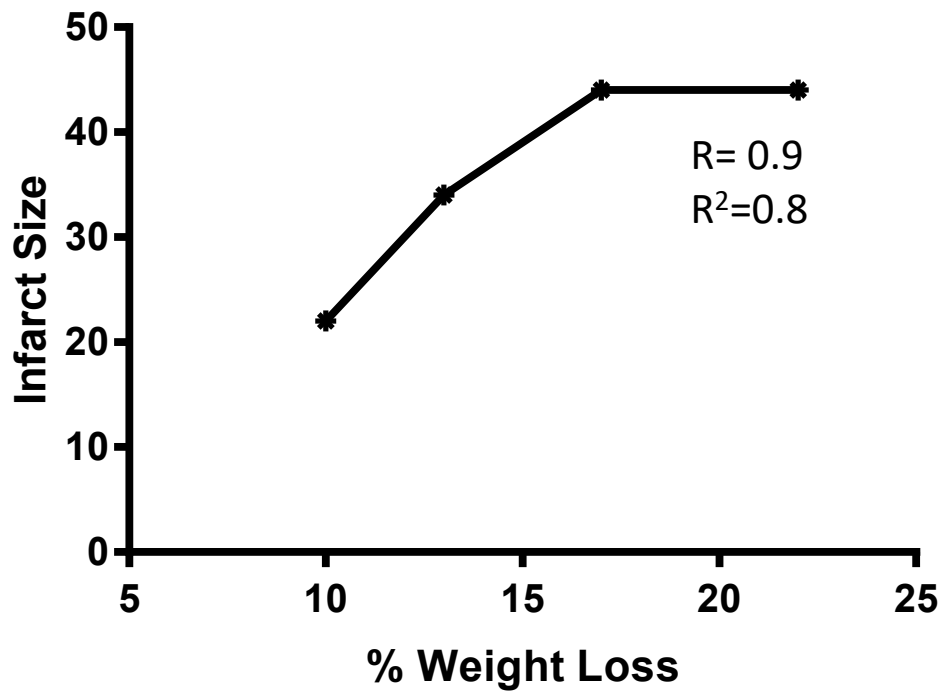


Figure 2.S1: The degree of weight loss correlated with lesion size

In order to set inclusion criteria, we first evaluated the correlation between weight loss at day 3 and the infarct size at day 3. We discovered that weight loss correlated with the size of the infarct ($R^2=0.8$), Pearson's Correlation. Since a 10% drop in weight loss only correlated with a 20% infarct size, we required the drop in weight loss of the included animals to be greater than 10%.

Blood Glucose Trend

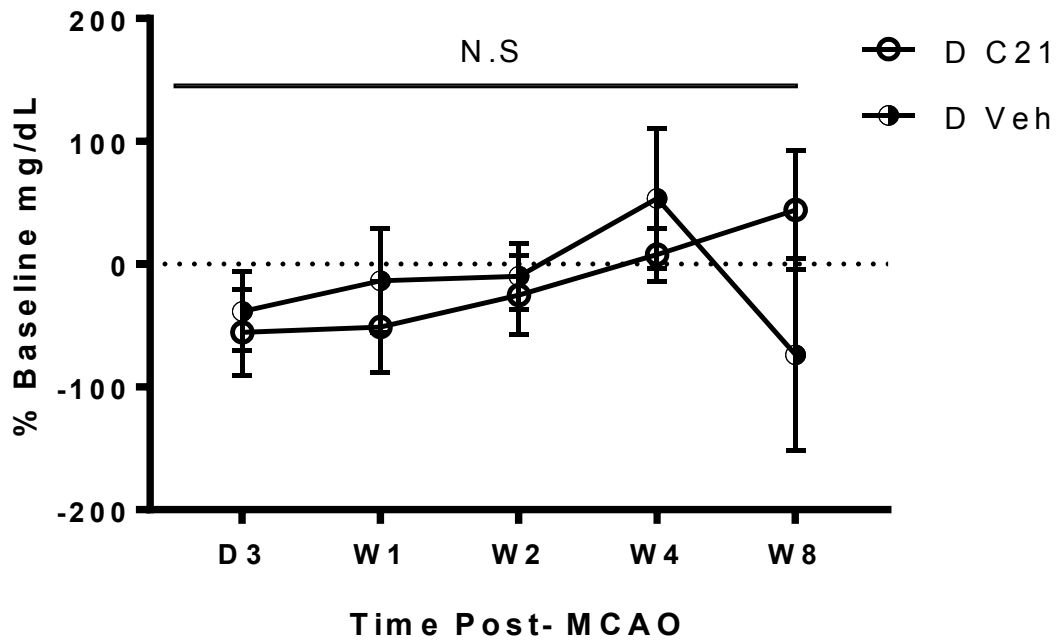


Figure 2.S2: Delayed C21 administration did not impact blood glucose

Blood glucose ranged from 300-350 mg/dL throughout the majority of the study.

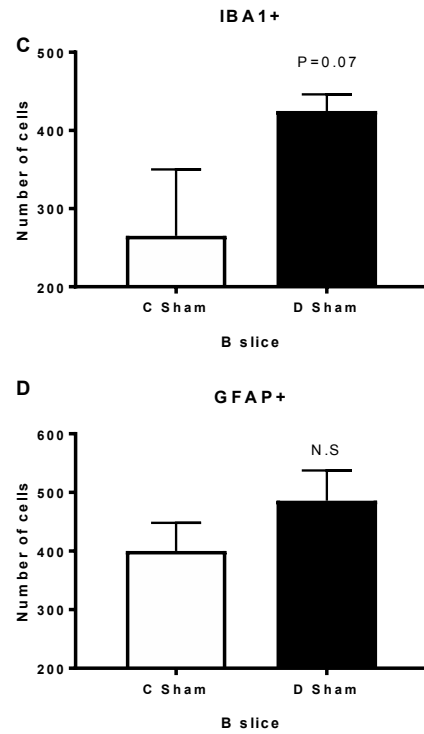
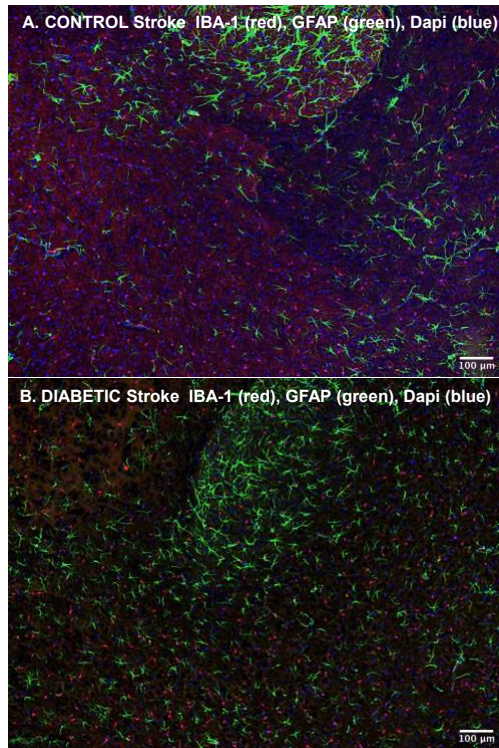


Figure 2.S3: Sham diabetic animals trended to show increased inflammation

A) 30 µm sections from the B slice were co-stained with IBA-1 and GFAP and 10x images were taken from the structures within the prefrontal cortex, limbic system and OVLT. Images derived from control sham (A) and a diabetic sham groups (B) were Z stacked and quantified throughout the layer. Diabetic sham animals trended to exhibit a chronic upregulation of C) IBA-1⁺ cells ($p < 0.07$). Student's t-test, (Control sham C vs Diabetic sham D) ⁺ compared to control sham ($p < 0.05$). No difference was found in D) GFAP⁺ cells compared to their control counterparts. (n=5/group)

Table 2.1: Flow Cytometry Markers Utilized to Identify Particular Cell Populations

	CD11b	CD45	TMEM119	CD86	TNF α	CD206
M1 (CD206+/IL10+)	+	+ low	N/A	+	N/A	N/A
M2 (CD86+/TNFα+) 	+	+ low	N/A	-	N/A	+
Residential Microglia (TMEM119+)	+	+	+	N/A	N/A	N/A
Infiltrating Macrophages	+	+	-	N/A	N/A	N/A
M1 macrophages	+	+	-	+	+	N/A
Inactivated microglia	+	+ low	N/A	-	N/A	-

Table 2.2: Diabetes Increases Mortality

	Diabetic animals	Control animals
Total Animals	50	28
Mortality Before Day 3	40%	25%
Mortality After Day 3	50%	0%

Table 2.3: Delayed Administration of C21 Prevents Early Mortality

	D Veh	D C21
Mortality After Day 3	50%	0%

References

1. Mozaffarian, D., et al., *Heart disease and stroke statistics--2015 update: a report from the American Heart Association*. Circulation, 2015. **131**(4): p. e29-322.
2. Mijajlovic, M.D., et al., *Post-stroke dementia - a comprehensive review*. BMC Med, 2017. **15**(1): p. 11.
3. Levine, D.A., et al., *Trajectory of Cognitive Decline After Incident Stroke*. JAMA, 2015. **314**(1): p. 41-51.
4. Li, W., et al., *Post-stroke neovascularization and functional outcomes differ in diabetes depending on severity of injury and sex: Potential link to hemorrhagic transformation*. Exp Neurol, 2018. **311**: p. 106-114.
5. Ward, R., et al., *Post Stroke Cognitive Impairment and Hippocampal Neurovascular Remodeling: The Impact of Diabetes and Sex*. Am J Physiol Heart Circ Physiol, 2018.
6. Hardigan, T., R. Ward, and A. Ergul, *Cerebrovascular complications of diabetes: focus on cognitive dysfunction*. Clin Sci (Lond), 2016. **130**(20): p. 1807-22.
7. Ergul, A., et al., *Cerebrovascular complications of diabetes: focus on stroke*. Endocr Metab Immune Disord Drug Targets, 2012. **12**(2): p. 148-58.
8. Wang, Q., et al., *Prediabetes is associated with post-stroke cognitive impairment in ischaemic stroke patients*. Brain Res, 2018. **1687**: p. 137-143.
9. Ergul, A., et al., *Impact of Comorbidities on Acute Injury and Recovery in Preclinical Stroke Research: Focus on Hypertension and Diabetes*. Transl Stroke Res, 2016. **7**(4): p. 248-60.
10. Felsky, D., et al., *Neuropathological correlates and genetic architecture of microglial activation in elderly human brain*. Nat Commun, 2019. **10**(1): p. 409.
11. Kalaria, R.N., R. Akinyemi, and M. Ihara, *Stroke injury, cognitive impairment and vascular dementia*. Biochimica et biophysica acta, 2016. **1862**(5): p. 915-925.
12. Gorelick, P.B., et al., *Vascular contributions to cognitive impairment and dementia: a statement for healthcare professionals from the american heart association/american stroke association*. Stroke, 2011. **42**(9): p. 2672-713.
13. Ma, S., et al., *Diabetes Mellitus Impairs White Matter Repair and Long-Term Functional Deficits After Cerebral Ischemia*. Stroke, 2018. **49**(10): p. 2453-2463.
14. Ladonya Jackson, W.L., Yasir Abdul, Guangkuo Dong, Babak Baban, Advije Ergul, *Diabetic Stroke Promotes a Sexually Dimorphic Expansion of T Cells*. NeuroMolecular Medicine 2019. **In Press**(71).
15. Jackson, L., et al., *Within the Brain: The Renin Angiotensin System*. Int J Mol Sci, 2018. **19**(3).
16. Ahmed, H.A., et al., *RAS modulation prevents progressive cognitive impairment after experimental stroke: a randomized, blinded preclinical trial*. J Neuroinflammation, 2018. **15**(1): p. 229.
17. Alhusban, A., et al., *Compound 21 is pro-angiogenic in the brain and results in sustained recovery after ischemic stroke*. J Hypertens, 2015. **33**(1): p. 170-80.
18. Ahmed, H.A., et al., *Role of angiotensin system modulation on progression of cognitive impairment and brain MRI changes in aged hypertensive animals - A randomized double- blind pre-clinical study*. Behav Brain Res, 2017.
19. Fouda, A.Y., et al., *Role of interleukin-10 in the neuroprotective effect of the Angiotensin Type 2 Receptor agonist, compound 21, after ischemia/reperfusion injury*. Eur J Pharmacol, 2017. **799**: p. 128-134.
20. Ahmed, H.A., et al., *Angiotensin receptor (AT2R) agonist C21 prevents cognitive decline after permanent stroke in aged animals-A randomized double- blind pre-clinical study*. Behav Brain Res, 2018.
21. Ishrat, T., et al., *Dose-response, therapeutic time-window and tPA-combinatorial efficacy of compound 21: A randomized, blinded preclinical trial in a rat model of thromboembolic stroke*. J Cereb Blood Flow Metab, 2018: p. 271678X18764773.

22. Schwengel, K., et al., *Angiotensin AT2-receptor stimulation improves survival and neurological outcome after experimental stroke in mice*. J Mol Med (Berl), 2016. **94**(8): p. 957-66.
23. Li, W., et al., *Diabetes Worsens Functional Outcomes in Young Female Rats: Comparison of Stroke Models, Tissue Plasminogen Activator Effects, and Sexes*. Transl Stroke Res, 2017.
24. Feeney, D.M., A. Gonzalez, and W.A. Law, *Amphetamine, haloperidol, and experience interact to affect rate of recovery after motor cortex injury*. Science, 1982. **217**(4562): p. 855-7.
25. Chen, J., Y. Li, and M. Chopp, *Intracerebral transplantation of bone marrow with BDNF after MCAo in rat*. Neuropharmacology, 2000. **39**(5): p. 711-6.
26. Holt, L.M. and M.L. Olsen, *Novel Applications of Magnetic Cell Sorting to Analyze Cell-Type Specific Gene and Protein Expression in the Central Nervous System*. PLoS One, 2016. **11**(2): p. e0150290.
27. Kumar, A., et al., *Microglial/Macrophage Polarization Dynamics following Traumatic Brain Injury*. J Neurotrauma, 2016. **33**(19): p. 1732-1750.
28. Hao, S., et al., *Dietary obesity reversibly induces synaptic stripping by microglia and impairs hippocampal plasticity*. Brain Behav Immun, 2016. **51**: p. 230-9.

CHAPTER 3

MICROGLIA KNOCKDOWN REDUCES INFLAMMATION AND COGNITIVE DEFICITS

IN DIABETIC ANIMALS¹

¹ Jackson L, Dumanli S, Johnson M, Fagan S.C, Ergul A. Microglia Knockdown Reduces Inflammation and Cognitive Deficits in Diabetic Animals. Submitted to [*Journal of Neuroinflammation*], [July 20, 2019]

Abstract

Introduction: Unfortunately over 40% of stroke victims have pre-existing diabetes which not only increases their risk of stroke up to 2-6 fold, but also worsens both functional recovery and the severity of cognitive impairment. Our lab has recently linked the chronic inflammation that persists in diabetic animals to their poor functional outcomes and exacerbated cognitive impairment, also known as post-stroke cognitive impairment (PSCI). Although we have shown that the development of PSCI in diabetes is associated with the upregulation and the activation of pro-inflammatory microglia, we have not established direct causation between the two. To this end, we evaluated the role of microglia in the development of PSCI. **Methods:** At 13 weeks of age, diabetic animals received bilateral intracerebroventricular (ICV) injections of short hairpin RNA (shRNA) lentiviral particles targeted at the colony stimulating factor 1 receptor (CSF1R). After 14 days, animals were subjected to 60 min middle cerebral artery occlusion (MCAO) or sham surgery. Adhesive removal task (ART), novel object recognition (NOR), and 2-trial Y-maze were utilized to evaluate sensorimotor and cognitive function. Samples from freshly harvested brains were analyzed by flow cytometry and immunohistochemistry. **Results:** CSF1R silencing resulted in a 94% knockdown of residential microglia to relieve inflammation and improve myelination of white matter in the brain. This also improved cognition in diabetic animals. **Conclusion:** CSF1R silencing should be considered as a potential therapeutic mechanism to treat the development of PSCI in comorbid conditions that present with pre-existing inflammation.

Introduction

Stroke is a leading cause of long-term disability worldwide, leaving patients both functionally and cognitively impaired [1]. 70% of stroke victims have pre-existing comorbidities such as diabetes and hypertension at the time of stroke [2]. Pre-diabetes alone doubles the risk of developing cognitive impairment [3]. Fully established diabetes increases the risk of stroke up to 2-6 fold and worsens functional recovery and the severity of cognitive impairment to an even greater extent [2, 4].

Elevated neuroinflammation has been linked to the exacerbated functional deficits and the development of post-stroke cognitive impairment (PSCI). Our lab has shown that diabetes chronically elevates the amount of pro-inflammatory microglia, as well as macrophage infiltration and the presence of other pro-inflammatory immune cells post-stroke [4-6]. Notably, the acute rise in anti-inflammatory M2 microglia to aid recovery after stroke in control animals is absent in diabetic animals [7]. This peaked our interest to investigate whether the depletion of microglia all together would be beneficial in diabetic animals, since the normal repair processes facilitated by anti-inflammatory M2 microglia are already blunted. To this end, we first aimed to eliminate microglia in diabetic animals. Colony-stimulating factor 1 receptor (CSF1R) signaling regulates proliferation, differentiation and function of macrophage lineage cells such as microglia and is involved in the regulation of homeostatic as well as inflammatory effects of microglia [8-11]. Depletion of microglia by inhibition of CSF1R by pharmacological approaches have been reported to be beneficial in Alzheimer's Disease [10, 11]. The use of short hairpin RNA (shRNA) lentiviral particles allows the strategic and localized knockdown of target gene expression *in vivo* [12]. Lentiviral particles are widely used in central nervous system research since they are

retroviruses that integrate in the host genome and can infect both dividing and non-dividing cells such as microglia [12]. Accordingly, the current study was designed to eliminate microglia using a molecular approach with CSF1R Knockdown (KD) by shRNA.

Diabetes, as a chronic inflammatory disease, increases macrophage infiltration, the presence of reactive astrocytes and exacerbates white matter damage [4-7]. Microglia, as the initiators of the inflammatory response in the brain, aid in these processes. Through the CCL2/CCR2 signaling pathway, microglia play a central role in regulating the recruitment of peripheral leukocytes and their infiltration into the brain during inflammatory reactions [13, 14]. They additionally aid in the modulation of astrocyte reactivity [15]. The inflammatory microglia activation, macrophage recruitment and the rise in astrocytic reactivity contribute to the demyelination that occurs acutely and persists chronically after stroke in diabetic animals [67, 68]. M2 microglia play a central role in re-myelinating after an ischemic injury [7]. Diabetic animals were found to have impaired myelination after a stroke that correlated with their rise in M1 activation and lack of acute M2 response [7]. Thus, the second aim of this study was to evaluate the impact of CSF1R silencing on chronic neuroinflammation after stroke in diabetic animals.

Our lab recently linked the chronically elevated M1/M2 ratio observed in diabetic animals to with the development of PSCI [6]. The elevated presence of pro-inflammatory microglia was accompanied by an upregulation of astrocytes and by demyelination of the hippocampus, an important region for learning and memory. When this ratio was modulated with therapeutic intervention using an Angiotensin II type 2 receptor (AT2R) agonist, the number of astrocytes were reduced, myelination of the hippocampus was preserved, the development of PSCI was

prevented and functional deficits were minimized [6]. Although we have shown that the development of diabetic PSCI is associated with the upregulation and the activation of pro-inflammatory microglia, we have not established a causal link between the two. Also the exact role of microglia activation in functional recovery has not been fully elucidated. Anti-inflammatory M2 microglia aid in the remodeling of synapses and secrete growth factors such as brain-derived neurotrophic factor (BDNF) [15]. The depletion of microglia-derived BDNF has been associated with altered synaptic protein levels and impaired spine formation during motor learning tasks, which resulted in the absence of training-induced improvement in motor behavior performance [16]. With the absence of the acute rise of M2 microglia in diabetic animals, our third aim was to evaluate whether the knockdown of microglia could alleviate the development of PSCI and functional deficits in diabetic animals.

Methods

Animal Model

Male Wistar rats (Envigo RMS, Inc., Indianapolis, IN) were housed in the animal care facility at Augusta University, which is approved by the American Association for Accreditation of Laboratory Animal Care. All experiments were conducted in accordance with the National Institute of Health (NIH) guidelines for the care and use of animals in research. Furthermore, all protocols were approved by the institutional animal care and use committee.

Type 2 Diabetes Mellitus (T2DM) Induction

Diabetes was induced by a high-fat diet/low-dose streptozotocin (HFD/STZ) combination. Male rats were received at 4 weeks of age and immediately started and maintained on a 45%

kcal fat diet for the remainder of the study (Research Diets Inc., New Brunswick, NJ). A single dose of STZ injection (35 mg/kg; Cayman Chemical, Ann Arbor, MI) was administered intraperitoneally (ip) at 6 weeks of age. If blood glucose was not above 150 mg/dL 5 days post-injection, a second small dose (20 mg/kg) was administered. Control rats were purchased at 10-11 weeks of age and maintained on regular chow with 4% kcal fat. Body weight and blood glucose were measured weekly.

In vivo CSF1R Silencing

In vivo CSF1R silencing was achieved by intracerebroventricular (ICV) injections using a stereotaxic instrument under isoflurane anesthesia. Stereotaxic coordinates used were -1 mm anteroposterior, 2 mm lateral and -3 mm dorsoventral relative to bregma. 2.5 μ l of lentiviral CSF1R shRNA (SMARTchoice lentiviral rat CSF1R hCMV-TurboGFP shRNA, 1×10^8 TU/mL, Dharmacon, #NC1650992) or non-targeting control vector (NTC) were slowly injected bilaterally over 5 minutes into each of the lateral ventricles. In the first round of experiments, a shRNA package that included 3 slightly different constructs were injected into control animals to determine the efficiency of the constructs. Animals were then kept for 14 days to allow for recovery and viral particle integration into their genome. We have previously shown that at least 10 days are required to achieve 70% or higher knockdown [12]. The control animals were sacrificed after those 14 days to optimize the shRNA selection. After selecting the best shRNA construct that achieved knockdown, the diabetic animals were injected with the NTC or CSF1R shRNA. 14 days later they underwent MCAO surgery. The animals were tested for behavioral deficits during the recovery phase and 3 weeks post-MCAO (5 weeks post-injection) the rats were sacrificed.

Middle Cerebral Artery Occlusion (MCAO) Surgery

Rats were subjected to transient focal cerebral ischemia (60 min MCAO) or sham surgery at 12-15 weeks of age using 4-0 silicon-coated nylon suture (Docol 403756). The rats were anesthetized using 2-5% isoflurane, a ventral mid-line neck incision was made, the right common carotid artery (CCA) was exposed and lightly tied, and the external carotid artery (ECA) was ligated and cut. The suture was marked at 1.8 and 2 mm then advanced from a nick at the ECA into the internal carotid artery (ICA) until positioned in-between the 1.8 and 2 mm marks, indicating the branching of the middle cerebral artery (MCA). The suture was tied in place for the duration of the occlusion and the rats were allowed to recover from anesthesia. At the end of the 60-minute occlusion time, the rats were re-anesthetized, the suture was removed for reperfusion and the small nick at the ECA was permanently ligated. In sham surgeries, the CCA was isolated and the ECA was cut and ligated without insertion of the suture. We began with a group of 25 animals. 3 animals died prior to stroke. A total of 8 NTC, 9 ShRNA and 5 sham underwent surgery. After post-stroke mortality the groups were as follows: NTC (N= 5), shRNA (N=7), sham (N=5), one shRNA animal was excluded due to a failed injection resulting in N=6. Although we planned to include another group of 25 animals the majority of them died with the injection of STZ, which is an abnormal occurrence.

Assessment of Sensorimotor Function

Sensorimotor function was evaluated by ART as previously described [17]. This was taken at baseline, day 3 and weeks 1, 2 and 3. For the ART, the rats were trained for 4 days and then baseline measurements were recorded prior to stroke, but after ICV injection. Contact and

removal latency of the adhesive paper dot was recorded and the average was taken from 3 trials with a maximum removal latency of 180 seconds per trial.

Assessment of Cognitive Function

All behavioral assessments were conducted by a blinded investigator. Cognition was assessed by the 2-trial Y-maze and novel object recognition (NOR). For Y-maze the rats were trained 4 days prior to baseline testing. Testing was conducted at baseline prior to stroke but after ICV injection, followed by weeks 1 and 3 post-MCAO. The 2-trial Y-maze was used to examine spatial memory. In the first trial, rats were allowed to freely explore 2 open arms for 10 minutes. The animal was returned to its home cage for a 45 min delay. In the second trial, rats were allowed to explore all 3 arms of the Y-maze apparatus freely for 3 mins. Total time spent in each arm was recorded. Results were expressed as % time spent in the novel arm (time in novel arm divided by total time in all arms x 100). NOR was utilized to examine working memory. On testing days, the rats participated in 2 phases: familiarization and novel. In the familiarization phase, rats were allowed to explore 2 identical objects placed equidistant from the walls with 20 cm between the objects for 5 mins. After a 45 min delay in their home cage, the rat was allowed to explore a novel object paired with the familiar object for 5 mins. Rats were started in the center of the testing apparatus for each session. Objects and the testing area were cleaned with vital oxide odor eliminator between each phase. The time spent exploring each object was recorded as the recognition index (RI; $RI = (T_N) / (T_N + T_F)$).

Euthanasia, Specimen Collection and Molecular Techniques

Rats were euthanized 3 weeks post-MCAO or sham surgery using isoflurane overdose and cardiac puncture. They were then perfused with 50 mLs of PBS and the brains were extracted.

Using a brain matrix, sections of slice B through slice D were taken for flow cytometric and immunocytochemistry (Fig 3.1).

Flow cytometry

Following isolation of the ipsilateral hemispheres of B-D slice containing the prefrontal cortex through the hippocampus, the tissue was minced into 1 mm³ pieces and was dissociated using Worthington's Papain Dissociation kit (catalog number LK003153) with the following modifications: 1) tissue was left in dissociation medium for 15–25 minutes and 2) oxygen was continuously perfused over (not bubbled in) the solution for the duration of the incubation period [18]. Microglia were isolated as described below.

Myelin debris removal and microglial isolation

A debris removal step was performed using modified protocols from Miltenyi Biotec's Myelin Removal Kit (catalog number (Miltenyi Biotec, Germany) and CD11b⁺ Microbeads (Miltenyi Biotec, Germany). Following dissociation, up to 10⁷ cells were suspended in 200 µL 0.5% BSA in PBS buffer and incubated with 20 µL anti-myelin microbeads for 15 mins at 4°C. The cells were then placed in the mini-MACS magnetic separator column and the clean supernatant was eluted out. The cells were then incubated with 20 µL of CD11b⁺ beads to isolate the microglia/macrophage population and isolated using the mini-MACS separator once again. CD11b⁺ cells were then further processed with surface and intracellular microglia makers.

Cellular staining

Cells were incubated with surface markers against pre-conjugated antibodies CD45-APC (ebioscience, San Diego, CA) and CD86-FITC (BD bioscience, San Jose, CA) for 20 minutes. Cells were then permeabilized for intracellular staining with a fixation/permeabilization solution kit

(ebioscience, San Diego, CA). Cells were then separated into two groups and incubated with markers CD206 (Abcam, Cambridge, MA), TNF α (BD bioscience, San Jose, CA), and IL-10 (BD bioscience, San Jose, CA), or TNF α (BD bioscience, San Jose, CA) and TMEM119 (Novus, Centennial, CO). Secondary antibodies PE (ebioscience, San Diego, CA) and PerCP (BD bioscience, San Jose, CA) were used in both groups. Cells were then washed and analyzed using the Cytoflex (Beckman Coulter, Indianapolis, Indiana).

Imaging and analysis

To minimize false-positive events in flow cytometry, the number of positive events detected with the negative staining control for each individual channel was subtracted from the number of positive cells stained with corresponding antibodies. Cells expressing a specific marker were reported as the number of gated events. The gating strategy is shown in Table 1. Microglia were first identified as CD11b⁺ /CD45⁺ low. M1 microglia were further identified as CD86⁺/TNF α ⁺, M2 cells were identified as CD206⁺/IL-10⁺. Residential microglia versus infiltrating macrophages were also identified as CD11b⁺/CD45⁺ without separation of low versus high. Residential microglia were then further identified as TMEM119⁺, while infiltrating macrophages were identified as TMEM119⁻. M1 macrophages were then identified as CD11b⁺/CD45⁺/TMEM119⁻/CD86⁺/TNF α ⁺ cells.

Immunohistochemistry (IHC)

Brains were extracted and post-fixed in 4% PFA overnight. Free-floating 30 μ m sections were incubated overnight with anti-IBA-1 (Ionized calcium-binding adaptor molecule 1, 1:500, Wako, Japan) and anti-GFAP (Glial fibrillary acidic protein, Sigma-Aldrich, Burlington, MA) for B slice sections containing the PFC and with anti-MBP (Myelin Basic Protein, Abcam, Cambridge,

MA) and NF200 (Neurofilament, Abcam, Cambridge, MA) for the D slice containing the cerebral cortex (CTX). Cells were then incubated with Texas Red and Alexa Flour 488-conjugated secondary antibodies (Cell Signaling Technology, Danvers, MA, USA) used at 1:200 for 2 h at room temperature. Nuclei were counterstained using Dapi (406-diamidino-2-phenylindole, Roche Basel, Switzerland) and sections were mounted on glass cover slips. Imaging was performed using the Keyence Microscope and Z stacked through the 30-um thickness to obtain a complete count of the tissue area (Itasca, IL) for IBA-1 and GFAP quantifications. The counts of IBA-1 and GFAP were completed utilizing a double extraction method where only the cells that also co-stained for DAPI were counted. Sections were derived from a single plane for MBP and NF200 quantifications. A double extraction method was also utilized, where only the MBP that co-stained for NF200 was counted. The area of MBP:NF200 was then compared to derive a ratio of myelination.

Statistical Analyses

Repeated measure ANOVA was performed for NOR to account for the measures taken across time utilizing the last observation carried forward method for any missing data. Sidak's multiple comparisons was evaluated from significant One-way ANOVAs and is displayed on the graph, unless an interaction occurred, in which case that is displayed on the graph instead. Lastly, student's t-test was used to compare 2 groups. The level of significance was marked by the number of symbols: 1 symbol indicates $p < 0.05$, 2 indicate $p < 0.01$ and 3 indicate $p < 0.001$, * indicates vs sham, + indicates vs NTC.

Results

Bilateral Injections of CSF1R ShRNA Resulted in a Significant Reduction of both Residential Microglia and Macrophages

In order to identify the best shRNA construct to silence the CSF1R, 3 different shRNAs were injected into the lateral ventricles for a global knockdown. The knockdown percentages were then evaluated in the B, C and D slice with IHC via IBA-1+ staining 14 days post-injection. Our shRNA of choice exhibited a global knockdown percentage of 72% as quantified by IHC 2 weeks after stroke. Specifically, there was a 48% knockdown in the B slice, 87% in the C slice and 68% in the D slice (Fig 3.1).

After identifying a shRNA of choice, we evaluated whether the silencing would produce similar results in diabetic animals, and whether that knockdown would be sustained over 5 weeks. 14 days after shRNA injection, the animals underwent MCAO or sham surgery. 3 weeks post-stroke (5 weeks post-injection) there was a 53% reduction in the PFC of the B slice and a 45% reduction in the limbic structure of the B slice (Fig 3.2). The PFC of NTC animals exhibited an upregulation of IBA-1+ cells 3 weeks post-stroke (Fig 3.2B, $p < 0.001$). However, CSF1R silencing lowered this upregulation to sham levels (Fig 3.2D, $p < 0.001$). Like the PFC, the limbic structures of NTC animals also had more IBA-1+ cells 3 weeks post-stroke stroke (Fig 3.2E, $p < 0.001$). In this case, CSF1R silencing prevented the upregulation, but it was still higher than that was observed in sham animals (Fig 3.2E, $p < 0.05$, $p < 0.05$, respectively).

We used flow cytometry to both quantify the knockdown globally and elucidate the residential microglia from the macrophages. CSF1R silencing resulted in a significant reduction of both residential microglia and macrophages. We gated for CD11b⁺/CD45⁺ cells indicative of both

microglia and macrophages as depicted in figure 3A and B. We then separated these cells utilizing a TMEM119 residential microglia marker. 3 weeks post-stroke diabetic animals had an increase in residential microglia and CSF1R KD resulted in a drastic 94% knockdown as measured by flow cytometry (Fig 3.3C, $p<0.01$, $p<0.001$, respectively). The residual IBA-1+ cells measured in IHC of the CSF1R silencing animals actually derived from the infiltrating macrophages, as the injection only lowered this population by 74% post-stroke when evaluated by flow cytometry (Fig 3.3D $p<0.01$).

CSF1R Silencing Exacerbated Sensorimotor Deficits

CSF1R silencing resulted in 28% mortality post-stroke, while the NTC animals experienced a 44% mortality (Fig 3.4A). Although the CSF1R silencing allowed more animals to survive, the surviving animals had worsened functional deficits. The CSF1R KD animals had higher blood glucose (BG) levels (Fig 3.4B, $p<0.05$). They also had lower body weights (Fig 3.4C $p<0.01$). Additionally, fine sensorimotor skills measured by ART were impaired in the CSF1R K/D group without apparent resolve (Fig 3.4D, $p<0.01$).

CSF1R Silencing Reduced Inflammation

In an effort to further investigate the ramifications of CSF1R silencing, we then evaluated the impact it had on neuroinflammation. Since we previously observed that the modulation of the M1/M2 ratio toward a more anti-inflammatory profile was able to preserve cognition, we evaluated the M1/M2 ratio that persisted in the remaining microglia population that was not depleted. To evaluate this, we gated for CD11b⁺/CD45⁺ low cells. The expression levels of CD45 (low versus high) have previously been accepted as a way to distinguish between microglia and macrophages. Out of the CD11b⁺/CD45⁺ low population, we then gated for M1 and M2 cells (Fig

3.5A and B). We discovered that 3 weeks post-stroke diabetic animals that received the NTC had a chronically elevated M1/M2 ratio compared to sham animals (Fig 3.5C, $p < 0.05$). The CSF1R KD animals however did not (Fig 3.5C). CSF1R silencing lowered the number of M1 residential microglia that remained chronically elevated in the NTC group (Fig 3.5D, $p < 0.001$, $p < 0.001$). CSF1R silencing also lowered the number of M1 infiltrating macrophages which too were chronically elevated after a stroke (Fig 3.5E, $p < 0.001$, $p < 0.001$).

GFAP⁺ cells are astrocytes that also play an essential role in the neuro-inflammatory response to stroke. With this in mind, we evaluated the impact of CSF1R silencing on astrocyte cell number in both the PFC as well as the limbic structures of the B slice. The limbic structures contained more GFAP⁺ cells than the PFC, and in that region there was no significant difference in the number of GFAP⁺ cells between groups (data not shown). However, CSF1R silencing significantly reduced the amount of GFAP⁺ cell in the PFC compared to the NTC animals 3 weeks post-stroke ($p < 0.05$)

Demyelination is a serious consequence of chronic inflammation. Although CSF1R silencing lowered the presence of inflammatory cells to alleviate inflammation, the anti-inflammatory M2 microglia have been shown to play a significant role in the re-myelination post-stroke. Thus, we wanted to evaluate the impact of CSF1R silencing on myelination of the cerebral cortex (CTX), a region of white matter in the rat [7]. Using MBP to stain myelin and NF200 to stain the axons, we evaluated the ratio of MBP: NF200 as a measure of myelination. The NTC animals exhibited extensive demyelination 3 weeks post-stroke (Fig 3.6H, $p < 0.001$). CSF1R silencing preserved the myelination in the CTX post-stroke, as the neurons were significantly more

myelinated compared to the NTC (Fig 3.6H, $p < 0.01$). Interestingly, CSF1R silencing was able to lower the presence of inflammatory cells and halt a consequence of chronic inflammation after stroke.

CSF1R Silencing Reduced Cognitive Deficits

Our lab has previously shown that cognitive deficits were improved when microglia polarization was modulated and chronic inflammation was relieved. Thus, we then evaluated the impact that a global microglia knockdown would have on cognition after stroke. CSF1R silencing improved working memory, particularly at week 2, as measured by NOR (Fig 3.7A, interaction $p < 0.01$). B) 2-trial Y-MAZE was employed to evaluate spatial memory. CSF1R silencing improved spatial memory at week 1 (Fig 3.7B, $p < 0.01$). CSF1R KD animals spent less time exploring at week 1 and at baseline in NOR and Y-Maze, respectively ($p < 0.05$, $p < 0.05$).

Discussion

We demonstrate in this study that under comorbid conditions such as diabetes, the CSF1R silencing dampened inflammation and reduced the cognitive deficits that accumulate post-stroke. Although CSF1R inhibition has been reported to reduce neuroinflammation leading to improved disease phenotype in several mouse models of neurodegenerative diseases, it has previously been shown to have detrimental effects on stroke recovery under non-comorbid conditions [8, 10, 11, 19]. A study utilizing oral administration of PLX3397 to silence the CSF1R reported that it exacerbated stroke severity and actually increased the infarct size by increasing the production of inflammatory mediators by astrocytes (IL-1b, iNOS, IL-6). Since the microglia function to restrict the ischemia-induced astrocyte response and provide neuroprotective

effects, this feature was lost upon their depletion [20]. Using similar methods another study reported a drastic 60% increase in infarct size. In that study, CSF1R silencing resulted in increased excitotoxicity, dysregulated calcium (Ca^{2+}) responses and a complete loss of spreading depolarization, which ultimately resulted in cognitive decline and/or death [19]. Since astrocytes play an essential role in Ca^{2+} regulation in neurons, and also function to protect them from excitotoxicity, it is likely that the altered astrocytic response in the absence of microglia also contributed to the worsened stroke recovery in that study.

M2 microglia have been reported to peak 3 days after a stroke and play an essential role in synapse remodeling through their release of microglia derived BDNF [15, 21]. They additionally play an essential role in synapse transmission through the re-myelination of axons after a stroke via the modulation of oligodendrogenesis [7, 22]. In patients, adult-onset leukoencephalopathy with axonal spheroids and pigmented glia (ALSP) is a progressive white matter disorder characterized by a depletion of microglia and a dominant loss-of function in CSF1R. This further emphasizes the importance of microglia in the myelination process. A pre-clinical study reported increased gliosis, demyelination and cognitive decline that accompanied CSF1R silencing [16]. Within the context of a neurodegenerative disease such as AD, however, astrocyte number and function was unaffected. In fact, similar to our study inflammation was downregulated [11]. In the context of stroke, microglia play an essential role in myelination post-stroke. Diabetic animals have been found to have impaired myelination post-stroke, consistent with their rise in M1 activation and lack of acute M2 response [6]. Although microglia support healthy synaptic pruning, brain connectivity and development, homeostatic functioning is lost in neurodegenerative diseases [10]. Unfortunately, the chronic inflammation in diabetes is similar

to that observed in neurodegenerative diseases. This difference could be why we observed positive results on cognition and a dampening of inflammation post-stroke in our study, contrary to what has previously been published.

Our study is the first to evaluate the impact of CSF1R silencing on stroke recovery under a comorbid neuroinflammatory condition. Within this study we actually observed a reduction in astrocytes located in the PFC, in agreement with the improvements observed in working memory evaluated with NOR. We also observed increased myelination in the white matter of the animals and improvements in spatial memory measured with Y-maze 1 week after stroke. The fact that the CSF1R silencing led to decreased exploration time after stroke may also be dampening some of the observed cognitive benefits. This could be due to the fact that diabetic animals have a dysfunctional M2 microglia response, so depletion does not impact their beneficial effects post-stroke. Taken together, these encouraging results suggest that perhaps CSF1R silencing should be tailored toward stroke victims that present with comorbid conditions that perpetuate neuroinflammation. That should not be a limiting factor since 70% of stroke victims present with pre-existing diabetes and or hypertension.

Although the targeted microglia knockdown appears to be a promising route to prevent cognitive decline, the effects that we observed on functional recovery are discouraging. Exacerbation of sensorimotor deficits may be due to the increase in the BG observed. Although we are perplexed that an ICV administered silencing of CSF1R could increase BG, the increase in BG alone does not void the encouraging results. Rather, the evaluation of microglia knockdown approaches with co-administration of a BG lowering agent such as metformin should be further investigated. Toward the end of the 3 weeks post-stroke some of the CSF1R KD animals did not

appear to maintain self-grooming. They were also smaller in weight and spent less time exploring during some of the behavioral tasks. A limitation of this study is that we did not incorporate open-field assessments that may have been beneficial to inform us of some of the potential contributing effects (i.e. pain, depression, anxiety).

With the bilateral ICV administration we noted a 94% reduction in TMEM119⁺ residential microglia 5 weeks post-injection and 3 weeks post-stroke as measured through flow cytometry. This was similar to the 87% reduction that we observed using IHC to quantify the number of IBA-1+ cells throughout the B-D slice in control animals 14 days post-injection. With this, we are confident that administering the CSF1R targeted ShRNA 14 days prior to MCAO surgery allowed enough time for integration of the ShRNA and for the full knockdown to be complete prior to ischemic insult. It is interesting that although there was a drastic reduction of residential microglia throughout the B-D slice, there was only a 45-53% reduction in the B slice as measured with IHC in diabetic animals. This was similar to the 48% reduction observed in the control animals during the optimization phase. This may be due to the placement of the B slice in location to the lateral ventricles and an artifact of the limited diffusion potential of the viral vector. It is interesting that although the PFC within the B slice received the lowest percentage of knockdown relative to the C and D slice, the NOR task, which evaluates working memory and is predominantly dependent upon the PFC, was drastically improved. This suggests that the partial but not complete knockdown of microglia within that region was enough to improve cognitive deficits post-stroke.

Our lab has previously shown that diabetic animals have a 50% increase in IBA-1+ cells compared to control animals 8 weeks post-stroke, with the majority of this increase occurring in the infiltrating macrophage population [6]. Although there was a 94% knockdown of residential microglia, there was only a 74% knockdown of infiltrating macrophages in this study. We learned from previous studies that 8 weeks post-stroke, diabetic animals had far more IBA+ cells than control animals, but the increase derived from an increase in macrophages. 71% of CD11b⁺/CD45⁺ cells in the PFC of diabetic animals were derived from infiltrating macrophages, while only 26% were derived from infiltrating macrophages in control animals [6]. The control animals in that study which exhibited a lesser degree of macrophage infiltration also displayed less functional and cognitive deficits. With the massive accumulation of macrophage infiltration in diabetic animals, the 74% knockdown may have restored balance to the diabetic brain, lowering the level of macrophage infiltration to that similar to what has been observed in our control animals.

The high degree of macrophage infiltration in the diabetic animals brings into question the blood brain (BBB) integrity. Utilizing the same HFD/STZ model reported here, our lab has previously shown that diabetic animals have a compromised BBB that persists 14 days post-stroke [23]. This brought into question whether the CSF1R silencing would improve or exacerbate the compromised BBB. Although our study was not able to address that directly, we can infer from the dampened percentage of macrophage infiltration (74% reduction) and the reduced inflammation, that it may in fact improve, not exacerbate BBB damage. A study utilizing an orally administered CSF1R inhibitor similarly reported that there were no BBB changes that accompanied the depletion of microglia [19]. On the contrary, other studies targeting the CSF1R

have reported that microglia depletion was associated with exacerbated BBB damage and peripheral cell infiltration [16, 24]. Some differences may arise from the timing of the depletion with various developmental stages. While damage to the BBB was detected when administered in young mice 2 week post-natal, it was not reported in 12-16 week old mice [15, 20]. Another variable may be that the 12-16 week old mice were analyzed post-stroke. An ischemic event can independently induce BBB alterations and may mask any potential BBB damage induced by the microglia depletion. In our study, diabetes and stroke both independently alter the BBB.

We utilized a recently identified marker, TMEM119, to differentiate infiltrating macrophages from residential microglia. This marker has recently been identified as a homeostatic marker for residential microglia. There is emerging evidence that suggests that damage associated microglia (DAMs) have been shown to decrease in expression of TMEM119 in association with the development of Alzheimer's disease. [25]. With this in mind, under neurodegenerative conditions, such as diabetic PSCI, the use of TMEM119 to differentiate residential versus infiltrating macrophages may be skewed by the number of DAMs that lose their TMEM119 expression. It may also be true that what they evaluated in that study was actually an increase in infiltrating macrophages with disease progression. Further studies are warranted in this regard to validate the efficacy of TMEM119 in neurodegenerative conditions.

Although we expect the CSF1R silencing to be localized to the brain, a limitation of our study is that we did not evaluate the possible peripheral effects of this injection. A study that used pharmacological intervention with 3 weeks of oral administration of PLX3397 reported that the particular CSF1R inhibitor was specific to microglia and did not impact the macrophage population in the splenic tissue [19]. On the contrary, a different study that also used PLX3397

administration for 3 weeks reported that diabetic mice exhibited a decrease in peripheral macrophages [26]. This study demonstrated that CSF1R silencing reduced inflammation in adipose tissue. Interestingly, it downregulated the M1/M2 ratio both in the blood and in visceral adipose tissue without impacting BG in those animals [19]. It completely depleted the number of circulating M1 macrophages, without altering the M2. Since these approaches were administered orally and ours was administered with ICV injection, one would expect a larger potential to impact the peripheral system compared to the localized injection in the brain.

Alteration of the M1/ M2 ratio in diabetic animals may be beneficial both in the central and the peripheral system. Our lab previously showed that the lowering of this M1/M2 ratio with oral administration of pharmacological intervention was beneficial to both functional recovery and the prevention of PSCI. Although M2 microglia are infamous for their role in tissue repair, the function of M2 microglia in diabetic subjects should be evaluated for the retention of this characteristic. A recent study reported increased heterogeneity in the response subtypes of microglia in the context of neurodegeneration [27]. This was also observed in our diabetic animals that developed PSCI where we reported a massive overlap of CD206⁺ M2 cells that also expressed a M1 CD86⁺ marker [6]. This increased heterogeneity in microglia markers and possibly, function, allows justification for a silencing approach since the microglia response with the diabetic subjects may be aberrant.

Although our approach of ICV injection is useful to elucidate the role of microglia post-stroke in diabetic subjects, and to lay the ground work for further investigation, an ICV injection in patients is not a feasible route. Pharmacological intervention with an orally available inhibitor, such as the ones currently in clinical trials, is the most likely route. This may be a beneficial

therapeutic intervention to treat the development of PSCI in diabetic subjects. A previous study reported that microglia were depleted orally with PLX3397 and then allowed to repopulate by mere withdrawal of the oral compound [9, 19]. The new microglia were less inflammatory when they repopulated the CNS [19], moreover the repopulation derived from nestin positive cells [9]. In addition to the role that microglia play post-stroke, they also play an essential role in protecting the brain from foreign invaders as well as the formation of brain tumors. In the context of a brain tumor, microglia are essential to ward off its formation. Since a permanent depletion could essentially leave the patient immune compromised for the rest of their life, a temporary depletion where the microglia are allowed to repopulate after some time may be the best therapeutic option.

In conclusion, although CSF1R silencing has been reported to exacerbate stroke recovery in previous experimental stroke studies, it actually lowered inflammation and improved cognition when diabetes was present. In this regard, CSF1R silencing appears to be a promising therapeutic strategy for the treatment of PSCI.

Acknowledgements: This study was supported by National Institute of Health (NIH); R01 NS104573 to Adviyee Ergul and Susan C. Fagan; R01 NS083559 to Adviyee Ergul. A Veterans Affairs (VA) Merit Review (BX000347), VA Senior Research Career Scientist Award and a TL1 award TL1 TR002382 and UL1TR002378 to Ladonya Jackson. We would also like to thank the Electron Microscope and Histology Core at Augusta University for the histological staining of our samples, with a special thank you to Ms. Penny Roon.

Figures

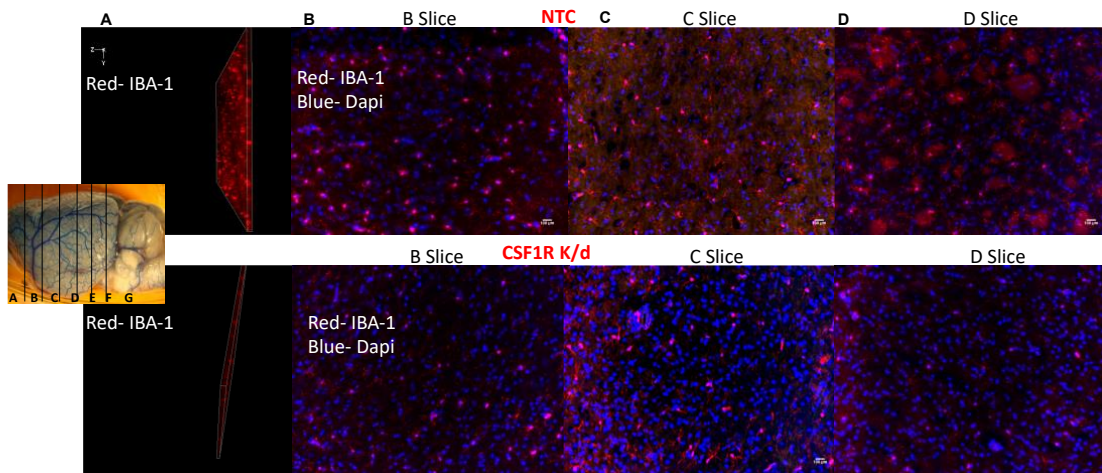


Figure 3.1: Bilateral CSF1R ShRNA injection resulted in a global knockdown of IBA-1+ cells brain 14 days post-injection

Images were derived from control animals and were Z stacked and quantified throughout the layer. 30 μm thick sections were taken from the B, C, D slice, both the layer and a representative image indicating the slides are illustrated in A. ShRNA injection resulted in a reduction of IBA-1⁺ cells in the B slide (B), C slice (C), and D slice (D).

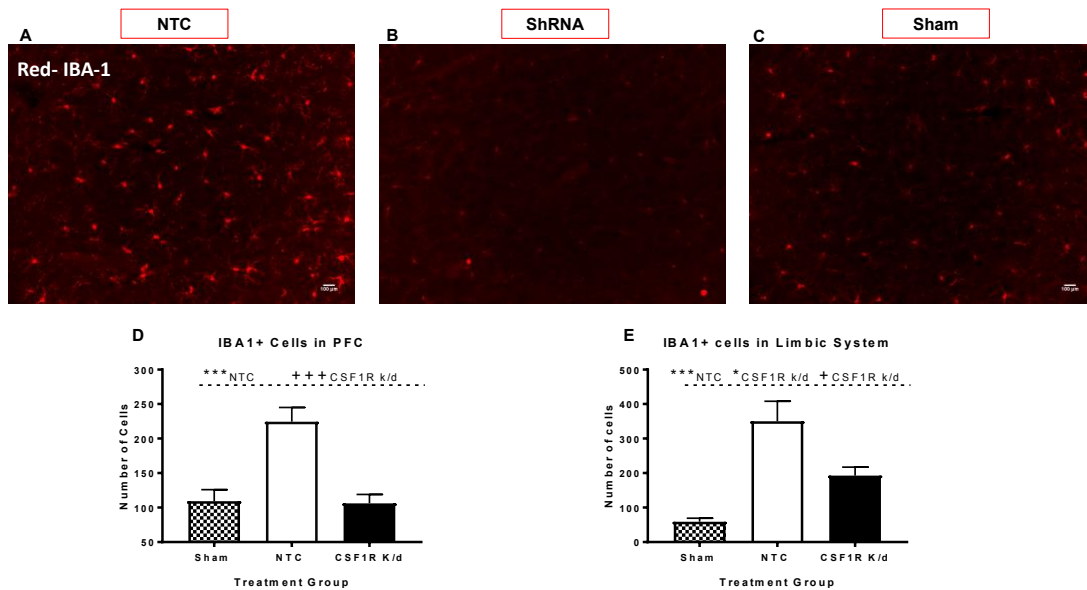


Figure 3.2: CSF1R silencing resulted in a sustained knockdown in diabetic animals 3 weeks post-stroke and 5 weeks post-injection

A-C depicts representative images of IBA-1⁺ cells in the PFC of slice B for NTC, CSF1R KD, and Sham animals, respectively. D) The PFC of diabetic animals have more IBA-1⁺ cells 3 weeks after a stroke. One-way ANOVA, Multiple Comparisons NTC vs Sham $p < 0.001$. However, CSF1R KD lowered this upregulation. One-way ANOVA, Multiple Comparisons CSF1R vs NTC $p < 0.001$. E) Like the PFC, the limbic structures of diabetic animals also have more IBA-1⁺ cells 3 weeks after a stroke. One-way ANOVA, Multiple Comparisons NTC vs Sham $p < 0.001$. In this case CSF1R KD lowered this upregulation, but is still upregulated compared to the shams. One-way ANOVA, Multiple Comparisons CSF1R vs NTC $p < 0.05$, CSF1R vs Sham $p < 0.05$.

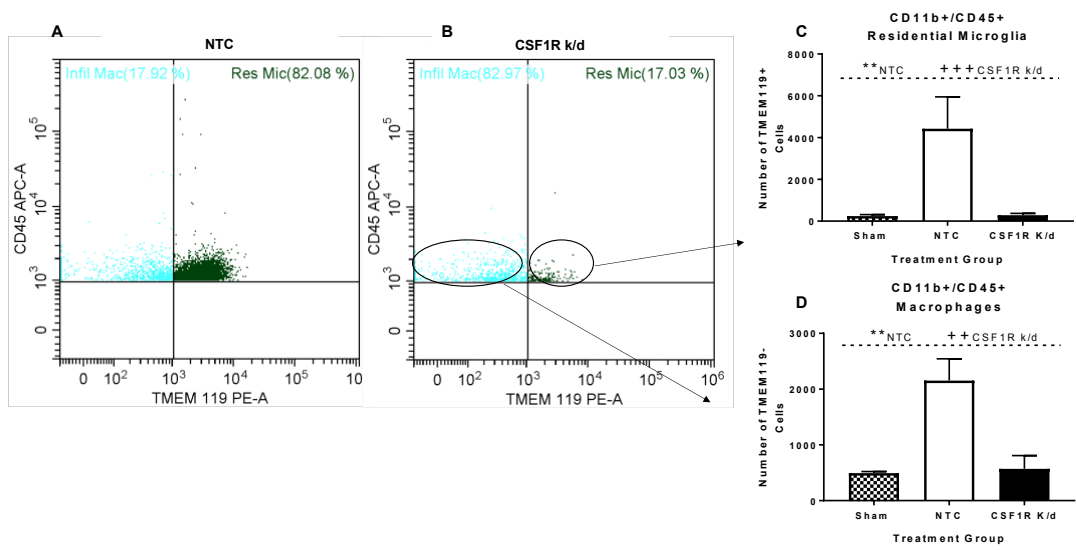


Figure 3.3: CSF1R silencing resulted in a significant reduction of both residential microglia and macrophages

We gated for CD11b⁺/CD45⁺ cells indicative of both microglia and macrophages as depicted in A and B. C) 3 weeks post-stroke diabetic animals had an increase in residential microglia, that CSF1R KD drastically lowered by 94%. One-way ANOVA, Multiple Comparisons NTC vs Sham p<0.01, CSF1R vs NTC p<0.001. D) The macrophage infiltration after stroke was also lowered by 74%. One-way ANOVA, Multiple Comparisons NTC vs Sham p<0.01, CSF1R vs NTC p<0.01.

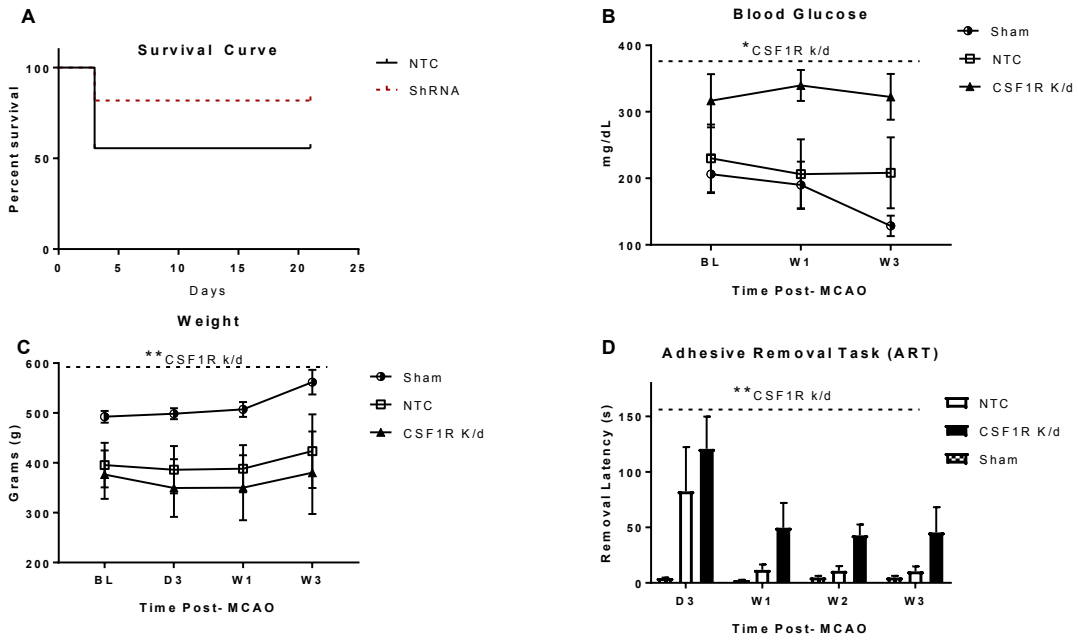


Figure 3.4: CSF1R silencing worsened functional recovery

A) CSF1R animals experienced a 28% mortality post-stroke, while the NTC animals experienced a 44% mortality. CSF1R KD increased B) BG and exacerbated C) and decreased weight over the 3 weeks post-stroke. Repeated measures ANOVA, Multiple Comparisons CSF1R vs Sham $p < 0.05$ BG, and $p < 0.01$ weight loss. D) The adhesive removal task (ART) was utilized to measure sensorimotor function. CSF1R KD animals also experienced worsened sensorimotor deficits. Repeated measures ANOVA, Multiple Comparisons CSF1R vs Sham.

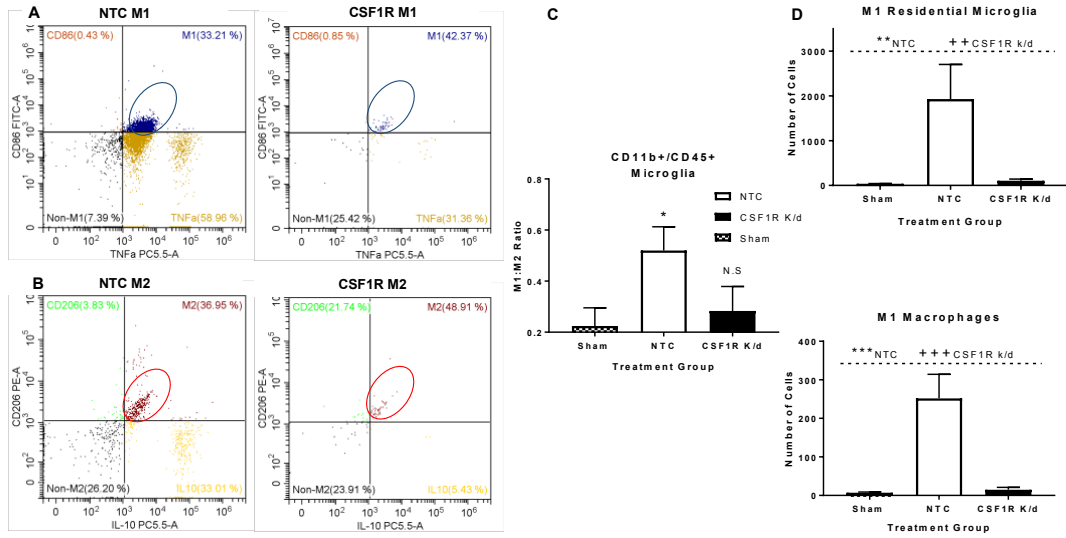


Figure 3.5: CSF1R silencing lowered the amount of inflammatory microglia

We gated for M1 and M2 cells as indicated in A and B. C) 3 weeks post-stroke diabetic NTC but not CSF1R animals have an increased M1/M2 ratio. Student's T test, NTC vs Sham $p < 0.05$. D) CSF1R KD lowered the number of M1 microglia, and M1 macrophages. One-way ANOVA, Multiple Comparisons NTC vs Sham $p < 0.01$ microglia, $p < 0.001$ macrophages, CSF1R vs NTC $p < 0.01$ microglia, $p < 0.001$ macrophages.

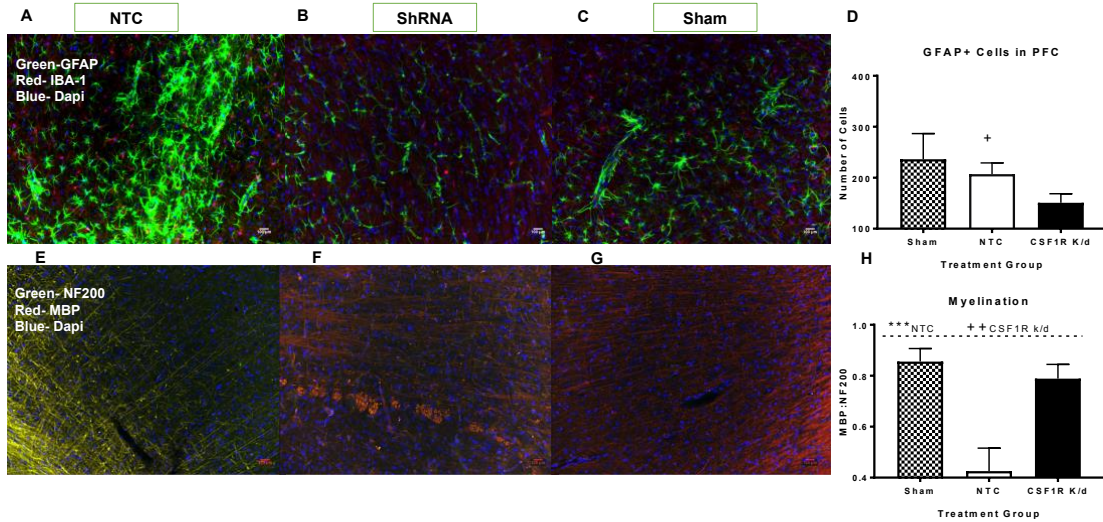


Figure 3.6: CSF1R silencing reduced inflammation and improved myelination

A-C depicts representative images of GFAP⁺ cells of slice B for NTC, CSF1R KD, and Sham animals, respectively. D) Although there was no significant difference in the number of GFAP⁺ cells in the limbic structures of slice B and GFAP⁺ cells were not increased compared to sham animals, CSF1R significantly reduced the amount of GFAP⁺ cell compared to control animals 3 weeks after a stroke. Student's T-Test CSF1R vs NTC $p < 0.05$. E-H Depicts representative images of NF200⁺ and MBP⁺ cells of slice B for NTC, CSF1R KD, and Sham animals, respectively. Using MBP to stain myelin and NF200 to stain the axons, we evaluated the ratio of MBP:NF200 as a measure of myelination. Although diabetic animals exhibited demyelination 3 weeks after stroke, CSF1R KD prevented this decline in myelination. One-way ANOVA, Multiple Comparisons, NTC vs Sham $p < 0.001$, CSF1R vs NTC $p < 0.01$.

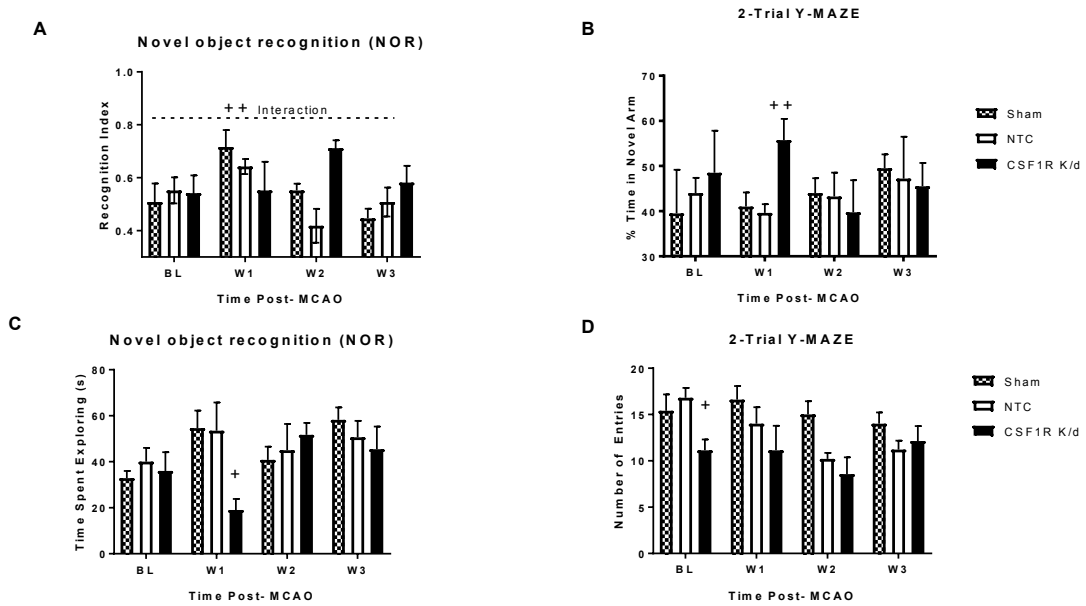


Figure 3.7: CSF1R silencing reduced cognitive deficits post-stroke

A) CSF1R KD reduced cognitive deficits as measured by NOR. Repeated measures ANOVA, interaction $p < 0.01$
 A) 2-trial Y-MAZE was employed to evaluate the impact of CSF1 knockdown post-stroke in spatial memory. Although NTC animals were only impaired acutely post-stroke, CSF1R KD improved the cognitive decline at W1. Student's T test, CSF1R vs NTC $p < 0.01$.

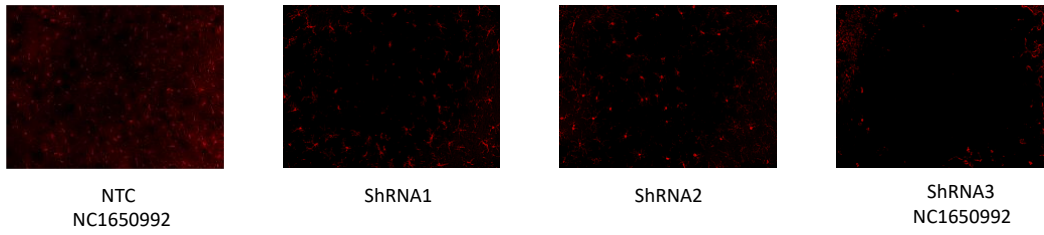


Figure 3.S1: ShRNA knockdown selection

ShRNA knockdown selection. Three ShRNA constructs all targeted at the CSF1R were evaluated 14 days post-injection. Based on this evaluation we choose the ShRNA with the best knockdown percentage to proceed with the study.

Table 3.1: Flow Cytometry Markers Utilized to Identify Particular Cell Populations

	CD11b	CD45	TMEM119	CD86	TNF α	CD206	IL10
M1 (CD206+/IL10+)	+	+ low	N/A	+	+	N/A	N/A
M2 (CD86+/TNFα+))	+	+ low	N/A	N/A	N/A	+	+
Residential Microglia (TMEM119+)	+	+	+	N/A	N/A	N/A	N/A
Infiltrating Macrophages	+	+	-	N/A	N/A	N/A	N/A
M1 macrophages	+	+	-	+	+	N/A	N/A
Inactivated microglia	+	+ low	N/A	-	N/A	-	N/A

References

1. Mozaffarian, D., et al., *Heart disease and stroke statistics--2015 update: a report from the American Heart Association*. Circulation, 2015. **131**(4): p. e29-322.
2. Tun, N.N., et al., *Diabetes mellitus and stroke: A clinical update*. World J Diabetes, 2017. **8**(6): p. 235-248.
3. Wang, Q., et al., *Prediabetes is associated with post-stroke cognitive impairment in ischaemic stroke patients*. Brain Res, 2017.
4. Ward, R., et al., *Post Stroke Cognitive Impairment and Hippocampal Neurovascular Remodeling: The Impact of Diabetes and Sex*. Am J Physiol Heart Circ Physiol, 2018.
5. Ladonya Jackson, W.L., Yasir Abdul, Guangkuo Dong, Babak Baban, Advie Ergul, *Diabetic Stroke Promotes a Sexually Dimorphic Expansion of T Cells*. NeuroMolecular Medicine 2019. **In Press**(71).
6. Ladonya Jackson, Guangkuo Donya, S.C.F., Advie Ergul, *Delayed Administration of Angiotensin Receptor (AT2R) Agonist C21 Downregulates Diabetes Induced Pro-inflammatory Microglia Activation to Improve Cognitive and Functional Recovery Post-Stroke*. AHA stroke abstract, 2019. **50**(1).
7. Ma, S., et al., *Diabetes Mellitus Impairs White Matter Repair and Long-Term Functional Deficits After Cerebral Ischemia*. Stroke, 2018. **49**(10): p. 2453-2463.
8. Gerber, Y.N., et al., *CSF1R Inhibition Reduces Microglia Proliferation, Promotes Tissue Preservation and Improves Motor Recovery After Spinal Cord Injury*. Front Cell Neurosci, 2018. **12**: p. 368.
9. Elmore, M.R., et al., *Colony-stimulating factor 1 receptor signaling is necessary for microglia viability, unmasking a microglia progenitor cell in the adult brain*. Neuron, 2014. **82**(2): p. 380-97.
10. Spangenberg, E.E. and K.N. Green, *Inflammation in Alzheimer's disease: Lessons learned from microglia-depletion models*. Brain Behav Immun, 2017. **61**: p. 1-11.
11. Spangenberg, E.E., et al., *Eliminating microglia in Alzheimer's mice prevents neuronal loss without modulating amyloid-beta pathology*. Brain, 2016. **139**(Pt 4): p. 1265-81.
12. Fouda, A.Y., et al., *Brain-Derived Neurotrophic Factor Knockdown Blocks the Angiogenic and Protective Effects of Angiotensin Modulation After Experimental Stroke*. Mol Neurobiol, 2017. **54**(1): p. 661-670.
13. El Khoury, J., et al., *Ccr2 deficiency impairs microglial accumulation and accelerates progression of Alzheimer-like disease*. Nat Med, 2007. **13**(4): p. 432-8.
14. Guruswamy, R. and A. ElAli, *Complex Roles of Microglial Cells in Ischemic Stroke Pathobiology: New Insights and Future Directions*. Int J Mol Sci, 2017. **18**(3).
15. Kirkley, K.S., et al., *Microglia amplify inflammatory activation of astrocytes in manganese neurotoxicity*. J Neuroinflammation, 2017. **14**(1): p. 99.
16. Paolicelli, R.C. and M.T. Ferretti, *Function and Dysfunction of Microglia during Brain Development: Consequences for Synapses and Neural Circuits*. Front Synaptic Neurosci, 2017. **9**: p. 9.
17. Chen, J., Y. Li, and M. Chopp, *Intracerebral transplantation of bone marrow with BDNF after MCAo in rat*. Neuropharmacology, 2000. **39**(5): p. 711-6.
18. Holt, L.M. and M.L. Olsen, *Novel Applications of Magnetic Cell Sorting to Analyze Cell-Type Specific Gene and Protein Expression in the Central Nervous System*. PLoS One, 2016. **11**(2): p. e0150290.
19. Szalay, G., et al., *Microglia protect against brain injury and their selective elimination dysregulates neuronal network activity after stroke*. Nat Commun, 2016. **7**: p. 11499.
20. Jin, W.N., et al., *Depletion of microglia exacerbates postischemic inflammation and brain injury*.

- J Cereb Blood Flow Metab, 2017. **37**(6): p. 2224-2236.
21. Hu, X., et al., *Microglia/macrophage polarization dynamics reveal novel mechanism of injury expansion after focal cerebral ischemia*. Stroke, 2012. **43**(11): p. 3063-70.
 22. Yuan, J., et al., *M2 microglia promotes neurogenesis and oligodendrogenesis from neural stem/progenitor cells via the PPARgamma signaling pathway*. Oncotarget, 2017. **8**(12): p. 19855-19865.
 23. Ward, R., et al., *NLRP3 inflammasome inhibition with MCC950 improves diabetes-mediated cognitive impairment and vasoneuronal remodeling after ischemia*. Pharmacol Res, 2019. **142**: p. 237-250.
 24. Bruttger, J., et al., *Genetic Cell Ablation Reveals Clusters of Local Self-Renewing Microglia in the Mammalian Central Nervous System*. Immunity, 2015. **43**(1): p. 92-106.
 25. Keren-Shaul, H., et al., *A Unique Microglia Type Associated with Restricting Development of Alzheimer's Disease*. Cell, 2017. **169**(7): p. 1276-1290 e17.
 26. Merry, T.L., et al., *The CSF1 receptor inhibitor pexidartinib (PLX3397) reduces tissue macrophage levels without affecting glucose homeostasis in mice*. Int J Obes (Lond), 2019.
 27. Mathys, H., et al., *Temporal Tracking of Microglia Activation in Neurodegeneration at Single-Cell Resolution*. Cell Rep, 2017. **21**(2): p. 366-380.

CHAPTER 4

INTEGRATED DISCUSSION

The overall goal of this thesis was to investigate the relative role(s) that diabetes, microglia activation and interaction thereof, play in the exacerbation of PSCI, and to investigate a potential therapeutic mechanism to alleviate this. For the first specific aim, our goal was to determine whether the accumulation of cognitive deficits post-stroke was augmented in diabetes and if it could be therapeutically targeted. We hypothesized that diabetes would exacerbate the progressive development of PSCI. Through thorough investigation we discovered that this was in fact true. Diabetes more than doubled the risk of developing cognitive impairment 8 weeks after stroke [1]. Even the diabetic sham group developed cognitive impairment at a higher rate than the control. This beautifully illustrated the impact that diabetes has on cognition and emphasized the importance of comorbid disease modeling into the investigation of PSCI [1]. If we studied this in control animals alone, only 20% would develop PSCI 8 weeks after stroke versus 100% of the diabetic animals. Taking the high diabetic mortality into account, it may actually be more financially feasible to study PSCI in control animals, but again, the low rate of occurrence could mask the impact of any therapeutic interventions.

We then hypothesized that AT2R agonist C21 could ameliorate the evolution of PSCI in diabetic rats. We in fact proved this hypothesis to be true. Treatment with C21 was able to ameliorate the evolution of PSCI in diabetic rats as evident by the 0% development of PSCI. This was remarkable to witness, but interestingly it actually exerted its effect independent of AT2R stimulation. Our *in vitro* data indicated that C21 was able to polarize microglia independent of AT2R stimulation [1]. Our lab has shown in the past that although C21 treatment improved stroke recovery, it did not increase the AT2R expression (Wael Eldahshan Thesis). On the

contrary, our lab also reported that the anti-apoptotic effect of C21 in neuronal cultures exposed to OGD/reoxygenation was blocked by co-administration of the AT2R blocker PD 123319.

One study claimed that C21 lowered MRI detectable brain damage in stroke-prone rats, and that this was blunted when PD 123319 was administered [2]. A limitation of this study is that they only administered PD 123319 with the highest dose of C21 (10 mg/kg), but compared it to doses of 0, 0.75, 5 mg/kg. The high dose of C21 (10 mg/kg) rather than the PD 123319 administration could underlie the detrimental effects reported [2]. This 10 mg/kg dose is much larger than our dose of 0.12 mg/kg. Our lab has shown that C21 treatment has an optimal threshold of around 0.3 mg/kg when administered intravenously (IV) [3]. In fact, higher doses of C21 are associated with increased cell death [4]. The oral dose of 0.12 mg/kg that we utilized in our study was calculated based on an oral bioavailability of 0.25, so it is equivalent to the dose of 0.03 mg/kg [5]. A different study which evaluated the role of C21 in pulmonary hypertension observed an increase in the AT2R expression with the administration of C21. In this study, the beneficial effects of C21 as well as the AT2R expression was attenuated when the AT2R was blocked with PD 123319 [6]. This is in accordance with what our lab previously reported in neuronal cultures [2]. Interestingly, this study also reported that C21 increased Mas receptor (MasR) expression [6]. MasRs and AT2Rs both work synergistically in the brain to improve cognition, and both are associated with M2 microglia polarization [7]. Although we did not see an attenuation of polarization with AT2R blockade, we cannot rule out the potential role of MasR stimulation on the improved cognition associated with M2 microglia polarization.

Invigorated by the findings in the first aim, we then desired to delve deeper into the mechanism of PSCI in diabetes. We hypothesized that chronic pro-inflammatory microglia activation was correlated with the enhanced development of PSCI in diabetic rats. We validated this by showing the increase in IBA-1⁺ cells in diabetic rats with PSCI compared to control rats [1]. In the IBA-1⁺ population, there was actually an increase in the amount of infiltrating macrophages in the diabetic animals that drove the number of IBA-1⁺ cells up compared to the control. Microglia have a low turnover rate so their function is susceptible to injury and age. Their renewal has been shown to derive from a nestin positive population [8, 9]. From our findings, an increase in the number of microglia does not appear to be the case. A combination of a compromised BBB and pro-inflammatory microglia signaling may be leading to the increase in macrophage infiltration. The CCL2/CCR2 (C-C motif chemokine ligand/ receptor 2) signaling pathway in microglia and macrophages play a central role in regulating their interaction [10]. Toll-like receptor (TLR) activation upregulates pro-inflammatory microglia and triggers their release of CCL2 in an autocrine and paracrine manner [10]. Diabetes is associated with an upregulation of both TLR-2 and 4 [11, 12]. Post-stroke, this cycle of increased TLR signaling can lead to more M1 microglia activation in diabetic subjects, which can then signal for more macrophage infiltration. The CCL2 released by M1 microglia can act to signal macrophages into the brain during inflammatory reactions [10]. Under non-comorbid conditions, there is a rise in M2 acutely post-stroke which is then followed by a rise in M1 [13]. This rise in M2 peaks around day 3, around the same time as the peak in macrophage infiltration [14]. This may contribute as a mechanism to limit macrophage infiltration. Unfortunately, diabetic subjects do not

experience an acute rise in M2 [15]. Instead this is replaced with an immediate rise in M1 and may act to enhance the recruitment of macrophages.

Although there is no difference in the number of microglia, our lab has shown that there is an increase in the activated microglia in diabetic animals post-stroke [16]. Within this thesis, we have now characterized the activated microglia sub-types and shown that M1 pro-inflammatory activated microglia predominate in diabetic animals. Interestingly, studies have shown that diet influences the gut microbiota which can modulate the activation and the function of microglia [17]. High-salt diet has been associated with inflammatory intestinal changes that upregulate pro-inflammatory Thelper (Th17) cells to exacerbate stroke outcome [18]. However recently our lab repeated this study to evaluate the impact of HFD on intestinal changes. Interestingly, this led to pro-inflammatory changes in the blood and brain but not in the intestines. Perhaps HFD alters the microbiota and exerts the bulk of its pro-inflammatory effects through the modulation of microglia activation.

As we hypothesized, therapeutic intervention with C21 was able to downregulate the pro-inflammatory M1: anti-inflammatory M2 ratio in *in vivo* and *in vitro*. The most encouraging aspect of this is that it was able to do so with delayed administration *in vivo*, and with post-treatment *in vitro*. This is exciting because it suggests that a therapeutic intervention with C21 can not only prevent, but actually reverse pro-inflammatory effects on microglia polarization. This is essential since it would not be administered to patients until after they have diabetes and after they have a stroke, in which substantial damage would have already occurred.

Although the upregulation of pro-inflammatory microglia was linked to the progressive development of PSCI, correlation does not necessarily indicate causation. With this in mind, we

lastly hypothesized that microglia knockdown could prevent the progressive development of PSCI, as a means to measure the degree of causation (chapter 3). Although microglia knockdown had previously been shown to exacerbate ischemic injury, this was not the case in diabetic animals. In diabetic animals the microglia knockdown prevented the cognitive decline, giving direct causation to microglia activation in the development of diabetic PSCI.

Findings within this study emphasize the essential need for more translational studies. In an effort to increase the translatability of our study, we followed the recommendations made by the Stroke Therapy Academic Industry Roundtable (STAIR) [19, 20]. We blinded and randomized our first study [1]. Although we were not able to randomize our second study due to personnel restraints, we did blind the behavioral assessments (chapter 3). The labs of Drs. Ergul and Fagan work together to evaluate the role of C21 in PSCI in both diabetes and hypertension, satisfying two aspects of the STAIR recommendations (the request for the efficacy in two laboratories and the replication in a second species). We did not include female studies within this thesis but our lab is in the process of completing female studies evaluating the impact of C21 on PSCI in both diabetic and hypertension animals. We chose an oral route of administration of C21 and a delayed administration to satisfy the request for consideration of route of administration and a clinically useful therapeutic window and dose response. Lastly, when we evaluated the impact of diabetes on PSCI development and C21 administration, we incorporated inclusion criteria as a means to ensure inclusion of animals with a significant degree of ischemic injury. This served to provide an accurate depiction of the impact of diabetes and C21 on PSCI devoid of false negative or false positive results. Unfortunately, with

the 2-week prior to stroke injection of CSF1R ShRNA, we were not able to set an inclusion criteria without potentially compromising the results.

In addition to the inability to apply pre-set inclusion criteria, another limitation of this thesis is that we were not able to evaluate the CSF1R KD animals at a time course past 3 weeks. In our C21 study, we experienced massive mortality in the diabetic animals (chapter 2). In addition to the acute mortality, we also experienced a peak in mortality 4 weeks post stroke. In an effort to avoid this spike in mortality, we halted our CSF1R silencing study at 3 weeks. It is

interesting that in both the knockdown study and the C21 study the animals appeared to improve after week 2. In the knockdown study the animals improved at week 3 and did not appear to be impaired. In the C21 study, the animals did not appear to be significantly impaired when evaluated at week 4 but then experienced a subsequent drop in cognition at week 8. This emphasizes the need for longer time course studies in the evaluation of PSCI. The rise and the subsequent drop was also evident in the ART

scores, indicative of their fine motor ability. Since there was no difference in the time these animals spent exploring at those timepoints we suspect that it is not their motor ability which is impacting the drop in their cognition but perhaps there may be secondary neurodegeneration

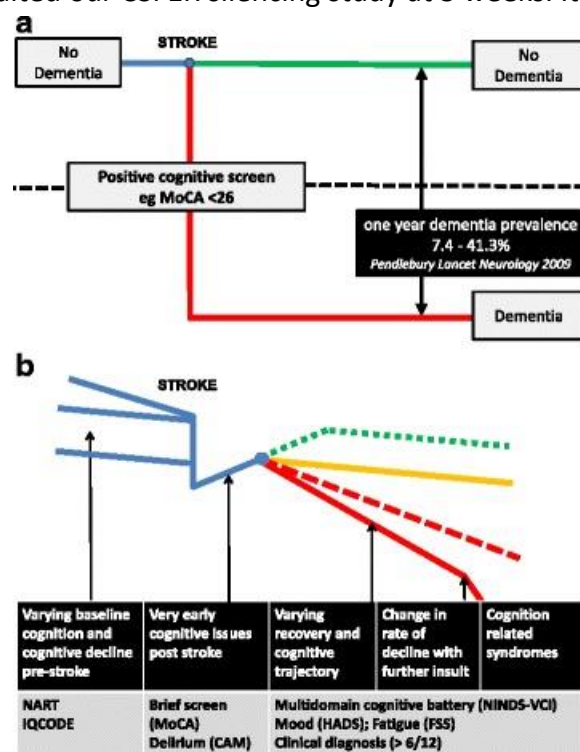


Figure 4.1: Cognitive "Trajectory" in Stroke
 Depicts the traditional view in A, and the "real-world" development of PSCI in B.
 Adapted from Milija D. Mijajlović 2017, BMC med.

that occur in the diabetic animals post-stroke after the week 4 time point. Interestingly, clinical studies have reported a similar trajectory in the development of PSCI in patients (Fig.1). If possible, studies beyond 8 weeks should be further evaluated in diabetic PSCI.

In summary, this thesis most importantly emphasizes the need for comorbid disease modeling of PSCI. Within the C21 study we found that control animals not only had a lower occurrence of PSCI, but they also experienced a dimorphic effect of C21. This could indicate the restriction of this drug to diabetic PSCI, or it could indicate a need to re-evaluate optimal dosing under non-comorbid conditions. In our knockdown study, we noticed that contrary to what has been reported in the literature about microglia knockdown post-stroke, when the animals were diabetic the effect was positive. This is because previous studies only modeled microglia knockdown under non-comorbid conditions, where the microglia present retained homeostatic functions. Both of the studies nicely illustrate the need for translational disease modeling for the advancement of scientific research and the improvement of patient outcomes.

References

1. Jackson, L., Dong, G., Fagan, S.C., Ergul, A, *Delayed Administration of Angiotensin Receptor (AT2R) Agonist C21 Downregulates Diabetes Induced Pro-inflammatory Microglia Activation to Improve Cognitive and Functional Recovery Post-Stroke*. AHA stroke abstract, 2019. **50**(1).
2. Gelosa, P., et al., *Stimulation of AT2 receptor exerts beneficial effects in stroke-prone rats: focus on renal damage*. J Hypertens, 2009. **27**(12): p. 2444-51.
3. Ishrat, T., et al., *Dose-response, therapeutic time-window and tPA-combinatorial efficacy of compound 21: A randomized, blinded preclinical trial in a rat model of thromboembolic stroke*. J Cereb Blood Flow Metab, 2018: p. 271678X18764773.
4. Fouda, A.Y., et al., *Role of interleukin-10 in the neuroprotective effect of the Angiotensin Type 2 Receptor agonist, compound 21, after ischemia/reperfusion injury*. Eur J Pharmacol, 2017. **799**: p. 128-134.
5. Alhusban, A., et al., *Compound 21 is pro-angiogenic in the brain and results in sustained recovery after ischemic stroke*. J Hypertens, 2015. **33**(1): p. 170-80.
6. Bruce, E., et al., *Selective activation of angiotensin AT2 receptors attenuates progression of pulmonary hypertension and inhibits cardiopulmonary fibrosis*. Br J Pharmacol, 2015. **172**(9): p. 2219-31.
7. Jackson, L., et al., *Within the Brain: The Renin Angiotensin System*. Int J Mol Sci, 2018. **19**(3).
8. Szalay, G., et al., *Microglia protect against brain injury and their selective elimination dysregulates neuronal network activity after stroke*. Nat Commun, 2016. **7**: p. 11499.
9. Elmore, M.R., et al., *Colony-stimulating factor 1 receptor signaling is necessary for microglia viability, unmasking a microglia progenitor cell in the adult brain*. Neuron, 2014. **82**(2): p. 380-97.
10. Guruswamy, R. and A. ElAli, *Complex Roles of Microglial Cells in Ischemic Stroke Pathobiology: New Insights and Future Directions*. Int J Mol Sci, 2017. **18**(3).
11. Hardigan, T., et al., *TLR2 knockout protects against diabetes-mediated changes in cerebral perfusion and cognitive deficits*. Am J Physiol Regul Integr Comp Physiol, 2017. **312**(6): p. R927-R937.
12. Abdul, Y., et al., *Inhibition of Toll-Like Receptor-4 (TLR-4) Improves Neurobehavioral Outcomes After Acute Ischemic Stroke in Diabetic Rats: Possible Role of Vascular Endothelial TLR-4*. Mol Neurobiol, 2018.
13. Hu, X., et al., *Microglia/macrophage polarization dynamics reveal novel mechanism of injury expansion after focal cerebral ischemia*. Stroke, 2012. **43**(11): p. 3063-70.
14. Jin, R., G. Yang, and G. Li, *Inflammatory mechanisms in ischemic stroke: role of inflammatory cells*. J Leukoc Biol, 2010. **87**(5): p. 779-89.
15. Ma, S., et al., *Diabetes Mellitus Impairs White Matter Repair and Long-Term Functional Deficits After Cerebral Ischemia*. Stroke, 2018. **49**(10): p. 2453-2463.
16. Ward, R., et al., *Post Stroke Cognitive Impairment and Hippocampal Neurovascular Remodeling: The Impact of Diabetes and Sex*. Am J Physiol Heart Circ Physiol, 2018.
17. Erny, D., et al., *Host microbiota constantly control maturation and function of microglia in the CNS*. Nat Neurosci, 2015. **18**(7): p. 965-77.
18. Faraco, G., et al., *Dietary salt promotes neurovascular and cognitive dysfunction through a gut-initiated TH17 response*. Nat Neurosci, 2018. **21**(2): p. 240-249.

19. Lapchak, P.A., *Scientific Rigor Recommendations for Optimizing the Clinical Applicability of Translational Research*. J Neurol Neurophysiol, 2012. **3**.
20. Lapchak, P.A., J.H. Zhang, and L.J. Noble-Haeusslein, *RIGOR guidelines: escalating STAIR and STEPS for effective translational research*. Transl Stroke Res, 2013. **4**(3): p. 279-85.